

INFORMATION TO USERS

This manuscript has been reproduced from the microfilm master. UMI films the text directly from the original or copy submitted. Thus, some thesis and dissertation copies are in typewriter face, while others may be from any type of computer printer.

The quality of this reproduction is dependent upon the quality of the copy submitted. Broken or indistinct print, colored or poor quality illustrations and photographs, print bleedthrough, substandard margins, and improper alignment can adversely affect reproduction.

In the unlikely event that the author did not send UMI a complete manuscript and there are missing pages, these will be noted. Also, if unauthorized copyright material had to be removed, a note will indicate the deletion.

Oversize materials (e.g., maps, drawings, charts) are reproduced by sectioning the original, beginning at the upper left-hand corner and continuing from left to right in equal sections with small overlaps.

ProQuest Information and Learning
300 North Zeeb Road, Ann Arbor, MI 48106-1346 USA
800-521-0600

UMI[®]

University of Alberta

Preconcentration Techniques in Capillary Electrophoresis with Laser-Induced
Fluorescence Detection

by

Jiang Jiang



A thesis submitted to the Faculty of Graduate Studies and Research in partial fulfillment
of the requirements for the degree of Doctor of Philosophy

Department of Chemistry

Edmonton, Alberta

Fall 2005



Library and
Archives Canada

Bibliothèque et
Archives Canada

Published Heritage
Branch

Direction du
Patrimoine de l'édition

0-494-08661-0

395 Wellington Street
Ottawa ON K1A 0N4
Canada

395, rue Wellington
Ottawa ON K1A 0N4
Canada

Your file *Votre référence*

ISBN:

Our file *Notre référence*

ISBN:

NOTICE:

The author has granted a non-exclusive license allowing Library and Archives Canada to reproduce, publish, archive, preserve, conserve, communicate to the public by telecommunication or on the Internet, loan, distribute and sell theses worldwide, for commercial or non-commercial purposes, in microform, paper, electronic and/or any other formats.

The author retains copyright ownership and moral rights in this thesis. Neither the thesis nor substantial extracts from it may be printed or otherwise reproduced without the author's permission.

AVIS:

L'auteur a accordé une licence non exclusive permettant à la Bibliothèque et Archives Canada de reproduire, publier, archiver, sauvegarder, conserver, transmettre au public par télécommunication ou par l'Internet, prêter, distribuer et vendre des thèses partout dans le monde, à des fins commerciales ou autres, sur support microforme, papier, électronique et/ou autres formats.

L'auteur conserve la propriété du droit d'auteur et des droits moraux qui protègent cette thèse. Ni la thèse ni des extraits substantiels de celle-ci ne doivent être imprimés ou autrement reproduits sans son autorisation.

In compliance with the Canadian Privacy Act some supporting forms may have been removed from this thesis.

Conformément à la loi canadienne sur la protection de la vie privée, quelques formulaires secondaires ont été enlevés de cette thèse.

While these forms may be included in the document page count, their removal does not represent any loss of content from the thesis.

Bien que ces formulaires aient inclus dans la pagination, il n'y aura aucun contenu manquant.


Canada

Abstract

Capillary electrophoresis (CE) is a separation technique based on the differential migration of solutes in an electric field. In CE, one of the long-standing problems is the poor detection sensitivity, especially when ultraviolet detection is used. Several pre-concentration techniques were utilized in this thesis for enhancing the detection sensitivity of CE with laser-induced fluorescence detection (LIF).

High-salt stacking, originally proposed by Lander *et al.*, was applied to enrich fluorescently labelled alkylphosphonic acids in micellar electrokinetic chromatography (MEKC). By adding sodium chloride to the sample solution, a discontinuous buffer system was created in the capillary. The difference in conductivity at the sample zone – MEKC buffer zone interface resulted in the deceleration and accumulation of sodium cholate micelles at the zone boundary and the subsequent concentration of hydrophobic analytes. An enrichment of approximately 10 fold was obtained.

Enrichment of analytes can also be achieved based on solid-phase extraction (SPE) in either an off-line or online manner. A 200- μ l micropipette tip packed with anion-exchanger beads was used for offline SPE extraction of glyphosate, a herbicide, from a spiked river water sample. Subsequent elution of the retained glyphosate and fluorescent labeling allowed detection of glyphosate in the sub-nanomolar range. An approximate 88-fold preconcentration was observed by using such an off-line resin-packed SPE pipette tip.

SPE-based on-capillary preconcentration was developed by entrapping HPLC bulk packing (PRP-1) into a sol-gel silica monolith in a short segment of capillary and attaching the prepared SPE capillary to the tip of separation capillary. After fluorescent

labeling, two herbicides, ampropylfos and glufosinate, were extracted onto the PRP-1 beads, followed by elution and CE-LIF analysis. The charge states of analytes were found to affect the extraction ratio, which can be improved significantly either by reducing the pH or by adding salt to the sample solution. Examination of the PRP-1 packed silica monolith by scanning electron microscopy (SEM) found that PRP-1 beads were encapsulated by a silica shell. A very small fraction of PRP-1 beads had exposed surface for extracting hydrophobic analytes. This problem was solved by partial digestion of the silica shell using a pH 9.4 borate buffer. With significantly increased PRP-1 bead surface and salt effect during sample loading, 1260- and 580- fold enhancement of detection sensitivity were achieved for ampropylfos and glufosinate, respectively.

Finally, in an alternate project, a capillary gel electrophoresis (CGE)-LIF method using a polyethylene oxide (PEO) polymer sieving matrix was developed for separation of five model proteins. For the first time, detergent differential fractionation (DDF) technique was combined with CGE for the sequential fractionation and protein profiling of HT29 human colon adenocarcinoma cell extract.

Acknowledgements

I would like to thank my supervisor, Dr. Charles Lucy, for accepting me into his group in Fall 2000 when Dr. Norm Dovichi moved to the University of Washington, and his continual guidance and support throughout the past five years. Dr. Norm Dovichi's support and guidance during my first year in graduate school are also greatly appreciated.

Past and present members of the Lucy group are greatly acknowledged for their help and friendship. In particular I would like to thank Dr. Chuanzhong Wang and Dr. Jeremy Melanson for their fruitful discussions. Past members of the Dovichi group are also acknowledged for their support. I would like to thank Lillian Cook for HT29 cell culture, Dr. Dawn Richards for her advice on detergent differential fractionation procedure and Dr. Shen Hu for his helpful ideas and discussions.

Numerous members of the department provided great help. In particular I would like to thank Jian Wang for preparing dry DMF, and Chengjie Ji, Dr. Huizhi Liu, Dr. Jianbin Bao, Jing Wen for their assistance. Dr. George Braybrook in the Department of Earth and Atmospheric Sciences is greatly appreciated for his help with SEM imaging.

Financial support for this thesis research was provided by the Natural Sciences and Engineering Research Council of Canada (NSERC), the Department of National Defense Canada and the University of Alberta. The work done in the Dovichi group was supported by the National Institutes of Health (USA).

I am grateful to my parents and sister for their continued encouragement. Their unconditional support has helped me overcome all obstacles during my graduate study in Canada.

Table of Contents

Chapter 1. Introduction

1.1 Principles of capillary electrophoresis.....	1
1.1.1 History	1
1.1.2 Basic instrumentation.....	2
1.1.3 Electroosmotic flow (EOF).....	3
1.1.4 Electrophoretic mobility.....	5
1.1.5 Major modes of separation.....	5
1.1.5.1 Capillary zone electrophoresis (CZE).....	5
1.1.5.2 Micellar electrokinetic chromatography (MEKC).....	9
1.1.5.3 Capillary gel electrophoresis (CGE).....	12
1.1.6 Detection.....	13
1.2 Electrophoresis-based online preconcentration.....	15
1.2.1 Field-amplified sample stacking (FASS).....	15
1.2.2 Dynamic pH-junction stacking.....	16
1.2.3 High-salt stacking.....	17
1.2.4 Sweeping.....	19
1.3 Solid phase extraction (SPE)-based online preconcentration.....	20
1.3.1 Online SPE methods.....	21
1.3.2 SPE phase immobilization techniques.....	25
1.4 Thesis overview.....	27
1.5 References.....	29

Chapter 2. Determination of Alkylphosphonic Acids Using Micellar Electrokinetic Chromatography with Laser-Induced Fluorescence Detection and High-Salt Stacking

2.1 Introduction.....	33
2.2 Experimental.....	35
2.2.1 Apparatus.....	35
2.2.2 Reagents.....	37
2.2.3 Derivatization reaction.....	37
2.2.4 CE parameters.....	38
2.2.5 Measurement of EOF.....	38
2.3 Results and discussion.....	39
2.3.1 CE separation parameters.....	39
2.3.2 Optimization of the derivatization reaction.....	45

2.2.3 High-salt stacking.....	48
2.3.3.1 Salt concentration.....	49
2.3.3.2 Dilution ratio.....	51
2.3.4 Calibration, detection limit and reproducibility.....	53
2.4 Conclusions.....	53
2.5 References.....	55

Chapter 3. Determination of Glyphosate Using an Off-Line Ion-Exchanger Resin Preconcentration Tip and Laser-Induced Fluorescence Detection

3.1 Introduction.....	58
3.2 Experimental.....	60
3.2.1 Reagents and Materials.....	60
3.2.2 Analysis Procedures.....	62
3.2.2.1 Preconcentration.....	63
3.2.2.2 Derivatization and fluorescence labeling.....	63
3.2.2.3 MEKC separation.....	63
3.2.2.4 Analysis of real samples.....	65
3.3 Results and discussion.....	65
3.3.1 Derivatization and fluorescent labeling.....	65
3.3.2 Preconcentration on AG1-X8 resin tip.....	75
3.3.3 Quantitative analysis of standard glyphosate solutions.....	76
3.3.4 Clean-up of real samples.....	79
3.4 Conclusions.....	81
3.5 References.....	84

Chapter 4. A Capillary-Tip Chromatographic Beads-Packed Monolithic Preconcentrator – Fabrication, Characterization and Application in Determination of Herbicides Using Capillary Electrophoresis – Laser Induced Fluorescence Detection

4.1 Introduction.....	89
4.2 Experimental.....	91
4.2.1 Reagents and Materials.....	92
4.2.2 Fabrication of PRP-1 packed monolith.....	92
4.2.3 SEM imaging.....	94
4.2.4 Fluorescence derivatization.....	95

4.2.5 CE separation.....	95
4.3 Results and Discussion.....	97
4.3.1 Fabrication and pre-conditioning of the PRP-1 monolith tips.....	97
4.3.2 Operation of the Pre-concentration Tip.....	106
4.3.2.1 Charge state of analytes.....	108
4.3.2.2 Effect of sample solution pH.....	110
4.3.2.3 Effect of salt in sample solutions.....	113
4.4 Quantitative studies.....	116
4.5 Conclusions and future work.....	119
4.6 References.....	121

Chapter 5. Capillary Gel Electrophoresis with Laser Induced Fluorescence and Detergent Differential Fractionation for Characterization of Cancer Cell Proteins

5.1 Introduction.....	124
5.2 Experimental.....	126
5.2.1 Apparatus.....	126
5.2.2 Reagents.....	127
5.2.3 Separation of model proteins.....	128
5.2.4 Differential detergent fractionation of HT29 cancer cells.....	128
5.3 Results and discussion.....	129
5.3.1 Separation of standard proteins.....	130
5.3.2 Characterization of HT29 cell proteins by CGE-LIF with DDF.....	136
5.4 Conclusions	142
5.5 References	143

Chapter 6. Summary and Future Work

6.1 Summary.....	146
6.2 Future work.....	148
6.2.1 Studies on the formation of the encapsulating shell.....	148
6.2.2 Other recognizing/preconcentration mechanisms.....	149
6.2.3 Applications in MEKC mode.....	150
6.2.4 Other monolith materials and CE separation channel layout.....	151

6.3 References.....153

Appendix

Curriculum Vitae.....155

List of Figures

Figure 1.1	Basic CE instrumentation.....	3
Figure 1.2	CZE separation mechanism.....	7
Figure 1.3	MEKC separation mechanism.....	11
Figure 1.4	CGE separation mechanism.....	13
Figure 1.5	Schematic diagrams of field-amplified sample stacking (FASS) in CZE.....	16
Figure 1.6	Schematic diagram of dynamic pH-junction stacking in CZE.....	17
Figure 1.7	Schematic diagrams of high-salt stacking for neutral analytes in MEKC.....	18
Figure 1.8	Schematic diagrams of sweeping for neutral analytes in MEKC.....	20
Figure 1.9	Schematic representation of SPE device on capillary tip.....	23
Figure 1.10	Online SPE preconcentration procedures.....	24
Figure 1.11	Fabrication reactions for alkoxide-based sol-gel silica monoliths.....	27
Figure 2.1	Structures of panacyl bromide, alkylphosphonic acids and the fluorescent derivatization product.....	36
Figure 2.2	Sodium cholate and its aggregate structures.....	41
Figure 2.3	Effect of cholate concentration on the separation.....	42
Figure 2.4	Effect of acetonitrile on the separation.....	44
Figure 2.5	Effect of dye concentration on the fluorescence response.....	46
Figure 2.6	Effect of <i>N, N</i> -diisopropylethylamine concentration on the fluorescence response.....	47
Figure 2.7	Effect of NaCl concentration in dilution buffer on the resolution.....	50
Figure 2.8	High-salt stacking performance.....	52
Figure 2.9	MPA/EPA/PPA Calibration curves.....	54

Figure 3.1	Oxidative conversion of glyphosate to glycine and subsequent fluorescence labeling reactions using OPA-ME or NDA-CN ⁻	62
Figure 3.2	Clean-up cartridge beside a Canadian one dollar coin and resin-packed pre-concentration tip.....	64
Figure 3.3	Effect of calcium hypochlorite concentration on glyphosate peak area.....	67
Figure 3.4	Effect of NDA derivatization reaction time at 60°C on glyphosate peak area.....	68
Figure 3.5	Effect of NDA concentration on glycine labeling.....	72
Figure 3.6	Effect of NaCN concentration on glycine labeling.....	73
Figure 3.7	Typical electropherogram of side-reaction products in blank reaction.....	74
Figure 3.8	Electropherogram of 50 ml of 1 nM glyphosate standard.....	77
Figure 3.9	Calibration curve of glyphosate standards.....	78
Figure 3.10	Calibration curve of spiked river water sample... ..	82
Figure 3.11	Lifetime of a Purolite mixed resin clean-up cartridge.....	83
Figure 4.1	Molecular structures of test analytes and derivatization products.....	91
Figure 4.2	PRP-1 packed monolith tip attached to the inlet of bare capillary.....	94
Figure 4.3	PRP-1 beads.....	98
Figure 4.4	Sol-gel monolithic structure (without packed PRP-1 beads).....	99
Figure 4.5	PRP-1-packed monolith before pre-conditioning.....	101
Figure 4.6	PRP-1-packed monolith, after pre-conditioning with 25 mM borate solution at 20 psi for 60 min.....	104
Figure 4.7	Effect of pre-conditioning time.....	105
Figure 4.8	RP-1-packed monolith, after pre-conditioning with 15 mM pH 4.8 acetate buffer at 20 psi for 60 min.....	107
Figure 4.9	Pre-concentration effect by changing pH and salt concentration.....	112

Figure 4.10 Effect of sample injection time at 20 psi in the absence of 100 mM NaCl.....	113
Figure 4.11 Effect of sample injection time at 20 psi in the presence of 100 mM NaCl.....	115
Figure 4.12 Performance comparisons.....	117
Figure 4.13 AMPR calibration curve.....	118
Figure 4.14 GLUF calibration curve.....	119
Figure 5.1 Molecular structure of FQ and its fluorescence labeling reaction.....	130
Figure 5.2 Effect of PEO concentration on the separation of five model proteins.....	131
Figure 5.3 Effect of electric field on the separation of standard proteins.....	133
Figure 5.4 Plot of migration time of standard protein vs. log (MW).....	135
Figure 5.5 CGE-LIF electropherogram of the cytosolic fraction of HT29 cell extract.....	137
Figure 5.6 CGE-LIF electropherogram of the membrane/organelle fraction of HT29 cell extract.....	139
Figure 5.7 CGE-LIF electropherogram of the nuclear fraction of HT29 cell extract...	140
Figure 5.8 CGE-LIF electropherogram of the cytoskeletal fraction of HT29 cell extract.....	141
Figure 6.1 A potential microfluidic format with LIF detection for SPE preconcentration and separation performed on different channels.....	152

List of Tables

Table 3.1	Effect of elution flow rate on the recovery of glyphosate standard.....	76
Table 5.1	CGE-LIF for separation of five standard proteins.....	134

List of Symbols and Abbreviations

Symbol	Parameter
α	separation factor
ε	dielectric constant
ε	molar absorptivity of the analyte,
η	viscosity coefficient
μ_a	apparent mobility
μ_e	electrophoretic mobility
μ_{EOF}	EOF mobility
$\Delta \mu$	mobility difference between two analytes
$\overline{\mu_a}$	mean apparent mobility of the analytes
ζ	zeta potential
σ^2_{Diff}	variance of peak width due to longitudinal diffusion
$\sum \sigma^2$	total variance of all bandbroadening factors
A	absorbance
b	length of light path
c	molar concentration of the analyte
d	inside diameter of the capillary
D	diffusion coefficient of the analyte
I	intensity of transmitted light
I_0	intensity of the incident light
k'	retention factor

L_d	capillary length from the inlet to the detection window
L_t	total length of capillary
N	efficiency, expressed in number of theoretical plates
ΔP	pressure difference across the capillary
q	ion charge
r	hydrated ion radius
R	resolution
t_0	migration time of the unretained solute
t_m	migration time of the analyte
t_{mc}	migration time of the micelles
t_r	retention time of the analyte
V	voltage applied across the total capillary length
AMPA	aminomethylphosphonic acid
AMPR	ampropylfos (3-aminopropylphosphonic acid)
APS	ammonium persulfate
BSA	bovine serum albumin
CE	capillary electrophoresis
CEC	capillary electrochromatography
CGE	capillary gel electrophoresis
CHES	2-(cyclohexylamino)-ethanesulphonic acid
CIEF	capillary isoelectric focusing
CITP	capillary isotachophoresis
CMC	critical micellar concentration

CZE	capillary zone electrophoresis
DDF	detergent differential fractionation
DMF	<i>N, N</i> -dimethylformamide
DOC	sodium deoxycholate
ELISA	enzyme-linked immunosorbent assay
ELSD	evaporative light scattering detection
EMPA	ethylmethylphosphonate
EOF	electroosmotic flow
ESI	electrospray ionization
FPD	flame photometric detection
FQ	3-(2-furoyl) quinoline-2-carboxaldehyde
GC	gas chromatography
GLUF	glufosinate
GLYP	glyphosate
HEPES	4-(2-hydroxyethyl)-1-piperazineethanesulfonic acid
HPLC	high performance liquid chromatography
IMPA	isopropylmethylphosphonate
LIF	laser-induced fluorescence
LOD	limit of detection
LPA	linear polyacrylamide
MAPS	γ -methacryloxypropyltrimethoxysilane
ME	2-mecaptoethanol
MEKC	micellar electrokinetic chromatography

MIP	molecularly imprinted polymer
MPA	methylphosphonic acid
mPC	membrane preconcentration
MS	mass spectrometry
NDA	naphthalene-2, 3-dicarboxaldehyde
ODS	octadecylsilane
OPA	<i>o</i> -phthalaldehyde
PAGE	polyacrylamide gel electrophoresis
PEG	poly (ethylene glycol)
PEO	polyethylene oxide
PIPES	piperazine- <i>N,N'</i> -bis(2-ethanesulfonic acid)
PMPA	pinacolylmethylphosphonate
PMSF	phenylmethylsulfonyl fluoride
PPA	propyl phosphonic acid
RSD	relative standard deviation
SDS	sodium dodecyl sulphate
SEM	scanning electron microscope
SPE	solid-phase extraction
TAPS	{[(2-hydroxymethyl)ethyl]-amino}-l-propanesulphonic acid
TEMED	<i>N, N, N', N'</i> -tetramethylethylenediamine
TEOS	tetraethyl ethylsilicate
TMOS	tetramethyl ethylsilicate
Tris	(hydroxymethyl) aminomethane

Chapter 1. Introduction

1.1 Principles of capillary electrophoresis

1.1.1 History

Electrophoresis, as a physical phenomenon, was reported as early as the late 1800s. For example, in 1886 Lodge reported H^+ migration in a U tube of phenolphthalein “jelly”¹. Since then, fundamental studies have been conducted for the development of a separation technique based on the differential migration of charged analytes in an electric field. Due to the major technique problem encountered in free solution - convective mixing - electrophoresis has been practiced for a long time in the slab gel format, in which stabilizing media such as acrylamide, agar or cellulose powder, is added. Also, to reduce thermal convection, the applied voltage had to be limited to several hundreds of volts. This limited the application of electrophoresis to macromolecules with low diffusion coefficients. Today, slab gel electrophoresis is still widely used in biochemical laboratories for the separation of macromolecules such as proteins and nucleic acids. In particular, two-dimensional polyacrylamide gel electrophoresis (2-D PAGE) can provide simple, inexpensive but powerful separation for complex matrices.

An alternate approach is to run electrophoresis in a capillary tube of small internal diameter. The capillary can dissipate joule heat much better than slab gel format and thus the applied voltage can be increased up to 30 kilovolts. Fast and high-performance separation is therefore possible. The experiments by Hjerten *et al.* with 3 mm i.d tubes in 1967 are commonly acknowledged as the first milestone in capillary electrophoresis (CE) history². The early days of CE were predominated by capillary zone electrophoresis

(CZE) and only ions can be separated. In 1984 Terabe and coworkers set another milestone in CE history by introducing micellar electrokinetic chromatography (MEKC)³. The analytes are no longer limited to the charged solutes because neutral analytes can be separated based on the difference in the analyte's affinity for the micelles. The last two decades of the 20th century have witnessed the explosive development of CE, including fundamental theories, instrumentation and applications^{1, 4-6}. The great success of CE in the Human Genome project made CE among the major separation techniques^{7, 8}.

1.1.2 Basic Instrumentation

Nowadays the commercial CE instruments consist of the following key components, as shown in Figure 1.1: (a) a bare silica capillary with uniform i.d of 10 ~100 μm and o.d of typically 360 μm . An air or coolant thermostating system is usually utilized to facilitate joule heat dissipation. (b) CE running buffer in the inlet and outlet buffer vials and also filling the capillary. (c) a pressure-driven system used to inject sample solution hydrodynamically and rinsing capillary between runs. (d) a high voltage source providing up to 30 kV DC voltage. (e) a detector such as ultraviolet-visible light spectrometry (UV) or diode array, mass spectrometry, laser-induced fluorescence (LIF) or electrochemical detector. More details will be discussed in Section 1.1.7. (f) control and data process devices, usually coming as a computer and specially-designed software.

The CE process can be briefly described as follows: A capillary is filled with a suitable buffer solution and both ends are immersed in the buffer vials. A short plug of sample solution is introduced into the capillary by voltage or pressure. After the inlet tip of capillary goes back to inlet buffer vial, high voltage is applied across the capillary.

Differential migration of analytes occurs. Detection is performed either on a transparent detection window several centimetres away from capillary outlet tip (as done in most UV and some LIF detection, shown in Figure 1.1) or at outlet-tip (as done in sheath-flow LIF detection and electrochemical detection) or connected to other post-column detectors (such as a mass spectrometer).

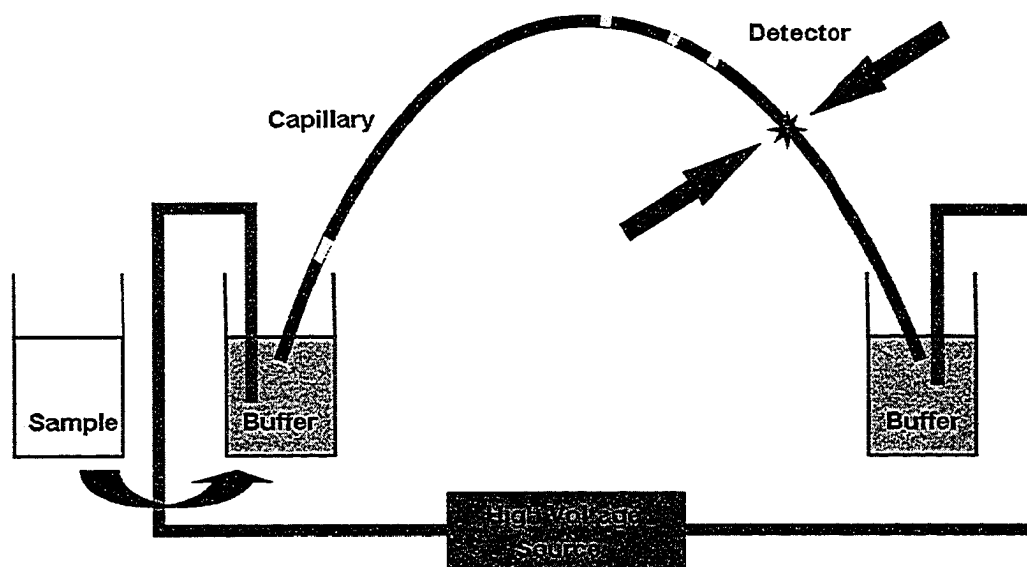


Figure 1.1 Basic CE instrumentation

1.1.3 Electroosmotic flow (EOF)

Electroosmotic flow (EOF) is the bulk flow of the CE running buffer in a capillary under an applied electric field. It is the major driving force in capillary. It results from the surface charge on the inner wall of capillary. Fused silica, for example, has weakly acidic silanol groups (-SiOH) with pKa of ~ 5.3 ⁹. If the CE running buffer is at pH 2 or

above, which is the case for most CE experiments, the inner wall of capillary is negatively charged and thus a negative plane is formed on capillary wall. To maintain the charge balance, cations in running buffer build up near the capillary wall to form a positively charged plane. Thus an electric double layer appears. A negative potential occurs between the double layers and decreases roughly linearly towards the bulk solution. Beyond the double layers, the diffusive layer of hydrated cations extends toward the bulk solution and thus the potential continues to decrease exponentially to zero. The potential at the plane of shear located slightly beyond the double layer is referred to as the zeta potential (ζ). Upon application of voltage, the hydrated cations in diffusive layer migrate toward the cathode and thus carry the bulk solution in the same direction. Since such driving force is uniform across the capillary, the flow profile is flat, unlike the parabolic profile in a pressure-driven system.

The EOF mobility (μ_{EOF}) is related to zeta potential by the Smoluchowski equation:

$$\mu_{EOF} = -\frac{\varepsilon \zeta}{\eta} \quad (\text{Eqn 1.1})$$

where ε is the dielectric constant and η is the viscosity coefficient of CE running buffer.

The zeta potential (ζ) is a function of the surface charge density on the capillary wall. Any experimental variable that changes the surface charge density can be used to adjust the zeta potential and thus the EOF. This can be accomplished by: changing the buffer pH or ionic strength; adding an organic solvent modifier; or using surfactant semi-permanent coatings /covalent permanent coatings to shield or alter the surface charge. The EOF may also be adjusted by varying the viscosity (η), for instance by changing the temperature or by adding organic solvents).

1.1.4 Electrophoretic mobility

When a charged particle, which may be an ion or even charged virus, is present in an electric field, it will migrate depending on its charge state. The steady state of migration is the result of the counterbalance of electric force and friction force. The mobility of steady-state migration is approximated from Debye-Huckel-Henry theory⁴:

$$\mu_e = \frac{q}{6\pi\eta r} \quad (\text{Eqn 1.2})$$

where μ_e is the ion electrophoretic mobility, q is the ion charge, and r is the hydrated ion radius. From the above equation, one can see that ions are separated in CZE roughly according to their charge-to-size ratios. For weak acid /base analytes, the change in buffer pH will lead to the change in charge (q) of the analytes¹⁰. This can be used to accelerate /decelerate the motion of charged analytes at the boundary of discontinuous buffer zones to stack such analytes (as discussed in Section 1.2.2).

1.1.5 Major modes of separation

Capillary zone electrophoresis (CZE) is the most commonly used CE operation mode. Micellar electrokinetic chromatography (MEKC) ranks the second, although there are many other modes of operation such as capillary gel electrophoresis (CGE), capillary isoelectric focusing (CIEF) and capillary isotachopheresis (CITP). In this thesis, CZE, MEKC and CGE were used and thus their separation mechanisms will be discussed here.

1.1.5.1 Capillary zone electrophoresis (CZE)

As mentioned above, CZE has been the predominant operation mode for CE. In CZE the apparent mobility (μ_a) of an ion is the summation of the ion's electrophoretic mobility (μ_e) and the EOF mobility (μ_{EOF}), as illustrated in Figure 1.2:

$$\mu_a = \mu_e + \mu_{EOF} \quad (\text{Eqn 1.3})$$

The apparent mobility is experimentally determined by:

$$\mu_a = \frac{L_t L_d}{t_m V} \quad (\text{Eqn 1.4})$$

where L_t is the total length of capillary, L_d is the capillary length from the inlet to the detection window, t_m is the migration time of the analyte, and V is the voltage applied across the total capillary length. A special case is when the solute is neutral (for example, mesityl oxide) and thus has no μ_e . In this case, μ_a equals μ_{EOF} .

Normally EOF is stronger than the electrophoretic mobility, and thus all solutes - cations, anions and neutral solutes - migrate in the same direction as EOF, i.e. from anode to cathode. The EOF is the major driving force. However, the electrophoretic migration velocity depends on the charge of ions. Cations intrinsically migrate with the EOF while anions migrate against the EOF. As a result, in CZE cations always come out more quickly than anions. For ions of same charge sign, the slight difference in charge /size ratio can still lead to separation. Neutral solutes have no electrophoretic mobility and thus all neutral compounds move at the same velocity as the EOF and can not be separated by CZE. However, neutral solutes such as mesityl oxide can be used to measure the EOF.

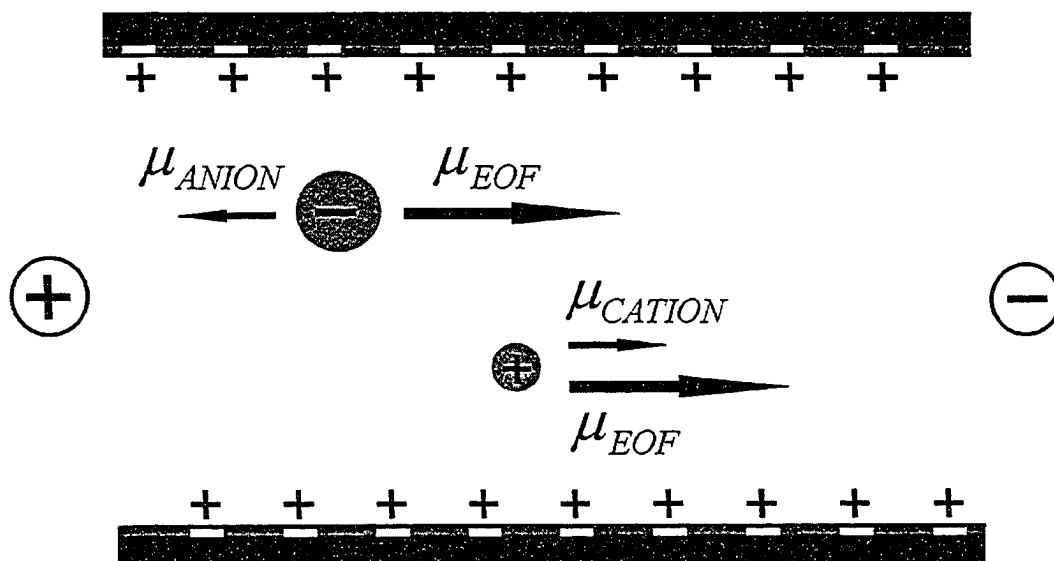


Figure 1.2 CZE separation mechanism.

Similar to chromatography, peak broadening is also observed in CE. This must be well studied and controlled to achieve optimal resolution. In CZE, the major bandbroadening factor is longitudinal diffusion, which refers to the axial diffusive spreading of the solutes in the sample zone into the bulk running buffer solution. The variance of peak width due to longitudinal diffusion is given by:

$$\sigma_{Diff}^2 = 2 D t_m \quad (\text{Eqn 1.5})$$

where D is the diffusion coefficient of the analyte and t_m is the migration time. To minimize the longitudinal diffusion term, a high voltage is essential to speed up the separation so that the analytes have less time to diffuse.

Radial diffusion is usually negligible due to the plug flow profile of the EOF in CE (Section 1.1.3). Convection bandbroadening is also unimportant because the small i.d

of capillary limits the convection. However, there are some other sources of bandbroadening which require attention in practical CE experiments:

- (a) Joule heating. The passage of electric current results in the generation of heat, which must be dissipated effectively by the air or coolant thermostating system. The excessive generation of heat is problematic and can cause temperature gradients which lead to local changes in viscosity and thus zone broadening. An Ohm's law plot can be used to check if Joule heating is a problem. To generate an Ohm's plot the current is monitored as different voltages are applied across a capillary filled with the CE running buffer. The loss of linearity in the current vs. voltage plot at higher voltages indicates that the generation of Joule heat has exceeded the thermostating capacity. To control Joule heating, voltage and/or buffer ionic strength should be decreased. Normally the power must be kept below 1 Watt per meter length of capillary.
- (b) Solute-wall interaction. Cationic analytes can adsorb onto the negatively charged capillary wall which will lead to peak tailing and broadening. This is especially evident for proteins and peptides. One way to minimize such adsorption is to operate at the extremes of pH to adjust charge state of analytes or capillary wall to decrease the charge interaction. Another approach is to coat the capillary wall permanently or semi-permanently and thus shield the charges on capillary wall.

The efficiency, expressed in number of theoretical plates, N , is given by:

$$N = \frac{L_d^2}{\sum \sigma^2} \quad (\text{Eqn 1.6})$$

where $\sum \sigma^2$ represents the total variance of all bandbroadening factors (*i.e.*, longitudinal diffusion, Joule heating, adsorption, *etc.*).

In chromatography and other separation techniques, the degree of peak separation is measured by the resolution (R). The resolution in CZE is given by:

$$R = \frac{1}{4} \sqrt{N} \left(\frac{\Delta\mu}{\mu_a} \right) \quad (\text{Eqn 1.7})$$

where N is the efficiency, $\Delta\mu$ is the mobility difference between two analytes and $\overline{\mu_a}$ is the mean apparent mobility of the analytes. This equation shows that the resolution is the combined effect of two factors: efficiency and selectivity. To achieve better resolution, it is desirable to improve the efficiency (N) as discussed above and increase the mobility difference ($\Delta\mu$) by, for example, changing the buffer pH or adding additives such as cyclodextrins or micelles.

1.1.5.2 Micellar electrokinetic chromatography (MEKC)

In MEKC, surfactant is added into running buffer at a concentration above its critical micellar concentration (CMC), such that the surfactant molecules aggregate to form micelles. Sodium dodecyl sulphate (SDS) is used in most MEKC experiments. It has a negatively charged hydrophilic head group and C12 hydrophobic tail. Above the CMC, SDS micelles have a spherical structure with the hydrophilic head groups facing the bulk solution and hydrophobic tails oriented towards the micelle core, as shown in Figure 1.3. Neutral analytes can partition into the core and thus migrate with the micelle, or come out of micelles and thus move with EOF. There is an equilibrium between the

“in” and “out” states. Note that the SDS micelles are negatively charged and thus migrate more slowly than the EOF. The higher affinity the analyte has for the SDS micelles, the lower the migration velocity. Analytes with differing affinity for the SDS micelles are thus separated.

Unlike CZE, MEKC has a “migration time window” that is defined by the migration times of the micelles (t_{mc}) and an unretained solute (t_0). A completely unretained neutral solute with no affinity for the micelles will always stay outside micelles and migrate with the same velocity as the EOF (t_0). On the other hand, a solute with extremely strong affinity for the micelles will always stay inside the micelle and co-elute with the micelles at t_{mc} . Thus all neutral solutes will elute within this period of time (t_0 to t_{mc}). A wider migration time window would increase the peak capacity and enhance resolution. This can be accomplished by selecting micelles with high mobility against the EOF, or decreasing EOF by the addition of organic solvents (as discussed in Chapter 2).

MEKC is the hybrid of chromatography and electrophoresis and the partitioning of solutes in and out of micelles is actually a chromatographic process, but the pseudo-stationary phase, i.e., the micelles are moving. To reflect this fact, the retention factor k' must carry a correction term:

$$k' = \frac{t_r - t_0}{t_0 \left(1 - \frac{t_r}{t_{mc}}\right)} \quad (\text{Eqn 1.8})$$

where t_r is the retention time of the analyte, t_0 is the retention time of a completely unretained solute, and t_{mc} is the micelle migration time.

Correspondingly the resolution equation in MEKC is given by ⁶:

$$R = \left(\frac{\sqrt{N}}{4}\right) \left(\frac{\alpha-1}{\alpha}\right) \left(\frac{k_2'}{k_2'+1}\right) \left(\frac{1-t_0}{1+\left(\frac{t_0}{t_{mc}}\right)k_1'}\right) \quad (\text{Eqn 1.9})$$

where N is the number of theoretical plates, α is the separation factor defined as $\left(\frac{k_2'}{k_1'}\right)$.

This equation illustrates that resolution is improved by extending the elution time window or by optimizing efficiency (N) and the separation factor (α). The separation factor can be easily optimized by varying the concentration and type of micelles or by adding buffer additives such as cyclodextrins.

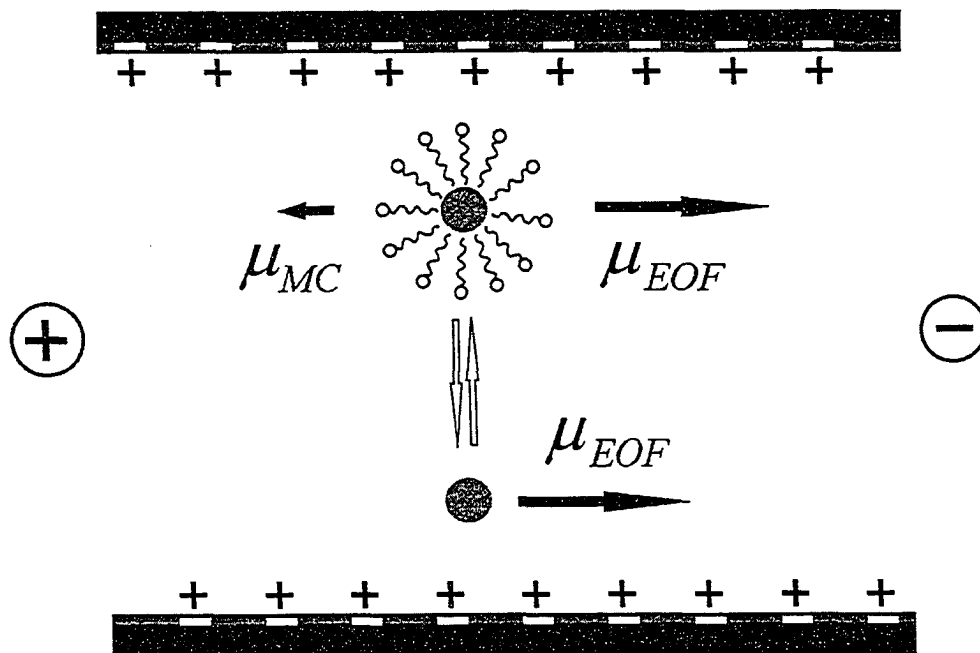


Figure 1.3 MEKC separation mechanism

1.1.5.3 Capillary gel electrophoresis (CGE)

Capillary gel electrophoresis (CGE) is actually the capillary version of traditional slab gel electrophoresis but is much faster due to the use of 10 ~ 100 times higher electric fields. CGE is used only for size-based separations of macromolecules such as proteins and nucleic acids. The key thing in CGE is to fabricate a polymer network with suitable pore size for “sieving” the analytes. This can be done using either cross-linked polymers or linear polymers. The former is performed by in-situ covalently cross-linking polyacrylamide to form a rigid sieving network. This approach has less flexibility and limited lifetime due to bubble formation and polymer degradation. The later is more flexible by adding a linear polyacrylamide, hydroxyalkyl cellulose, polyethylene oxide or other linear polymers to running buffer to make a polymer solution. If the linear polymer is above its entanglement threshold concentration, it forms a dynamic entangled mesh structure with “transient pore” size depending on the type and concentration of linear polymer. Size-based mechanism means larger analytes are more strongly hindered than smaller ones when migrating through the polymer network (Figure 1.4).

In CGE, electric injection is usually preferred since the viscous linear polymer solution or rigid cross-linked polymer network makes it difficult to inject sample hydrodynamically. The column efficiency is satisfactory primarily because (a) the macromolecules have lower diffusion coefficients and (b) high viscosity of polymer solution decreases the diffusion bandbroadening.

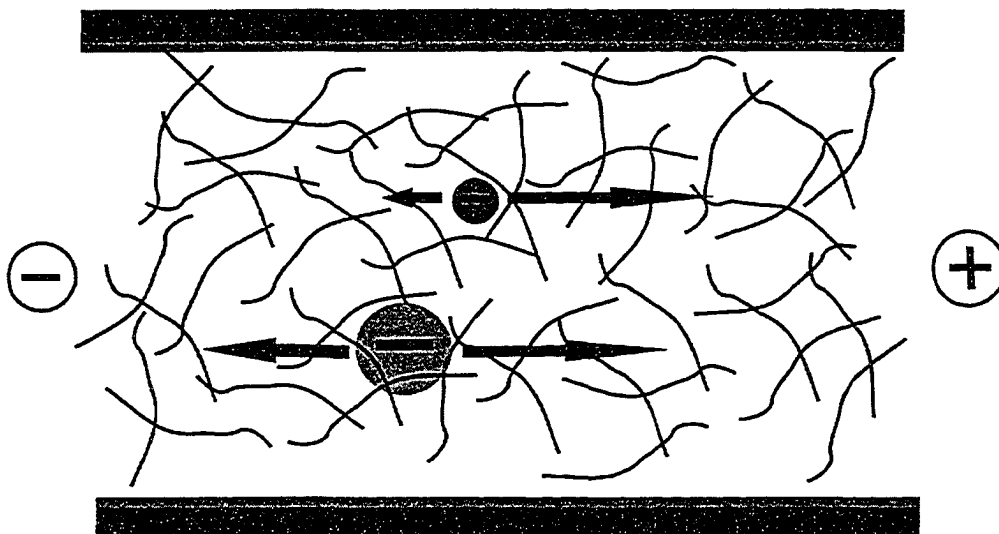


Figure 1.4 CGE separation mechanism. The arrows pointing to the right represent the electrophoretic forces that are equal for analytes with the same charge-to-size ratio (e.g., SDS-denatured proteins). Note that normally the EOF is suppressed in CGE by capillary coatings. The arrows pointing to the left represent the resistance that the analytes experience when they go through the gel network. Large analytes experience greater resistance and thus migrate more slowly.

1.1.6 Detection

Almost all commercial CE instruments are equipped with a UV absorbance detector because of its low cost and wide range of applicability. Many analytes can absorb light to in the UV or visible region. According to Beer's law, absorbance (A) is given by:

$$A = \log \frac{I_0}{I} = \epsilon b c \quad (\text{Eqn 1.10})$$

where I_0 is the intensity of the incident light, I is the intensity of transmitted light, ϵ is the molar absorptivity of the analyte, b is the length of light path, and c is the molar concentration of the analyte. One can see clearly that the extremely short light path is the bottleneck for highly sensitive detection. Typically detection limits for UV absorbance are in the micromolar range. To overcome this problem, many online preconcentration techniques have been developed. These will be discussed in Sections 1.2 and 1.3.

Alternately, fluorescence detection can provide much more sensitive detection than UV absorbance, especially when a laser is used as the excitation light source. Laser-induced fluorescence (LIF) can be performed on-column as shown in Figure 1.1, or off-column using a sheath-flow cuvette¹¹. The sheath-flow cuvette was first introduced by Dovichi and coworkers. Its advantage is that the laser beam is focused on the sample stream immediately after capillary tip, rather than on capillary. Light scattering is thus minimized and detection limits in the nanomolar to picomolar range can be achieved^{1,4}.

Ar-ion, HeCd and HeNe lasers are the most commonly used lasers in CE-LIF and many fluorescence labeling reagents have been synthesized specifically to match the excitation wavelengths of these lasers. However, the rapid development of miniaturized instrument makes these bulky lasers inappropriate to couple to miniaturized CE devices. Diode lasers are more promising in this respect. Their lasing mechanism is based on the junction between positively-doped (p-type) and negatively doped (n-type) semiconductors constructed from the same material. Upon application of voltage across the p-n junction, excess electrons flow from the n-type to the p-type region, generating a population inversion and thus a coherent monochromatic light is emitted. Compared with the above conventional lasers, diode lasers are relatively inexpensive, need no

maintenance, and have longer lifetimes (up to 50,000 h) and higher output stability (0.01%)^{12, 13}. Most of the work in this thesis was done using an InGaN-based violet diode laser at 415 nm.

1.2 Electrophoresis-based online preconcentration

Given the poor detection sensitivity of the standard UV absorbance detection in CE, many online preconcentration techniques have been proposed to enrich analytes of interest from a large volume of dilute sample. This can be done based on the change in migration velocity occurring when the analytes cross the boundary of discontinuous buffer zones. Only some of the more frequently used techniques in CZE and MEKC are discussed here. These include field-amplified sample stacking (FASS), dynamic pH-junction stacking, high-salt stacking and sweeping.

1.2.1 Field-amplified sample stacking (FASS)

Field-amplified sample stacking (FASS) is the simplest stacking technique for ionic analytes. The stacking mechanism is shown in Figure 1.5. Briefly, the sample solution is prepared in a low-conductivity buffer, usually a 1/100 ~ 1/1000 diluted running buffer, and then injected into a capillary filled with a high-conductivity running buffer (Figure 1.5A). Upon application of a positive voltage, the cationic and anionic analytes migrate towards the cathode-side and anode-side of the sample zone – running buffer zone boundaries, respectively (Figure 1.5B). Note that the EOF is strong enough to carry all analytes towards the detection window at the cathode end of the capillary. Since the sample zone has a lower conductivity and thus higher electric field, the migration of the

ionic analytes slows at these boundaries. As a result, cationic and anionic analytes will be focused near the cathode-side and anode-side of the sample zone – running buffer zone boundaries, respectively (Figure 1.5C). Normally, the sample can fill 10 ~ 30% of the capillary length so long as enough length is left for the subsequent CZE separation. Concentration factors of 10 ~ 10,000 fold have been reported¹⁴⁻¹⁹.

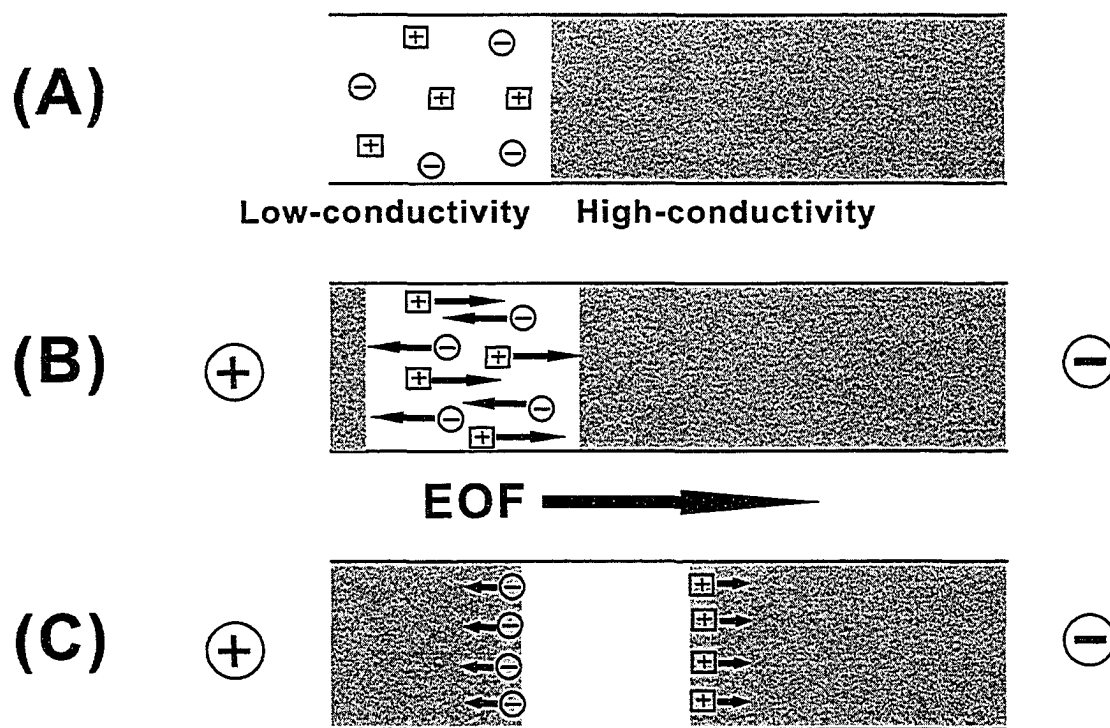


Figure 1.5 Schematic diagrams of Field-amplified sample stacking (FASS) in CZE

1.2.2 Dynamic pH-junction stacking

A change in electric field strength at the buffer zone boundaries is not the only reason to cause migration to slow down. This can also be done by varying the intrinsic electrophoretic mobility of the analytes via a change in pH. Dynamic pH-junction

stacking is suitable for zwitterionic and weakly acidic compounds²⁰. For instance, for a weakly acidic compound, the analytes are dissolved in a low pH buffer so that they are neutral species. This sample solution is injected into a capillary filled with a higher pH running buffer. After application of voltage, in sample zone, the neutral analyte (denoted by HA in Figure 1.6) migrate with EOF. When the analyte crosses the low-high pH boundary, HA is deprotonated to form A⁻ and thus obtains an intrinsic electrophoretic mobility against EOF. As a result, the migration of A⁻ becomes slower and thus focuses near the pH-junction. The focusing efficiency is determined by the pKa values of analytes, pH and concentrations of both zones²⁰. The reported concentration ratios range from 30 to 1700²¹⁻²⁴.

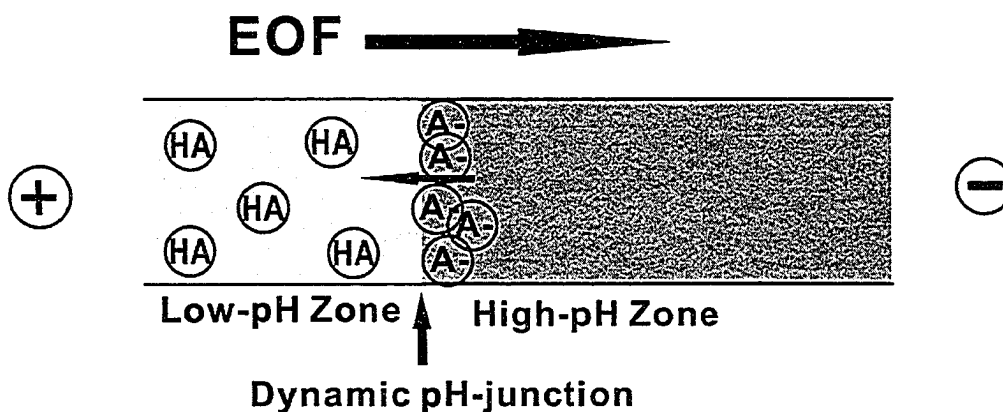


Figure 1.6 Schematic diagram of dynamic pH-junction stacking in CZE

1.2.3 High-salt stacking

High-salt stacking was proposed for online concentration of neutral analytes in MEKC by Landers and coworkers in 1999²⁵⁻²⁷. Again a discontinuous buffer system

plays an important role. The neutral analytes are dissolved in a buffer with added salt but no micelles. The MEKC running buffer has no added salt and thus lower conductivity than the sample solution (Figure 1.7A). As shown in Figure 1.7B, after the separation voltage is applied, the electrophoretic motion of the negatively charged micelles is slowed when they enter the high-salt sample zone due to the sudden decrease in electric field strength. The micelles thus accumulate near the cathode side of the high-salt sample zone which means a higher phase ratio of micellar phase at the sample - buffer boundary. The analytes in the sample zone then stack near the boundary due to their high affinity for the micelles (Figure 1.7C).

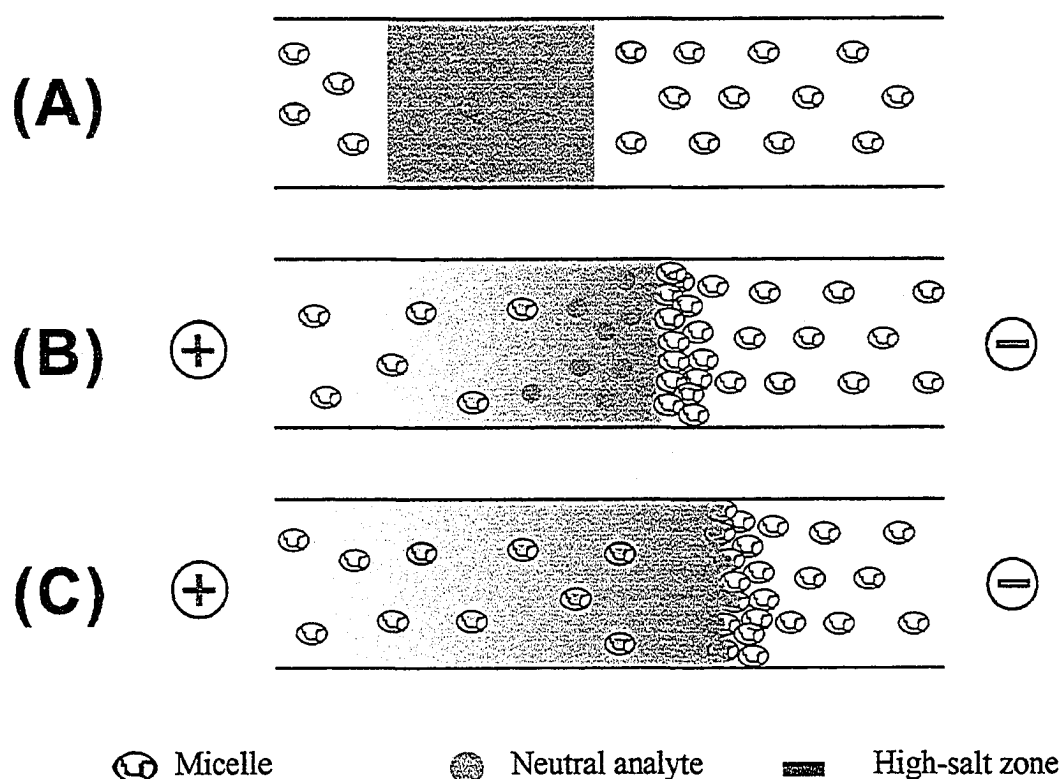


Figure 1.7 Schematic diagrams of high-salt stacking for neutral analytes in MEKC.

Based on Figure 3 from reference ²⁵.

Actually this type of stacking is achieved by first stacking negatively charged micelles using a mechanism similar to FASS and then extracting neutral analytes to a highly retentive micelle narrow-band. So the concentration ratio strongly depends on the affinity of analytes for the micelles. In Chapter 2, this technique has been successfully used to online preconcentrate fluorescent labeled products of three alkylphosphonic acids.

1.2.4 Sweeping

First introduced by Quirino and Terabe, sweeping is another great technique for online concentration in MEKC²⁸⁻³¹. Unlike high-salt stacking, there is no difference in conductivity between discontinuous zones. Instead, the sample solution has similar conductivity as the MEKC running buffer but no micelles (Figure 1.8A). When positive polarity is applied, the negatively charged micelles have an electrophoretic mobility against the EOF and thus enter the sample zone from the cathode side (Figure 1.8B). The neutral analytes originally migrate with the EOF in the sample zone. However, when the analytes come in contact with the micelles, they partition into the micelle, and obtain the same counter-EOF mobility as micelles. As a result, the apparent migration velocity of the analyte decreases. As more and more micelles enter the sample zone, the analytes are swept into a narrow band of analyte- micelle complex (Figure 1.8C). Similar to high-salt stacking, the enhancement factor strictly depends on the analyte affinity for the micelle phase. Detection sensitivity enhancement of 80 ~5000 fold have been reported^{28, 30, 32}. The recent development of combining sweeping and other stacking techniques already allows the online concentration of both neutral and charged analytes^{20, 29} and up to million fold enhancement can be achieved³³.

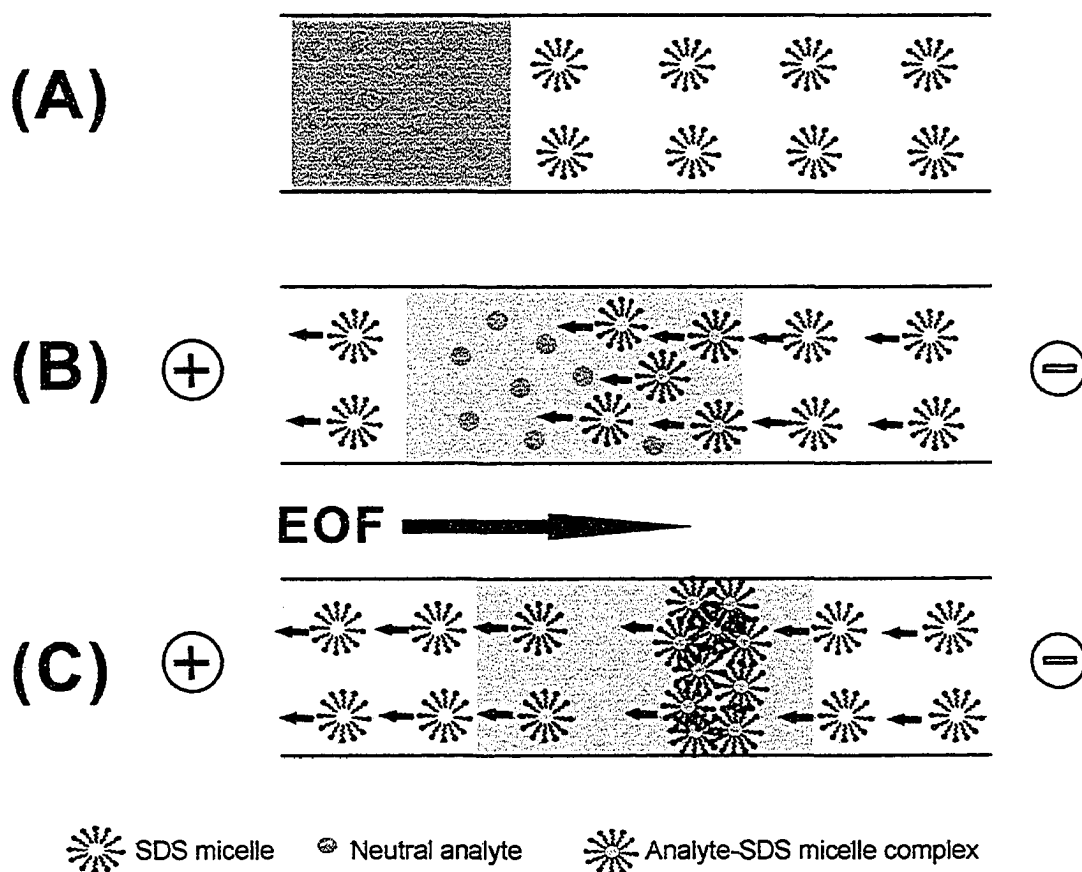


Figure 1.8 Schematic diagrams of sweeping for neutral analytes in MEKC

1.3 Solid phase extraction (SPE) – based online preconcentration

In stacking and sweeping techniques, no physical modification of the capillary is required. Only a discontinuous buffer system is needed to generate the acceleration or deceleration of the solute migration at the buffer zone boundaries. Another approach to preconcentrate sample is to extract the analytes of interest onto a solid phase from a large volume of dilute solution. If only the analyte of interest is retained on the solid phase, interfering compounds within complex matrices can simultaneously be removed. After the preconcentration is complete, the absorbed analytes can be eluted into a smaller amount of solution for subsequent analysis. This technique is called solid-phase

extraction (SPE)^{34,35} and can be done either off-line, as described in Chapter 3 or on-line as discussed in Chapter 4. However, online SPE preconcentration is preferred to reduce manual sample manipulation and obtain reproducible results. Thus, this approach will be introduced here.

1.3.1 Online SPE methods

The SPE methods reported so far can be grouped as either low-specificity or high-specificity preconcentration techniques according to their concentration mechanisms. The former includes hollow fibers^{36,37}, membrane preconcentration (mPC)³⁸⁻⁴⁰ and chromatography packings⁴¹⁻⁴³ and the latter uses immunoaffinity phases (such as antibodies)^{44,45} and molecularly imprinted polymers (MIP)^{46,47}.

Semi-permeable hollow fibers allow the free passage of water through the pores on the fiber wall, but restrict passage of large molecules such as peptides and proteins. Water is removed by evaporation, or Donnan effect which is accomplished by immersing the hollow fiber filled with dilute sample solution into a polymer solution, thus large molecules can be enriched by thousands folds. Hjerten and coworkers reported such an offline preconcentration method for 3000-fold enrichment of proteins³⁶. Hobo's group³⁷ designed an online hollow fiber preconcentration system by coupling a 2-mm long hollow fiber to the inlet of a capillary. They were able to enrich four basic proteins 1000-fold using their online system.

Conventional chromatography adsorbents can be packed into a miniaturized precolumn / SPE cartridge and placed at the capillary inlet⁴¹⁻⁴³, as shown in Figure 1.9. The SPE cartridge is rinsed with organic eluent and then CE running buffer to prepare it

for preconcentration (Figure 1.10A). Then a large volume of sample solution is introduced hydrodynamically into SPE cartridge (Figure 1.10B). The hydrophobic analytes are extracted onto the SPE packing. The excess sample solution in capillary is washed away by CE running buffer containing no organic solvent (Figure 1.10C). A small volume of organic eluent is injected to elute the preconcentrated analytes from SPR adsorbents (Figure 1.10D). Care should be taken because the introduction of organic solvent may change EOF and compromise the subsequent CE separation. Then the voltage is applied for the CE separation (Figure 1.10E). The capillary is then rinsed with organic solvent and CE running buffer to prepare the SPE column for another preconcentration (Figure 1.10A).

As stated above, the packing within the SPE column may be a conventional HPLC packing. For example, Petersson and co-workers used an on-capillary extractor packed with C₁₈-alkyl-diol silica to enrich terbutaline, a β -receptor agonist, by 7000-fold from plasma sample⁴³. Alternatively, immunoaffinity phases, such as antibodies specific to a particular analyte, can be covalently bonded to porous silica⁴⁴ or glass beads⁴⁵ and afford highly selective preconcentration. For example, Guzman coupled monovalent Fab antibody fragments to controlled-porous glass beads and packed these beads into an on-capillary concentrator. As low as 1 ng/ml of gonadotropin-releasing hormone in serum/urine samples were enriched and determined using this online immunoaffinity preconcentration CE system⁴⁵.

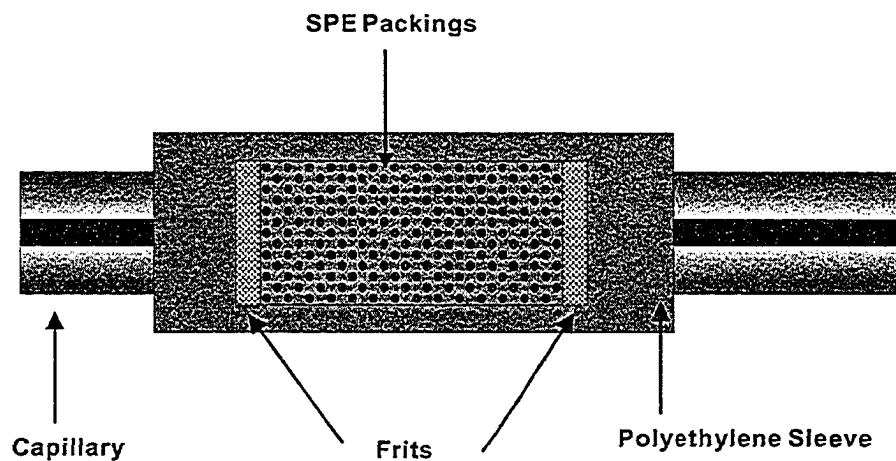


Figure 1.9 Schematic representation of SPE device on capillary tip. Redrawn from reference ⁴²

Coated or impregnated membranes can also be used for online preconcentration ³⁸. The polymeric membrane is modified with a chromatography stationary phase such as C2, C4, C8, C18, polystyrene divinylbenzene or ion exchanger capable of extracting solutes. Such membranes are then installed into a cartridge, usually a short Teflon tubing connecting inlet capillary and separation capillary. Compared with conventional bonded-phase adsorbents, membrane preconcentration (mPC) has a lower bed volume of absorptive phase and so less organic eluent is needed to remove concentrated analytes ³⁸. Rode *et al.* demonstrated that a C2 impregnated mPC cartridge allowed not only the enrichment of 15 proteins in aqueous humor but also the removal of unwanted matrix components ^{39,40}.

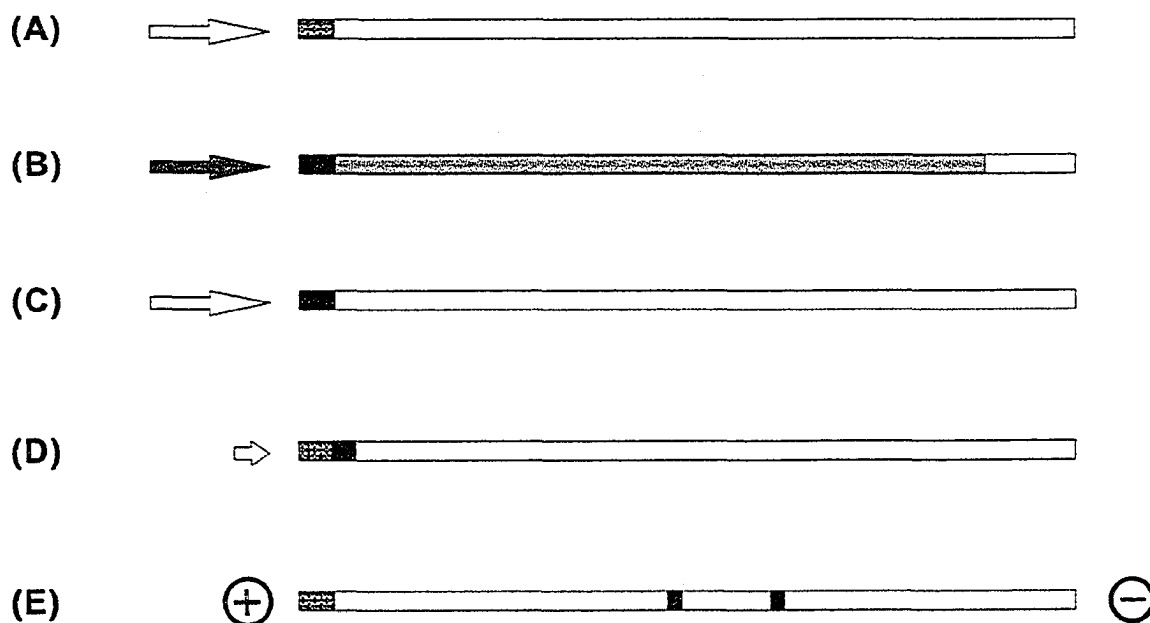


Figure 1.10 Online SPE preconcentration procedures. The grey segment on the lefthand end of the capillary is the online SPE column. The steps in online SPE preconcentration are: A) Column is rinsed with organic solvent and then equilibrated with the aqueous CE buffer. B) Sample solution (depicted in blue) is flushed through the capillary. Analyte is retained on the SPE column. C) The capillary is rinsed with CE buffer to remove the sample matrix. D) A small volume of organic solvent is introduced into the capillary to elute the analytes from the SPE column. E) Voltage is applied across the capillary to perform the electrophoretic separation.

Molecularly imprinted polymer (MIP) is a copolymer with artificial macromolecular receptors ⁴⁶. First, to prepare a MIP, functional and cross-linking monomers are copolymerized in the presence of a target analyte, which acts as an imprint or template molecule. The target analyte is complexed by functional groups in the

functional monomers and thus is immobilized within the highly cross-linked polymer. After removal of the target analyte by simple solvent extraction, binding sites are left with the specific size, shape and functional groups for the target analyte. In this way, a robust polymer can be prepared in the form of a bulky monolith or micrometer-sized particles for high-specific extraction. Recently Lai's group reported a MIP-based online preconcentration coupled to a microfluidic CE device for detection of ochratoxin A as low as 0.05 ppb ⁴⁷.

1.3.2 SPE phase immobilization techniques

Most of SPE adsorbents are in the physical form of particles, such as HPLC packings, antibody-coated glass beads, and some MIP particles. Usually frits such as shown in Figure 1.9 are necessary to retain these particulate packings in the capillary. However, the presence of the frits in the capillary causes problems related to mismatch in the EOF and thus the formation of bubbles ⁴⁸.

The monolith technique is a more reliable and promising immobilization method ⁴⁹. An organic polymer or silica rod with a porous structure can be fabricated in the capillary. SPE beads are then held in place within these pores. Alternatively, the monolith can be modified with retentive elements such as C18 phase ⁵⁰. The porous structure ensures high permeability and thus low resistance to flow. To eliminate the problem due to mismatched EOF, the monolith may be designed by introduction of ionic groups ⁴⁹.

There are two types of monoliths: polymeric and silica-based. Polymer monoliths are prepared by an *in situ* polymerization reaction using monomers, porogens and an

initiator⁴⁹. Although the fabrication methods of polymer monoliths and their applications in CEC have been extensively reported and reviewed^{51,52}, there are few reports of on-capillary preconcentration using polymer monolith^{53,54}. Baryla and Tolti reported a 1 cm methacrylate monolithic polymer at the capillary inlet for online preconcentration of S-propranolol in the low nanomolar range without significant sacrifice of column separation efficiency⁵⁴.

The fabrication of alkoxide-based sol-gel silica monoliths usually starts with precursors such as tetramethyl ethylsilicate (TMOS) or tetraethyl ethylsilicate (TEOS). The hydrolysis and a series of polycondensation reactions lead to the growth of siloxane oligomers, which link together to form a huge gel network (Figure 1.11)⁵⁵. After gelation and aging, a porous silica monolith is formed. Also the monolith is fixed firmly to the capillary wall. The physical characteristics, such as pore size and skeleton size, strongly depend on the fabrication conditions, such as pH, water concentration, temperature, substituting group of precursor, gelation time, the presence and concentration of catalyst⁴⁹. Silica sol-gel monoliths have been widely used in HPLC for fast separations and capillary electrochromatography (CEC) for fabricating fritless columns. For example, Tanaka's group made silica monoliths and then modified the silica surface by introducing C18 phase and used it as CEC column⁵⁰. Zare's group reported an octadecyl silica (ODS) particles entrapped monolith and used it for CEC separation⁵⁶. So far, all packed silica monolith columns were developed for HPLC or CEC separation. However, the column performance, denoted by theoretic plate number, is just "modest", because of the inhomogeneous packing⁵⁶. In Chapter 4, HPLC beads entrapped in a monolith are employed for online preconcentration, rather than separation.

However, online SPE is always more desirable. In Chapter 4, polymeric HPLC beads were immobilized into an alkoxide-based silica monolith to preconcentrate fluorescently labelled herbicides at the capillary tip. The silica shell encapsulating PRP beads were characterized by scanning electron microscope (SEM). It was also found that the preconcentration performance can be improved by changing pH and adding salt to sample solution.

Finally, work done under the supervision of Dr. Dovichi is presented as Chapter 5. A CGE-LIF method using polyethylene oxide (PEO) as sieving polymer was developed. Optimum separation conditions were established for five model proteins. Detergent differential fractionation (DDF) was used for the sequential fractionation of HT29 human colon adenocarcinoma cell extract. The resulting four fractions were analyzed using the optimized CGE-LIF method and the different protein profiles for the four sequential fractions were obtained and discussed.

1.5 References

- (1) Li, S. F. Y. *Capillary Electrophoresis: Principles, Practices and Applications*; Elsevier, **1992**.
- (2) Hjerten, S. *Chromatogr. Rev.* **1967**, *9*, 122.
- (3) Terabe, S.; Otsuka, K.; Ichikawa, K.; Tsuchiya, A.; Ando, T. *Analytical Chemistry* **1984**, *56*, 111-113.
- (4) Landers, J. P. *Handbook of Capillary Electrophoresis*, 3 ed.; CRC Press, **1996**.
- (5) Khaledi, M. Z. *High Performance Capillary Electrophoresis: Theory, Techniques and Applications*; John Wiley & Son Inc., **1998**.
- (6) Heiger, D. *High Performance capillary electrophoresis, An Introduction*; Agilent Technologies: Palo Alto, CA, USA, **2000**.
- (7) Roberts, L.; Davenport, R. J.; Pennisi, E.; Marshall, E. *science* **2001**, *291*, 1195.
- (8) Dovichi, N. J.; Zhang, J. Z. *Angewandte Chemie-International Edition* **2000**, *39*, 4463-4468.
- (9) Schwer, C.; Kenndler, E. *Analytical Chemistry* **1991**, *63*, 1801-1807.
- (10) Smith, S. C.; Khaledi, M. G. *Analytical Chemistry* **1993**, *65*, 193-198.
- (11) Cheng, Y. F.; Dovichi, N. J. *Science* **1988**, *242*, 562-564.
- (12) Melanson, J. E.; Lucy, C. A. *Analyst* **2000**, *125*, 1049-1052.
- (13) Melanson, J. E.; Boulet, C. A.; Lucy, C. A. *Analytical Chemistry* **2001**, *73*, 1809-1813.
- (14) Wey, A. B.; Thormann, W. *Journal of Chromatography A* **2001**, *924*, 507-518.
- (15) Liu, S. H.; Li, Q. F.; Chen, X. G.; Hu, Z. D. *Electrophoresis* **2002**, *23*, 3392-3397.

- (16) Alnajjar, A.; McCord, B. *Journal of Pharmaceutical and Biomedical Analysis* **2003**, *33*, 463-473.
- (17) Chen, Z. L.; Lin, J. M.; Naidu, R. *Analytical and Bioanalytical Chemistry* **2003**, *375*, 679-684.
- (18) Zhao, Y. P.; McLaughlin, K.; Lunte, C. E. *Analytical Chemistry* **1998**, *70*, 4578-4585.
- (19) Liu, W. P.; Lee, H. K. *Electrophoresis* **1999**, *20*, 2475-2483.
- (20) Lin, C. H.; Kaneta, T. *Electrophoresis* **2004**, *25*, 4058-4073.
- (21) Nesbitt, C. A.; Lo, J. T. M.; Yeung, K. K. C. *Journal of Chromatography A* **2005**, *1073*, 175-180.
- (22) Wang, S. J.; Tseng, W. L.; Lin, Y. W.; Chang, H. T. *Journal of Chromatography A* **2002**, *979*, 261-270.
- (23) Britz-McKibbin, P.; Ichihashi, T.; Tsubota, K.; Chen, D. D. Y.; Terabe, S. *Journal of Chromatography A* **2003**, *1013*, 65-76.
- (24) Britz-McKibbin, P.; Chen, D. D. Y. *Analytical Chemistry* **2000**, *72*, 1242-1252.
- (25) Palmer, J.; Munro, N. J.; Landers, J. P. *Analytical Chemistry* **1999**, *71*, 1679-1687.
- (26) Palmer, J.; Landers, J. P. *Analytical Chemistry* **2000**, *72*, 1941-1943.
- (27) Palmer, J.; Burgi, D. S.; Munro, N. J.; Landers, J. P. *Analytical Chemistry* **2001**, *73*, 725-731.
- (28) Quirino, J. P.; Terabe, S. *Analytical Chemistry* **1999**, *71*, 1638-1644.
- (29) Quirino, J. P.; Kim, J. B.; Terabe, S. *Journal of Chromatography A* **2002**, *965*, 357-373.
- (30) Quirino, J. P.; Terabe, S. *Science* **1998**, *282*, 465-468.

- (31) Quirino, J. P.; Terabe, S. *Analytical Chemistry* **1998**, *70*, 149-157.
- (32) Quirino, L. P.; Terabe, S.; Otsuka, K.; Vincent, J. B.; Vigh, G. *Journal of Chromatography A* **1999**, *838*, 3-10.
- (33) Quirino, J. P.; Terabe, S. *Analytical Chemistry* **2000**, *72*, 1023-1030.
- (34) Sentellas, S.; Puignou, L.; Galceran, M. T. *Journal of Separation Science* **2002**, *25*, 975-987.
- (35) Guzman, N. A.; Majors, R. E. *LC-GC Europe* **2001**.
- (36) Zhang, R.; Hjerten, S. *Analytical Chemistry* **1997**, *69*, 1585-1592.
- (37) Wu, X. Z.; Hosaka, A.; Hobo, T. *Analytical Chemistry* **1998**, *70*, 2081-2084.
- (38) Yang, Q.; Tomlinson, A. J.; Naylor, S. *Analytical Chemistry* **1999**, *71*, 183a-189a.
- (39) Rohde, E.; Tomlinson, A. J.; Johnson, D. H.; Naylor, S. *Electrophoresis* **1998**, *19*, 2361-2370.
- (40) Rohde, E.; Tomlinson, A. J.; Johnson, D. H.; Naylor, S. *Journal of Chromatography B-Analytical Technologies in the Biomedical and Life Sciences* **1998**, *713*, 301-311.
- (41) Waterval, J. C. M.; Hommels, G.; Bestebreurtje, P.; Versluis, C.; Heck, A. J. R.; Bult, A.; Lingeman, H.; Underberg, W. J. M. *Electrophoresis* **2001**, *22*, 2709-2716.
- (42) Strausbauch, M. A.; Xu, S. J.; Ferguson, J. E.; Nunez, M. E.; Machacek, D.; Lawson, G. M.; Wettstein, P. J.; Landers, J. P. *Journal of Chromatography A* **1995**, *717*, 279-291.
- (43) Petersson, M.; Wahlund, K. G.; Nilsson, S. *Journal of Chromatography A* **1999**, *841*, 249-261.

- (44) Dalluge, J. J.; Sander, L. C. *Analytical Chemistry* **1998**, *70*, 5339-5343.
- (45) Guzman, N. A. *Journal of Chromatography B-Analytical Technologies in the Biomedical and Life Sciences* **2000**, *749*, 197-213.
- (46) Haupt, K. *Analyst* **2001**, *126*, 747-756.
- (47) Revesz, E.; Lai, E. P. C., 88th Canadian Chemistry Conference and Exhibition. Saskatoon, Canada **2005**; 141.
- (48) Robson, M. M.; Cikalo, M. G.; Myers, P.; Euerby, M. R.; Bartle, K. D. *Journal of Microcolumn Separations* **1997**, *9*, 357-372.
- (49) Tanaka, N.; Kobayashi, H.; Nakanishi, K.; Minakuchi, H.; Ishizuka, N. *Analytical Chemistry* **2001**, *73*, 420a-429a.
- (50) Motokawa, M.; Kobayashi, H.; Ishizuka, N.; Minakuchi, H.; Nakanishi, K.; Jinnai, H.; Hosoya, K.; Ikegami, T.; Tanaka, N. *Journal of Chromatography A* **2002**, *961*, 53-63.
- (51) Hilder, E. F.; Svec, F.; Frechet, J. M. *Journal of Chromatography A* **2004**, *1044*, 3-22.
- (52) Hilder, E. F.; Svec, F.; Frechet, J. M. J. *Electrophoresis* **2002**, *23*, 3934-3953.
- (53) Ping, G. C.; Zhang, Y. K.; Zhang, W. B.; Zhang, L.; Zhang, L. H.; Schmitt-Kopplin, P.; Kettrup, A. *Electrophoresis* **2004**, *25*, 421-427.
- (54) Baryla, N. E.; Toltl, N. P. *Analyst* **2003**, *128*, 1009-1012.
- (55) Hench, L. L.; West, J. K. *Chemical Reviews* **1990**, *90*, 33-72.
- (56) Dulay, M. T.; Kulkarni, R. P.; Zare, R. N. *Analytical Chemistry* **1998**, *70*, 5103-5107.

Chapter 2. Determination of Alkylphosphonic Acids Using Micellar Electrokinetic Chromatography with Laser-Induced Fluorescence Detection and High-Salt Stacking *

2.1 Introduction

Alkylphosphonic acids and their derivatives have found wide applications as herbicides (glyphosate, glufosinate), antibiotics (fosfomycin) and antiviral compounds (foscarnet) ¹. Further, some nerve agents such as sarin, soman and VX hydrolyze to alkylphosphonates and ultimately to methylphosphonic acid (MPA) ². Many approaches for the determination of alkylphosphonic acids and related compounds have been reported ³⁻²⁰.

The first challenge in such determinations is detecting the alkylphosphonic acids because they have no chromophore or fluorophore that would enable direct UV or fluorescence detection. Various methods have been developed to circumvent this problem. Phenylphosphonic acid has been used as a UV absorbing probe in indirect UV detection methods in capillary electrophoresis (CE) ^{4-8, 10}. Using this approach Melanson *et al.* reported detection limits of 2 μM for MPA ¹⁰. Alternatively, Katagi *et al.* reported indirect photometric detection after separation with ion chromatography with detection limit of 0.4 μM MPA ⁹. Recently, Melanson *et al.* lowered the detection limit for indirect

* A version of this chapter has been published as: Jiang Jiang and Charles A. Lucy (2002), "Determination of Alkylphosphonic Acids Using Micellar Electrokinetic Chromatography with Laser-Induced Fluorescence Detection and High-Salt Stacking", *Journal of Chromatography A*, 966, 239-244.

detection in CE to 0.1 μM MPA using indirect fluorescence detection with a violet diode laser³. However, while these indirect detection methods are simple and quick, they lack specificity. This makes them difficult to apply directly to real samples.

A similar lack of specificity plagues many other detection schemes used such as conductivity⁶ and evaporative light scattering detection (ELSD)^{11,12}. Mercier *et al.* developed an anion exchange-ELSD method with detection limits of 10 μM MPA or EPA in the presence of high levels of inorganic anions¹². Greater specificity in detection of MPA has been achieved using mass spectrometry (MS)^{11,13-15,20}, flame photometric detection (FPD)¹⁶⁻¹⁸ and fluorescence¹⁹. However, quenching of the phosphorus emission by organic compounds is the main disadvantage of FPD, resulting in lower sensitivity, especially in high performance liquid chromatography (HPLC). So far, the only report of a direct fluorescence detection method was by Rough *et al.* using precolumn derivatization by panacyl bromide before HPLC separation¹⁹.

Separation of alkylphosphonic acids can be achieved in a number of manners. Both chromatographic^{9,11-17,19,20} and electrophoretic^{3-8,10,13,18} methods have been used to separate these compounds in both their native^{3-12,15,16,18} and derivatized forms^{13,14,17,19,20}. However, given the detection challenges associated with the alkylphosphonic acids discussed above, one of the key issues in selecting the separation method is its compatibility with a sample preconcentration step. Sega *et al.* extracted MPA, ethyl methylphosphonate (EMPA), and isopropyl methylphosphonate (IMPA) from water sample using a solid phase extraction column packed with a quaternary amine phase on silica¹⁷. Similarly, Meng and Liu⁴ synthesized molecularly imprinted polymers (MIP) for pinacolyl methylphosphonate (PMPA), EMPA and MPA. They used a solid-phase

extraction cartridge packed with such MIP particles to isolate and pre-concentrate these compounds from human serum solution. However, these methods require numerous offline steps prior to separation and detection.

In this chapter, a series of linear alkylphosphonic acids, methyl, ethyl and propyl phosphonic acids were derivatized with the fluorescent dye panacyl bromide (Figure 2-1). The resultant products were separated by micellar electrokinetic chromatography (MEKC)²¹⁻²⁶ using cholate / acetonitrile / borate as the separation buffer followed by laser-induced fluorescence detection (LIF). The recently introduced MEKC stacking procedure of Landers and co-workers²⁷⁻²⁹, as schematically discussed in Section 1.2.3, was successfully used to enhance detection sensitivity.

2.2 Experimental

2.2.1 Apparatus

All MEKC experiments were performed on a P/ACE 2100 capillary electrophoresis system equipped with an LIF detector and *P/ACE Station* software (Version 1.2) for instrument control and data acquisition (Beckman Instruments, Fullerton, CA, USA). A 325 nm He-Cd laser (Model # 3056-8M; Omnicrome, Chino, CA, USA) with an output power of 5 mW was utilized as the excitation source. The laser beam was coupled to the LIF detector through an SMA fiber optic receptacle (Omnichrome), a 1 m multimode fiber optic patchcord with a 100/140- μm (core/cladding) diameter and SMA 906 connectors (Polymicro Technologies, Phoenix, AZ, USA). An XB84-500DF25 band pass filter (Omega Optical, Brattleboro, VT, USA) was used to

collect the fluorescence signal at 500 ± 12.5 nm. Data were collected at 10 Hz with a detector response time of 0.5 s. The capillary was always thermostated at 25°C.

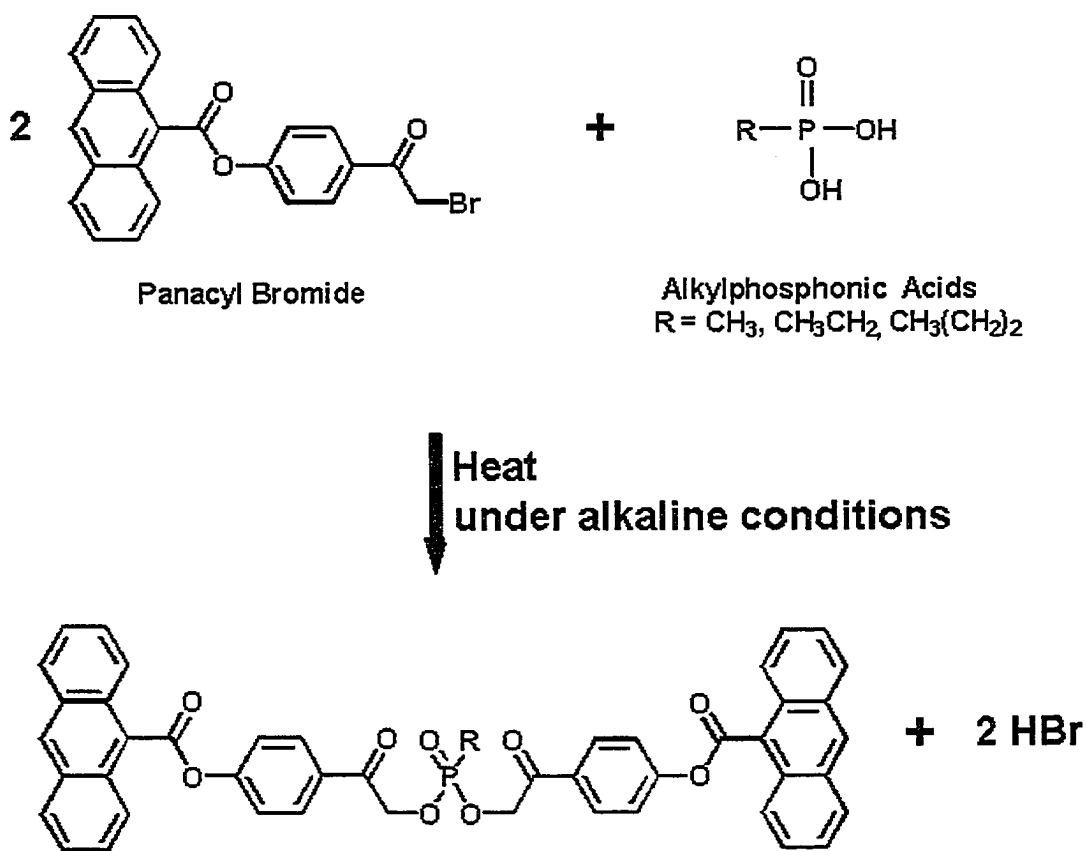


Figure 2.1 Structures of panacyl bromide (Ex/Em: 362/494 nm), alkylphosphonic acids and the fluorescent derivatization product.

2.2.2 Reagents

Methyl phosphonic acid (98%, MPA), ethyl phosphonic acid (98%, EPA), propyl phosphonic acid (95%, PPA, Figure 2-1), *N, N*-diisopropylethylamine (99.5%, redistilled), cholic acid (sodium salt), *N, N*-dimethylformamide (DMF), mesityl oxide (98%), calcium hydride (95%), and 3A molecular sieve were purchased from Aldrich (Milwaukee, WI, USA). Panacyl bromide (Figure 2-1) was from Molecular Probes (Eugene, OR, USA). Acetonitrile (HPLC grade) was from Fisher Scientific (Fair Lawn, NJ, USA). Sodium tetraborate and sodium chloride were analytical grade from BDH (Toronto, Ontario, Canada).

Commercially available DMF was refluxed over CaH_2 (5% w/v) for 5 hours at 60°C and then distilled onto 3A molecular sieves at 56 °C and 20 mm Hg to remove water. The prepared dry DMF was stored under N_2 for later use. Stock solutions of 5 mM alkylphosphonic acids, 120 mM *N, N*-diisopropylethylamine and 10 mM panacyl bromide were prepared using dry DMF and kept strictly airtight against moisture in the air. All the other solutions were prepared with Nanopure 18 M Ω water (Barnstead, Chicago, IL, USA). The separation buffer was 50 mM sodium borate, 50 mM sodium cholate and 40% (v/v) of acetonitrile (pH 10.6, without further pH adjustment) prepared every other day and degassed prior to use unless stated otherwise.

2.2.3 Derivatization reaction

The derivatization procedure was adapted from Rough *et al.*'s method¹⁹. Briefly, the optimized procedure was as follows: 60 μl of the alkylphosphonic acids in DMF was mixed with 50 μl of 120 mM *N, N*-diisopropylethylamine solution, 100 μl of 10 mM

panacyl bromide solution and 190 μl of dry DMF in a 4-ml capped borosilicate glass vial. This ensures that there is an excess of panacyl bromide. The vial was heated in an 80°C water bath for 30 min. Then 200 μl of the reaction mixture was added to 200 μl of the dilution buffer containing 100 mM borate and 400 mM sodium cholate. Finally, the sample was vortexed for 10 seconds to ensure thorough mixing prior to injection.

2.2.4 CE parameters

MEKC separation was performed at 30 kV (normal polarity) in a 57 cm-long (50 cm to the detection window), 75 μm -i.d, 365 μm -o.d, fused-silica capillary (Polymicro Technologies, Phoenix, AZ, USA). Injections were 30-s hydrodynamic at 0.5 psi unless otherwise stated. Before use each new capillary was conditioned by flushing at 20 psi with 1 M NaOH for 10 min, distilled water for 10 min, 0.1 M NaOH for 5 min and distilled water for 10min. Between runs the capillary was washed at 20 psi with 0.1 M NaOH for 2 min, distilled water for 2 min and running buffer for 5 min.

2.2.5 Measurement of EOF

Mesityl oxide was used as the EOF marker in this study. After a 2-s injection of 10 mM mesityl oxide at 0.5 psi, 30 kV voltage was applied across the capillary. UV detection at 214 nm was used to determine the migration time of the mesityl oxide peak. The other conditions were same as in Sections 2.2.1 and 2.2.4. EOF was calculated using:

$$\mu_{eof} = \frac{L_d L_t}{tV} \quad (\text{Eqn 2.1})$$

where L_d is the capillary length to the detection window, L_t is the total capillary length, t is the migration time of EOF marker and V is the voltage across the capillary.

2.3 Results and discussion

2.3.1 CE separation parameters

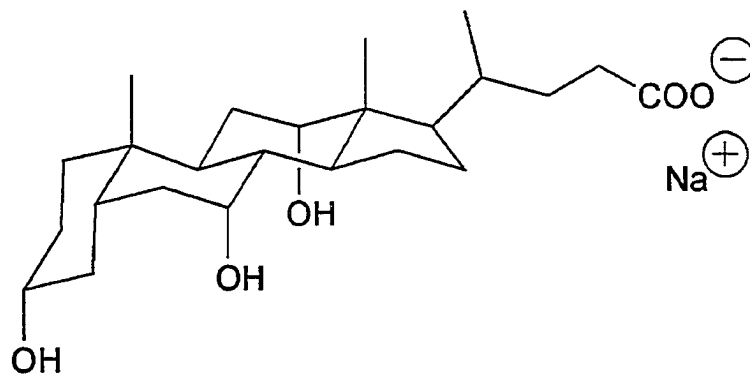
The molecular structures of panacyl bromide, alkylphosphonic acids and their derivatization products are shown in Figure 2.1. Panacyl bromide has excitation and emission maxima of 362 and 494 nm, respectively. This dye reacts with alkylphosphonic acids via a substitution reaction in basic nonaqueous medium in high yield (~ 90%)¹⁹ and shows no reactivity to the esters of alkylphosphonic acids. However, the resulting products are strongly hydrophobic, making them insoluble in most HPLC mobile phases / CE separation buffers. Rough *et al.*¹⁹ had to use very strong eluents (60% - 100% acetonitrile) to elute the alkylphosphonic acid derivatives from a C₁₈ column in reasonable time.

Sodium dodecyl sulfate (SDS) is typically used as the pseudo-stationary phase in MEKC. However SDS is not effective for strongly hydrophobic analytes because SDS exhibits high partitioning even at low SDS concentrations or after addition of organic modifier²². Our preliminary studies showed that the derivatization products could not be separated from excess dye using SDS. A number of alternative approaches have been proposed in the literature for the separation of very hydrophobic analytes in MEKC. Addition of urea or cyclodextrins increases the solubility of hydrophobic compounds in aqueous solutions, thus decreasing their retention factor in the micellar phase²³⁻²⁵. However, preliminary studies indicated that neither 6M urea nor 30 mM γ -cyclodextrin had a noticeable improvement on the resolution of our analytes.

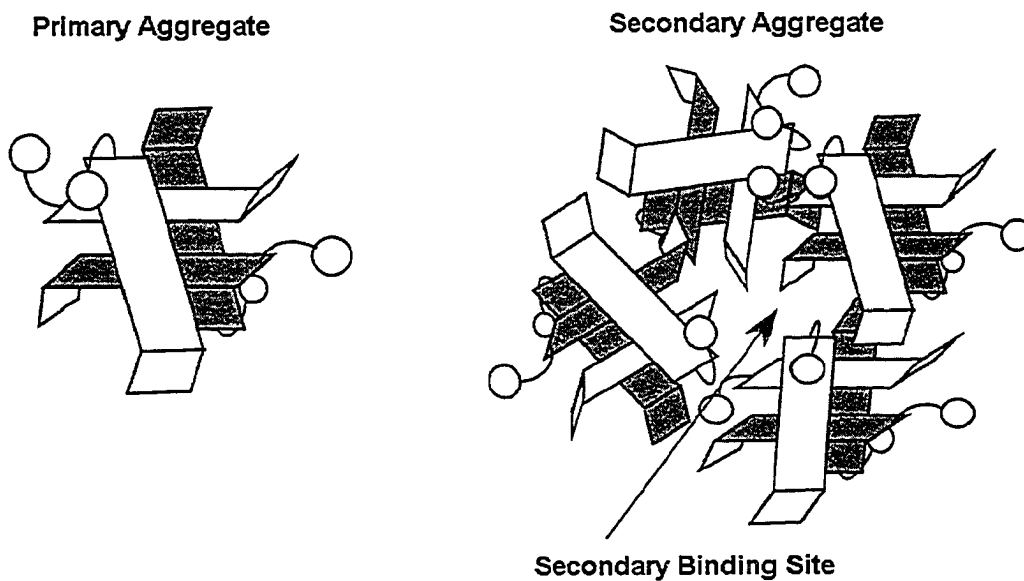
Alternatively, natural surfactants, such as sodium cholate, sodium deoxycholate and their taurine conjugates, have been reported to be suitable for the separation of very hydrophobic compounds²²⁻²⁵. The structures of sodium cholate and its micelles are

shown in Figure 2.2. Bile salts form aggregates that are more complex than the spherical micelles of conventional surfactants such as SDS³⁰⁻³². At low concentrations, bile salts form primary aggregates containing a small number (3-10) of monomers (Figure 2.2B). In Figure 2.2B, the primary aggregates contain four cholate molecules. In the primary aggregates, the convex hydrophobic surfaces of the cholate monomer form a hydrophobic binding site. At higher cholate concentrations, these primary aggregates combine to form larger aggregates known as secondary aggregates. The core of this secondary aggregate is relatively hydrophilic in nature. Thus, unlike the typical spherical SDS micelles, the cores of such bile salt micelles contain both hydrophobic and hydrophilic regions^{22,33}. The different structure properties of cholate micelles result in much lower partitioning than SDS micelles.

In MEKC, the analyte distribution between the micelle phase and aqueous phase can be adjusted by simply changing the surfactant concentration^{22,23,25}. First the effect of cholate concentration was examined by adding 30 ~ 60 mM sodium cholate to a separation buffer containing 50 mM borate and 40% (v/v) of acetonitrile. The resulting electropherograms are shown in Figure 2.3. Excess dye (D) eluted prior to the alkylphosphonic acid derivatives (peak 1-3, corresponding to MPA, EPA and PPA, respectively), as would be expected. Other by-product peaks (not shown in Figure 2.3, but indicated as B in Figure 2.4) eluted after the analyte peaks.



A. Sodium Cholate



B. Cholate Micelle

Figure 2.2 Sodium cholate (A) and its aggregate structures (B). Figures reproduced from reference 31 by permission of The Royal Society of Chemistry on behalf of the European Society for Photobiology and the European Photochemistry Association.

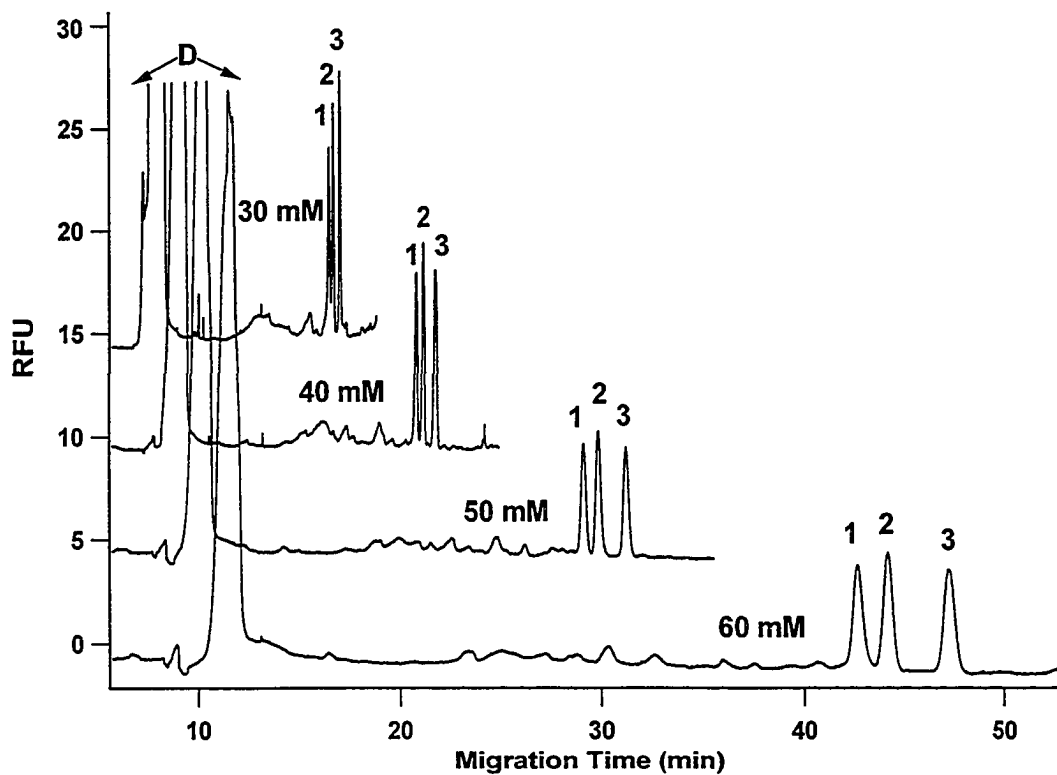


Figure 2.3 Effect of cholate concentration on the separation. MEKC separation buffer: cholate / 40 % (v/v) of acetonitrile / 50 mM borate; Voltage: 30 kV; Injection: 30 s at 0.5 psi; Dilution buffer: 100 mM borate / 400 mM NaCl; Dilution ratio: 50%:50% (v/v, reaction mixture vs. dilution buffer); Sample injected: 2.5 μ M; Peak designation: (D) excess dye, (1) MPA, (2) EPA, (3) PPA. Byproduct peaks not shown (see Figure 2.4).

As shown in Figure 2.3, the migration time of the analyte peaks (1-3) increases with the increasing cholate concentration. Also, the resolution between MPA and EPA (peaks 1 and 2, the critical pair since it is more difficult to separate than EPA / PPA pair) increased from 0.80 at 30 mM cholate to 1.64 at 60 mM cholate. Due to the limited solubility of sodium cholate in 40% acetonitrile and concerns associated with Joule heating, 50 mM sodium cholate was used in all further experiments.

Another advantage of bile salts is that, they can tolerate higher concentrations of organic modifiers such as acetonitrile (up to 50%)²². More acetonitrile results in a slower EOF. Generally a lower EOF leads to extended elution time window and thus better resolution²² (as discussed in Section 1.1.5.2). Figure 2.4 illustrates the effect of varying acetonitrile concentration in separation buffer containing 50 mM borate and 50 mM of sodium cholate. The peaks (B) eluting after the analytes (1-3) were evident in blank experiments and thus believed to be degradation products of panacyl bromide. However, as these by-product peaks (B) were consistently well resolved from the analyte peaks, they were not studied further. There are also a number of small byproduct peaks between the excess dye (D) and product peaks 1-3. These byproduct peaks are probably due to side reactions, presumably hydrolysis since these peaks were lower and simpler when freshly-prepared dry DMF was used.

As can be seen in Figure 2.4, the migration times of the excess dye (D) and analytes (1-3) increased as the acetonitrile concentration was increased. The longer migration times are not unexpected because EOF decreases from 3.00×10^{-4} to 1.71×10^{-4} $\text{cm}^2/\text{V}\cdot\text{s}$ upon going from 30 to 45% acetonitrile. Thus, the increase in migration time due to the slower EOF is greater than the decrease in migration time due to the change in the retention factor. More importantly, the resolution between MPA and EPA (peaks 1

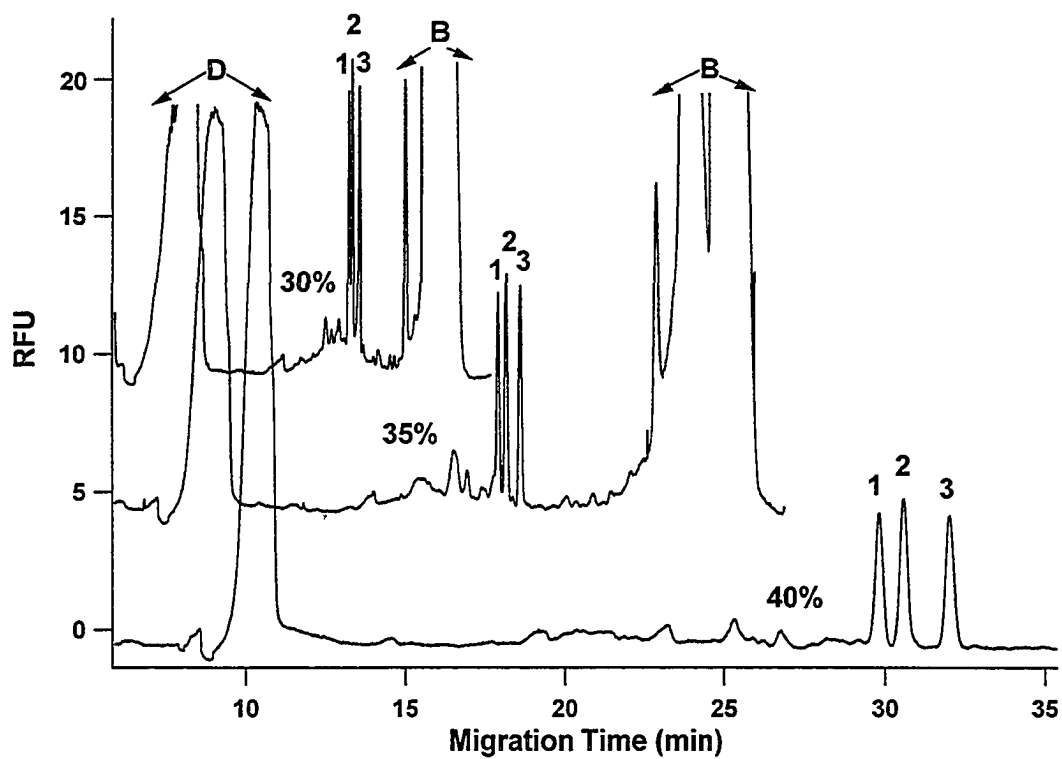


Figure 2.4 Effect of acetonitrile on the separation. MEKC separation buffer: 50 mM cholate / acetonitrile / 50 mM borate; Peak designation: (B) byproduct peaks. The other conditions and peak designations are as in Figure 2.3.

and 2) increased from 0.94 to 1.64 as the acetonitrile concentration is increased from 30% to 45%. The hydrolysis products were also better resolved from the analyte products peaks 1-3 at higher acetonitrile concentrations and therefore caused no interference. When the acetonitrile concentration was increased above 45%, MPA, EPA and PPA eluted after 90 min. As a compromise between separation time and resolution, 40% acetonitrile was used in subsequent experiments.

2.3.2 Optimization of the derivatization reaction

The reaction conditions of Rough *et al.*'s method¹⁹ were used as a starting point for optimization of the reaction conditions to obtain best sensitivity and least interference from byproducts in the reaction mixture. This derivatization procedure is shown schematically in Figure 2.1. Briefly, under the alkaline conditions the alkylphosphonic acids are converted to their anionic forms for higher nucleophilicity. Subsequent nucleophilic substitution in DMF generates the panacyl esters of the alkylphosphonic acids.

The effect of dye concentration was studied first. Different amounts of 10 mM panacyl bromide were mixed with 60 μ l of 0.2 mM mixed sample solution, 50 μ l of 120 mM *N, N*-diisopropylethylamine solution and then diluted to a total volume of 400 μ l with dry DMF. The other conditions were as described in Section 2.3. As shown in Figure 2.5, the response of each phosphonic acid increased significantly with increasing dye concentration used and reached a plateau at approximately 2.5 mM. This concentration of panacyl bromide corresponds to the derivatization procedure described in Section 2.2.3, and was used in all further experiments.

The concentration of *N, N*-diisopropylethylamine in the reaction mixture is critical as it consumes the HBr produced (Figure 2.1) and thus pulls the whole reaction to completion. However, too much base leads to hydrolysis of the dye and can cause severe interference with detection¹⁹. Different amounts of 120 mM *N, N*-diisopropylethylamine solution were added to 60 μ l of 0.2 mM mixed sample solution and 100 μ l of 10 mM panacyl

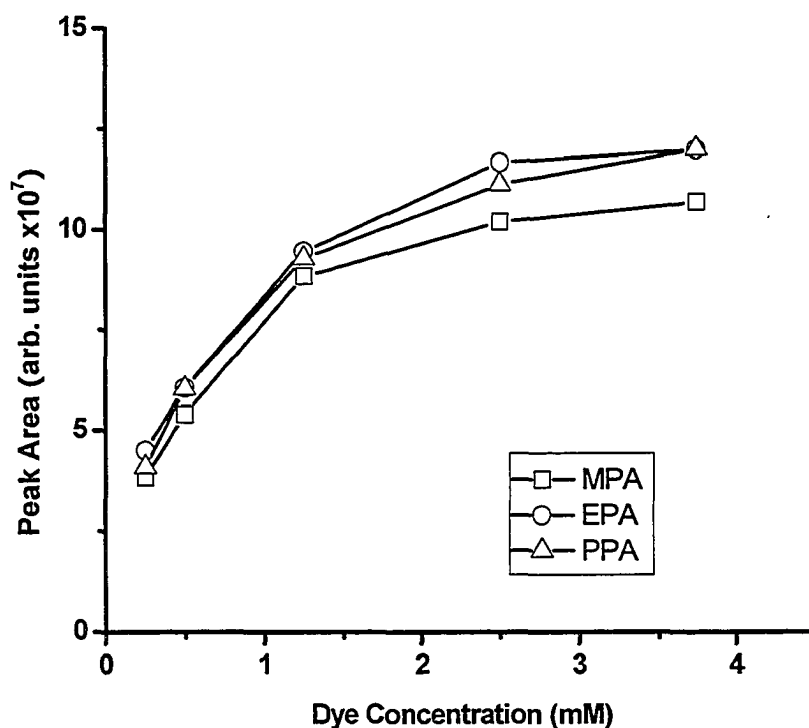


Figure 2.5 Effect of dye concentration on the fluorescence response. MPA/EPA/PPA: 30 μ M each; *N, N*-diisopropylethylamine: 15 mM; Reaction time: 30 min; Reaction Temperature: 80°C. Each data point is the average of duplicate reactions. The size of the data points approximately reflects the reproducibility of within 10%.

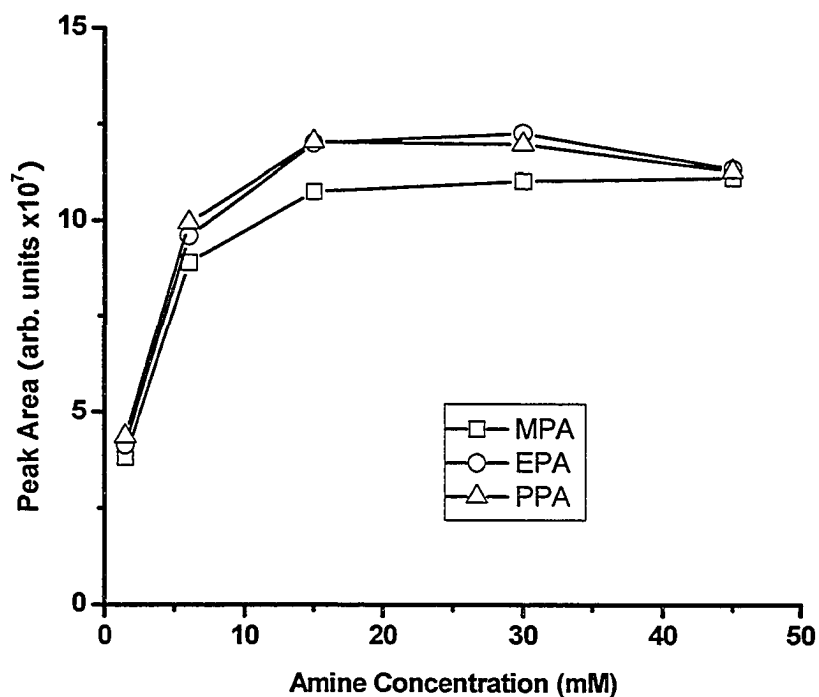


Figure 2.6 Effect of *N, N*-diisopropylethylamine concentration on the fluorescence response. MPA/EPA/PPA: 30 μ M each; Panacyl bromide: 2.5 mM; Reaction time: 30 min; Reaction Temperature: 80°C. Each data point is the average of duplicate reactions. The size of the data points approximately reflects the reproducibility of within 10%.

bromide, and then diluted to a total volume of 400 μ l with dry DMF. The other conditions were same as above. Figure 2.6 shows that the product peak areas increased as the concentration of *N, N*-diisopropylethylamine was increased up to 15 mM. Higher concentration of base yielded no further increase in response.

Thus, 2.5 mM panacyl bromide and 15 mM *N, N*-diisopropylethylamine were chosen as optimal reaction conditions, as described in Section 2.3. Under these reaction conditions the derivatization reaction is more than 2/3 complete within 5 min as determined by comparing with 40 min reaction time, and complete by 20 min. No degradation of the products was observed up to 40 min, the maximum reaction time studied. A reaction time of 30 min was used in our work.

2.3.3 High-salt stacking

A number of online concentration techniques for MEKC have been reported to increase the detection sensitivity and lower detection limit in MEKC^{27-29, 34-38}. Recently Landers and co-workers developed a universal stacking technique for MEKC which utilizes higher salt concentration in the sample matrix than in the separation buffer²⁷⁻²⁹. Its concentration mechanism has been schematically illustrated in Figure 1.7. Briefly, after the separation voltage is applied, the negatively-charged micelles move into the sample zone from the detector side of the sample zone / separation buffer interface. The electric field strength is lower in the higher-conductivity sample zone than in the separation buffer. As a consequence the micelle migration velocity decreases. The net effect is that micelles accumulate near the detector side of the sample zone / separation buffer interface resulting in a higher phase ratio of micellar phase at the sample / buffer interface. Consequently, the hydrophobic analyte is concentrated in this zone.

2.3.3.1 Salt concentration

Palmer and Landers have demonstrated that two requirements are critical to successful high-salt stacking in MEKC²⁸. First, the conductivity of sample matrix must exceed that of the separation buffer so that the electric field decreases significantly inside the sample zone. Second, the sample matrix must contain a co-ion (chloride in our work) with a higher intrinsic electrophoretic mobility than cholate. The second condition guarantees the formation of a pseudo-steady-state boundary between the micelle and co-ion component in the sample matrix. Figure 2.7 shows the effect of the addition of 0 to 700 mM NaCl in the dilution buffer on the resolution. As the NaCl concentration added to the sample is increased, the resolution for the MPA/EPA pair initially improved from 1.02 at 0 mM to 1.67 over a broad optimum at 200 ~ 400 mM, as expected based on the stacking mechanism above. The resolution then decreased as the peak shape degrades at higher salt concentrations. Similar behavior was observed if the peak efficiency is monitored. This behavior is consistent with that of Palmer *et al.*²⁷. The degradation of resolution at higher salt concentrations is probably due to the disappearance of the pseudo-steady-state boundary between the micelle and co-ion component. That is, as the conductivity of the sample matrix is further increased, the electrophoretic movement of co-ion against EOF is further slowed down, causing poor stacking (destacking).

The volume of sample injected can be determined using the Hagen-Poiseuille equation²⁶:

$$\text{Injection Volume} = \frac{\Delta P d^4 \pi t}{128 \eta L_t} \quad (\text{Eqn 2-2})$$

where ΔP is the pressure difference across the capillary, d is the inside diameter of the capillary, η is the separation buffer viscosity and L_t is the total capillary length.

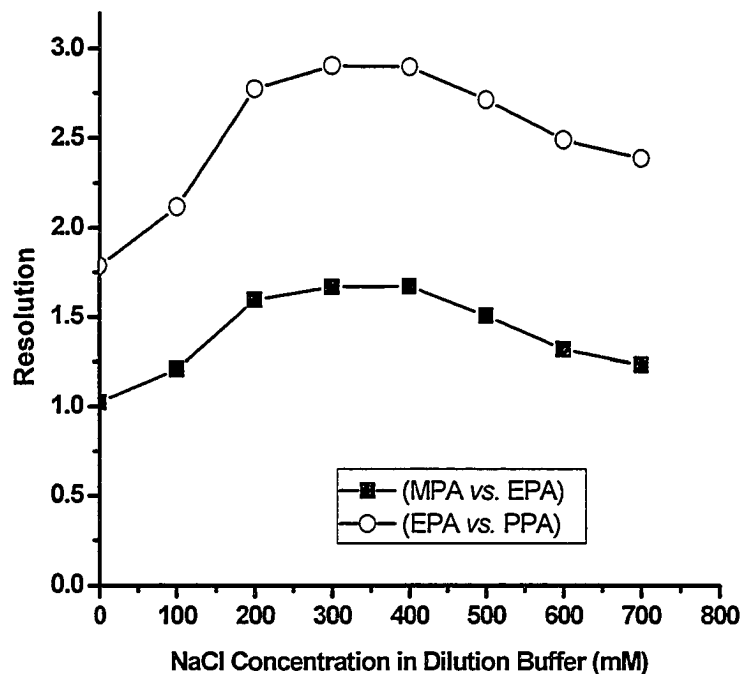


Figure 2.7 Effect of NaCl concentration in dilution buffer on the resolution. 200 μ l of fluorescence derivatization reaction solution in dry DMF was mixed with 200 μ l of dilution buffer containing NaCl and 100 mM borate. Each data point is the average of duplicate injections. The size of the data points approximately reflects the reproducibility of within 5%.

Based on this expression, the injection plug lengths of 3-s and 30-s injections were calculated to be 3.3 mm and 32.8 mm long, respectively. While the high-salt stacking was successfully applied in this work, the injection sample plug length was limited to 32.8 mm (30-s injection). Longer injection times lead to loss of baseline resolution. This agrees with Landers and coworkers' results that the stacking efficiency decreases dramatically at longer injection lengths (Figure 5 in reference ²⁷). Figure 2.8 shows high-salt stacking performance. A 30 s injection allows 10-fold more sample to be injected, compared with 3 s injection typically used in normal MEKC.

2.3.3.2 Dilution ratio

In HPLC and MEKC, the solvent used to dissolve sample should not be stronger than the mobile phase. Usually the mobile phase itself is recommended to dissolve the sample. If the injection solvent is stronger than the eluent, poor separation performance or even peak splitting may be observed ³⁹. In our work, the fluorescent dye and its derivatization products are soluble in acetonitrile or DMF. As discussed in Section 2.3.1, the optimum separation buffer contained 40% (v/v) of acetonitrile. However, the sample matrix contained 50% DMF (v/v) after final dilution. To investigate the effect of the DMF in the sample, the DMF concentration was varied while keeping the final concentrations of cholate and NaCl constant at 50 mM and 200 mM, respectively. No effect on resolution was observed up to 50% DMF. However, 70% DMF showed a distorted and broad peak shape, indicating the presence of strong solvent effect. Therefore, 50 % DMF was used.

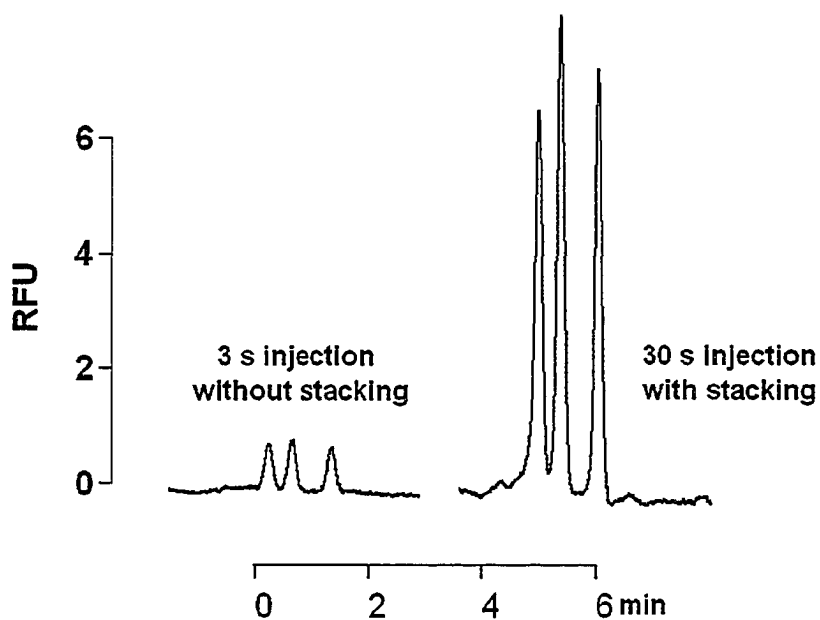


Figure 2.8 High-salt stacking performance. Separation buffer: 50 mM borate / 40 mM cholate / 40% acetonitrile; Sample injected: 7.5 μM each. Other conditions are as stated in Section 2.2.

2.3.4 Calibration, detection limit and reproducibility

Quantitative studies were conducted in the concentration range of 3.3 μM - 0.33 mM each analyte before reaction, corresponding to 0.25 μM - 25 μM injected (Figure 2.9). Calibration curves were recti-linear with correlation coefficients (R) greater than 0.999 and intercepts equal to zero within the 95% confidence interval. However the calibration data were best-fit by quadratic equations, as shown in Figure 2.9. Each data point is an average of duplicate injections.

The reproducibility ($n = 11$) of the migration time and corrected peak area (defined as the ratio of peak area to migration time) were studied using a 0.2 mM mixed sample (corresponding to 15 μM injected). Migration time reproducibility was 2.9 - 3.6% and the corrected peak area reproducibility was 3.7 - 4.3%.

Based on an S/N of 3, the limit of detection (LOD) is 0.13 μM MPA, 0.13 μM EPA and 0.14 μM PPA injected. These are better than most previous reports^{4, 6-10, 12, 13, 18, 19}.

2.4. Conclusions

A fluorometric determination of three linear alkylphosphonic acids is reported. After derivatization with panacyl bromide in dry DMF, baseline resolution was achieved using MEKC with cholate micelles and 40% acetonitrile. The addition of an optimal concentration of salt resulted in high-salt stacking which decreased the detection limit 10-fold while maintaining baseline resolution.

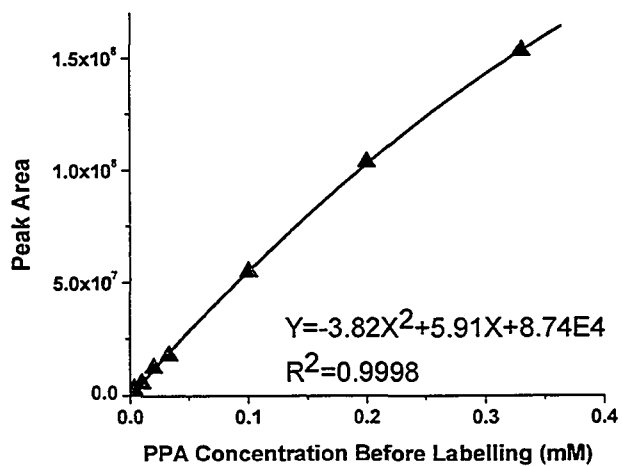
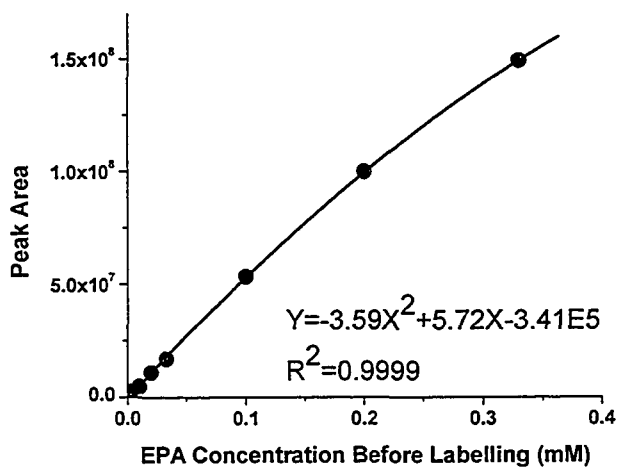
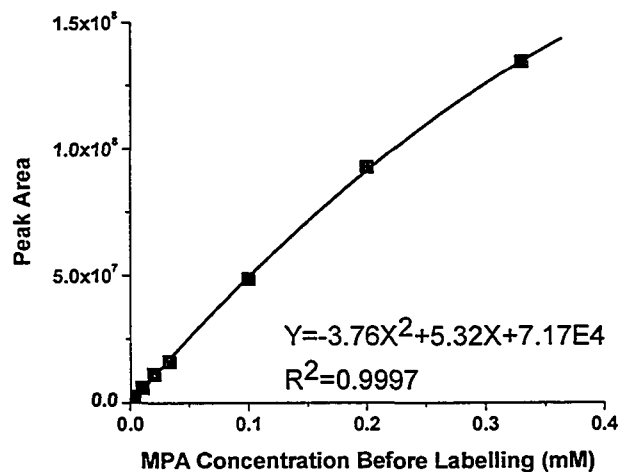


Figure 2.9 MPA/EPA/PPA Calibration curves

2.5 References

- (1) Stalikas, C. D.; Konidari, C. N. *Journal of Chromatography A* **2001**, *907*, 1-19.
- (2) Kientz, C. E. *Journal of Chromatography A* **1998**, *814*, 1-23.
- (3) Melanson, J. E.; Boulet, C. A.; Lucy, C. A. *Analytical Chemistry* **2001**, *73*, 1809-1813.
- (4) Meng, Z. H.; Qin, L. *Analytica Chimica Acta* **2001**, *435*, 121-127.
- (5) Nassar, A. E. F.; Lucas, S. V.; Hoffland, L. D. *Analytical Chemistry* **1999**, *71*, 1285-1292.
- (6) Nassar, A. E. F.; Lucas, S. V.; Jones, W. R.; Hoffland, L. D. *Analytical Chemistry* **1998**, *70*, 1085-1091.
- (7) Pianetti, G. A.; Taverna, M.; Baillet, A.; Mahuzier, G.; Baylocqferrier, D. *Journal of Chromatography* **1993**, *630*, 371-377.
- (8) Mercier, J. P.; Morin, P.; Dreux, M.; Tambute, A. *Journal of Chromatography A* **1996**, *741*, 279-285.
- (9) Katagi, M.; Nishikawa, M.; Tatsuno, M.; Tsuchihashi, H. *Journal of Chromatography B* **1997**, *698*, 81-88.
- (10) Melanson, J. E.; Wong, B. L. Y.; Boulet, C. A.; Lucy, C. A. *Journal of Chromatography A* **2001**, *920*, 359-365.
- (11) Mercier, J. P.; Morin, P.; Dreux, M.; Tambute, A. *Journal of Chromatography A* **1999**, *849*, 197-207.
- (12) Mercier, J. P.; Elfakir, C.; Dreux, M.; Lazar, S.; El Haddad, M.; Akssira, M. *Journal of Liquid Chromatography & Related Technologies* **2000**, *23*, 2345-2359.
- (13) Kataoka, M.; Tsuge, K.; Seto, Y. *Journal of Chromatography A* **2000**, *891*, 295-304.

- (14) Sng, M. T.; Ng, W. F. *Journal of Chromatography A* **1999**, *832*, 173-182.
- (15) Read, R. W.; Black, R. M. *Journal of Chromatography A* **1999**, *862*, 169-177.
- (16) Hooijschuur, E. W. J.; Kientz, C. E.; Brinkman, U. A. T. *Journal of Chromatography A* **2001**, *907*, 165-172.
- (17) Segal, G. A.; Tomkins, B. A.; Griest, W. H. *Journal of Chromatography A* **1997**, *790*, 143-152.
- (18) Sangervandegriend, C. E.; Kientz, C. E.; Brinkman, U. A. T. *Journal of Chromatography A* **1994**, *673*, 299-302.
- (19) Roach, M. C.; Ungar, L. W.; Zare, R. N.; Reimer, L. M.; Pompliano, D. L.; Frost, J. W. *Analytical Chemistry* **1987**, *59*, 1056-1059.
- (20) Riches, J.; Morton, I.; Read, R. W.; Black, R. M. *Journal of Chromatography B- Analytical Technologies in the Biomedical and Life Sciences* **2005**, *816*, 251-258.
- (21) Li, S. F. Y. *Capillary Electrophoresis: Principles, Practices and Applications*; Elsevier, 1992.
- (22) Landers, J. P. *Handbook of Capillary Electrophoresis*, 3 ed.; CRC Press, **1996**.
- (23) Khaledi, M. Z. *High Performance Capillary Electrophoresis: Theory, Techniques and Applications*; John Wiley & Son Inc., **1998**.
- (24) Grossman, P. D.; Colburn, J. C. *Capillary electrophoresis: Theory and Practice*; Academic Press Inc.: San Diego, **1992**.
- (25) Terabe, S. *Micellar Electrokinetic Chromatography*; Beckman Instruments: Fullerton, CA, USA, **1993**.
- (26) Heiger, D. *High Performance capillary electrophoresis, An Introduction*; Agilent Technologies: Palo Alto, CA, USA, **2000**.
- (27) Palmer, J.; Munro, N. J.; Landers, J. P. *Analytical Chemistry* **1999**, *71*, 1679-1687.

- (28) Palmer, J.; Landers, J. P. *Analytical Chemistry* **2000**, *72*, 1941-1943.
- (29) Palmer, J.; Burgi, D. S.; Munro, N. J.; Landers, J. P. *Analytical Chemistry* **2001**, *73*, 725-731.
- (30) Ju, C.; Bohne, C. *Journal of Physical Chemistry* **1996**, *100*, 3847-3854.
- (31) Rinco, O.; Nolet, M. C.; Ovans, R.; Bohne, C. *Photochemical & Photobiological Sciences* **2003**, *2*, 1140-1151.
- (32) Yihwa, C.; Quina, F. H.; Bohne, C. *Langmuir* **2004**, *20*, 9983-9991.
- (33) Sen, S.; Dutta, P.; Mukherjee, S.; Bhattacharyya, K. *Journal of Physical Chemistry B* **2002**, *106*, 7745-7750.
- (34) Quirino, J. P.; Kim, J. B.; Terabe, S. *Journal of Chromatography A* **2002**, *965*, 357-373.
- (35) Quirino, J. P.; Terabe, S. *Science* **1998**, *282*, 465-468.
- (36) Quirino, J. P.; Terabe, S. *Analytical Chemistry* **1998**, *70*, 149-157.
- (37) Quirino, J. P.; Terabe, S. *Analytical Chemistry* **1999**, *71*, 1638-1644.
- (38) Quirino, J. P.; Terabe, S.; Bocek, P. *Analytical Chemistry* **2000**, *72*, 1934-1940.
- (39) Lindsay, S. *High Performance Liquid Chromatography*, second ed.; John Wiley & Sons, **1992**.

Chapter 3. Determination of Glyphosate Using an Off-Line Ion-Exchanger Resin Preconcentration Tip and Laser-Induced Fluorescence Detection

3.1 Introduction

Introduced by Monsanto Company in 1971, glyphosate (N-(phosphonomethyl) glycine, Figure 3.1) has become one of the most widely used broad-spectrum herbicides. Its market is still growing at an annual rate of 20% because of the expiration of the Monsanto patent on glyphosate in the early 1990s and the introduction of crops genetically-engineered to be more glyphosate-tolerant¹. Due to its strong retention on soil components, high solubility in water and long half-time in the environment (about 47 days)², glyphosate may still be detected long after application or even far from the site of application. For decades, the long-term environmental and ecological effects of glyphosate have been the target of research and discussion. A reliable method for the determination of glyphosate in environmental samples is therefore a must for this research and environmental monitoring.

Almost all available analytical methodologies have been applied to the determination of glyphosate, including gas chromatography (GC)³⁻¹³, high performance liquid chromatography (HPLC)¹⁴⁻²⁶, capillary electrophoresis (CE)²⁷⁻³⁸, and enzyme-linked immunosorbent assay (ELISA)^{24,25,39}. Stalikas *et al.* have comprehensively reviewed the literature on the analysis of glyphosate and other phosphonic and amino acid group-containing pesticides⁴⁰. To date, most reports were

based on chromatographic separations. For example, Grey *et al.* developed a liquid chromatography/electrospray/mass spectrometry (LC/ES/MS) method for the analysis of glyphosate and its metabolite aminomethylphosphonic acid (AMPA) using isotope-labeled glyphosate as a method surrogate. The reported method detection limits were 0.06 and 0.30 $\mu\text{g/L}$, respectively, for glyphosate and AMPA in water matrices ⁴¹. Far fewer CE methods have been reported for glyphosate ²⁷⁻³⁸. Molina and Silva used nonionic surfactant micellar electrokinetic chromatography (MEKC) with laser-induced fluorescence (LIF) detection to determine glyphosate at a LOD of 0.06 $\mu\text{g/L}$ ³⁵. Safarpour and Asiaie reported a CE-electrospray ionization mass spectrometry (CE-ESI-MS) method for rapid and selective detection of glyphosate with LOD of 10 ng/ml with minimal sample handling ³⁷.

Prior to chromatographic or CE separation, ion-exchange solid-phase extraction (SPE) preconcentration techniques were utilized in many reports ^{6, 42-46} to greatly enhance the detection sensitivity. So far, the most sensitive method was reported by Patsias and coworkers ⁴⁴. They coupled a PRP-X100 poly (styrene-divinylbenzene)-trimethylammonium anion-exchange cartridge to a cation-exchange liquid chromatography separation followed by post-column derivatization and fluorescence detection. By processing 100-ml samples, a detection limit better than 20 ng/l for glyphosate was achieved in river water.

As glyphosate has no chromophore or fluorophore, derivatization is usually required prior to detection. Specifically, for fluorescence detection, most previous

reports used hypochlorite to convert glyphosate to glycine and then labeled glycine with *o*-phthalaldehyde (OPA) and 2-mercaptoethanol (ME). In this work, another fluorogenic reagent, naphthalene-2, 3-dicarboxaldehyde (NDA) was used to label glycine. Like OPA, NDA labels primary amine (-NH₂) groups in the presence of excess cyanide under mild conditions (Figure 3.1). However, the product of the NDA reaction is more strongly fluorescent and more stable than the OPA-ME product⁴⁷. NDA is also suitable for more compact 415 nm violet diode laser used in this work. In this chapter, an anion-exchanger SPE method similar to Patsias and coworkers' work⁴⁴ was developed for off-line preconcentration of glyphosate at the nM range from water samples. After elution of glyphosate from the SPE device, it is fluorescently labeled with NDA and analyzed by MEKC-LIF. As low as 0.2 nM of glyphosate in original samples can be detected using a 415 nm violet diode laser.

3.2 Experimental

3.2.1 Reagents and Materials

Sodium glyphosate (GLYP, 97.0%) and sodium dodecyl sulfate (SDS, 99%) were from Fluka (Buchs, Switzerland). Sodium cyanide (99.98%), calcium hypochlorite (available chlorine 65%) and naphthalene-2, 3-dicarboxaldehyde (NDA, 98%) were from Aldrich (Milwaukee, WI, USA). Sodium tetraborate was from BDH (Poole, England). Methanol (HPLC grade) was from Fisher (Fair Lawn, NJ, USA). Hydrochloric acid and sodium hydroxide were from EM Science (an affiliate of Merck KGaA, Darmstadt,

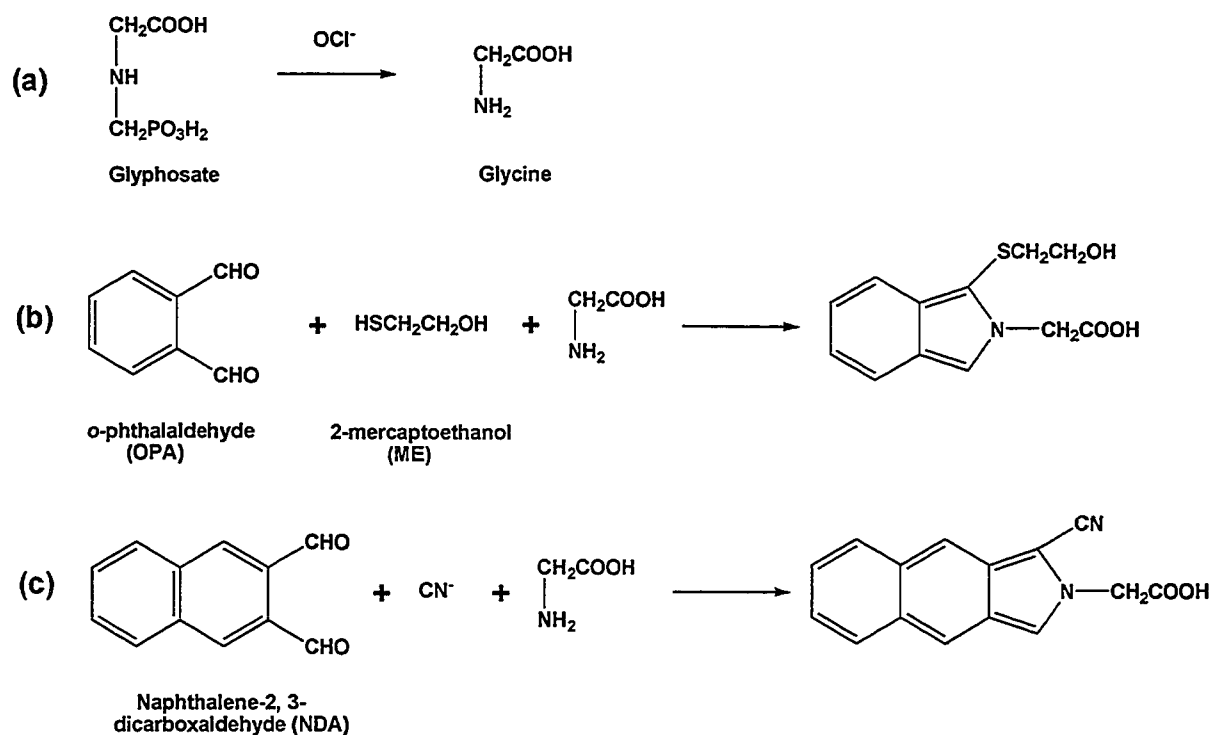


Figure 3.1 (a) Oxidative conversion of glyphosate to glycine and subsequent fluorescence labeling reactions using (b) OPA-ME or (c) NDA-CN⁻.

Germany). All solutions were prepared with Nanopure 18 MΩ water (Barnstead, Chicago, IL, USA) except NDA which was in methanol.

AG1-X8 strong-acid anion exchange resin (50-100 mesh, chloride form) was purchased from Bio-Rad (Richmond, CA, USA). Strong-acid cation exchange resin C-100H ((polystyrene-divinylbenzene)-sulfonate, 16~50 mesh) and macroporous type II strong-base anion exchange resin A-510S ((polystyrene-divinylbenzene)-dimethyl-ethylammonium, 16~50 mesh) were gifts kindly provided by Purolite (Philadelphia, PA, USA). Medium size Maxi-Clean™ solid-phase extraction cartridge and frits / caps were

from Alltech (Deerfield, IL, USA). 60 ml plastic syringes were from Beckton, Dickinson and Company (Franklin Lakes, NJ, USA).

3.2.2 Analysis Procedures

3.2.2.1 Preconcentration

The sample solution was pumped by a BS-9000-8 syringe pump (Braintree Scientific Inc., Braintree, MA, USA) through a clean-up cartridge followed by a resin preconcentration tip, as shown in Figure 3.2. The clean-up cartridge was a medium size Maxi-Clean™ solid-phase extraction cartridge with 0.2 µm frits, to which 300 mg of mixture of Purolite A-510 macroporous type II strong base anion exchange resin (chloride form) and Purolite C-100H strong acid cation exchange resin (hydrogen form) at a mass ratio of 60:40 was packed. The resin preconcentration tip was a 200 µl micro-pipette tip, in which 50 mg of Bio-Rad AG1-X8 resin was added. Glass wool was used to avoid loss of AG1-X8 resin when in use. Before use, both clean-up cartridge and resin preconcentration tip were rinsed with 10 ml of 18 MΩ water.

50 ml of sample solution was pumped at 5 ml/min through the clean-up cartridge and resin preconcentration tip. After extraction, the cleanup cartridge and resin preconcentration tip were removed and washed separately with 5ml of 18 MΩ water each. The resin preconcentration tip was eluted with 10 mM HCl at 0.1 ml/min. 500 µl of effluent was collected in a 4 ml borosilicate glass vial for subsequent derivatization reactions. After elution, the resin tip was regenerated with 2.5 ml of 1M HCl at 0.5

ml/min and then 5 ml of 18 MΩ water to be ready for next run.

3.2.2.2 Derivatization and fluorescence labeling

Glyphosate was converted to glycine using a previously reported method⁴⁴. Briefly, to the 4 ml glass vial containing 500 μl of effluent, 60 μl of 200 mM sodium borate buffer (pre-adjusted to pH 10.4 by NaOH) and 40 μl of 1 mM Ca(ClO)₂ were added. The mixture was vortexed and then placed in a 60°C water bath for 5 min. Then 20 μl of 10 mM NaCN and 20 μl of 2.5 mM NDA were added, mixed thoroughly by vortexing, and allowed to react in the dark at room temperature for 3 min only.

3.2.2.3 MEKC separation

All CE experiments were performed on a P/ACE 2100 capillary electrophoresis system (Beckman Instruments, Fullerton, CA, USA) equipped with a laser-induced fluorescence detector and *P/ACE Station* software (version 1.2) for instrument control and data acquisition (Beckman). A 415 nm violet diode laser (model LDCU 12/4673, Power Technology Inc., Little Rock, AR, USA) was used as the excitation source. The laser was coupled to the LIF detector through an SMA fiber optic receptacle (Omnichrome, Chino, CA, USA), a 1 m multimode fiber optic patchcord with a 100/140-μm (core/cladding) diameter and SMA 906 connectors (Polymicro Technologies, Phoenix, AZ, USA). The laser output power was 1 mW as measured at the outlet of optic fibre. An XB84-500DF25 band pass filter (Omega Optical, Brattleboro, VT,

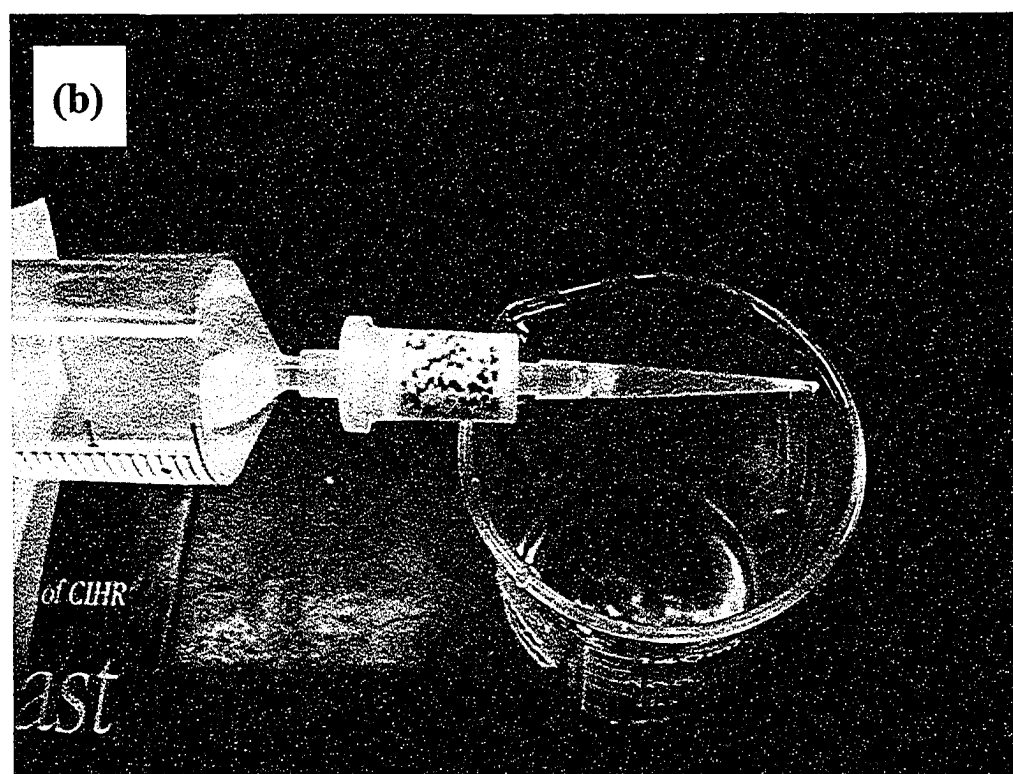


Figure 3.2 (a) Clean-up cartridge beside a Canadian one dollar coin and (b) resin-packed pre-concentration tip.

USA) was used to collect the fluorescence signal at 500 ± 12.5 nm. Data were collected at 10 Hz with a detector response time of 0.1 s. The capillary was always thermostated at 25°C.

MEKC separations were performed at 12 kV (normal polarity) across a 37 cm-long (30 cm to the detection window), 50 μm -i.d fused-silica capillary (Polymicro Technologies, Phoenix, AZ, USA). Injections were 3 s hydrodynamic at 0.5 psi. The running buffer was 50 mM SDS and 20 mM sodium borate (pH 9.3). Before use each new capillary was conditioned by flushing at 20 psi with 1 M NaOH for 10 min, distilled water for 10 min, 0.1 M NaOH for 5 min and distilled water for 10min. Between runs the capillary was washed at 20 psi with 0.1 M NaOH for 2 min, distilled water for 2 min and running buffer for 3 min.

3.2.2.4 Analysis of real samples

The river water was taken from North Saskatchewan River and stored in Nalgene™ plastic bottles (Nalge Nunc International, Rochester, NY, USA) at 4°C for no more than one week. The river water sample was spiked with glyphosate for testing of the proposed method.

3.3 Results and discussion

3.3.1 Derivatization and fluorescent labeling

Many previous papers have used hypochlorite to convert glyphosate to glycine

quantitatively, followed by fluorescence labeling using *o*-phthalaldehyde and 2-mercaptoethanol (Figure 3.1b)^{20, 21, 45, 48, 49} or Thiofluor (N,N-dimethyl-2-mercapto-ethylamine hydrochloride)⁴⁴. However hypochlorite can continue to react with the glycine product and thus reduce the overall conversion efficiency of glyphosate. So the derivatization must be carefully optimized to obtain the highest yield of glycine. In this work, the effluent from resin tip was in 10 mM HCl, and its pH must be adjusted to basic to be suitable for subsequent reactions. Addition of 60 μ l of 200 mM sodium borate buffer (pre-adjusted to pH 10.4 by NaOH) to 500 μ l of 10 μ M glyphosate in 10 mM HCl results in a final pH of 9.5, which is the recommended pH for NDA labeling reaction⁴⁷. However this may not be the best pH for conversion of glyphosate to glycine⁴⁴.

To determine the effect of hypochlorite concentration, 40 μ l of 0.1 ~ 7 mM Ca(ClO)₂ (concentration before mixing) were added to 60 μ l of 200 mM sodium borate buffer (pH 10.4) and 500 μ l of 10 μ M glyphosate. Note that the amount of glyphosate in this study was always kept well below that of chlorite ion. After oxidation and fluorescence labeling as described in Section 3.2.2.2, MEKC experiments showed that the glyphosate peak area increased sharply upon addition of hypochlorite and then reached a plateau at 0.5 ~ 2 mM (Figure 3.3). At higher Ca(ClO)₂ concentrations, the glyphosate peak area decreased slowly because the excess hypochlorite can convert glycine to chloramines, which are inactive to NDA. Thus 40 μ l of 1 mM Ca(ClO)₂ was used in all further experiments.

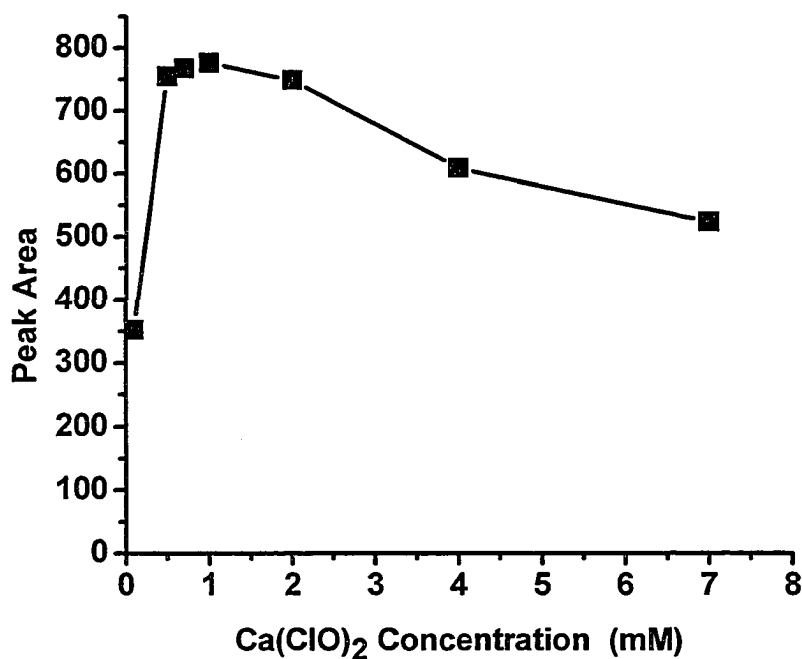


Figure 3.3 Effect of calcium hypochlorite concentration on glyphosate peak area.

Experimental conditions: 500 μ l of 10 μ M glyphosate in 10 mM HCl, 60 μ l of 200 mM sodium borate buffer (pH 10.4), 40 μ l Ca(ClO)₂, 60°C water bath for 5 min. MEKC separation conditions as in Section 3.2.2.3. Each data point is the average of duplicate reactions. The size of the data points approximately reflects the reproducibility of within 10%.

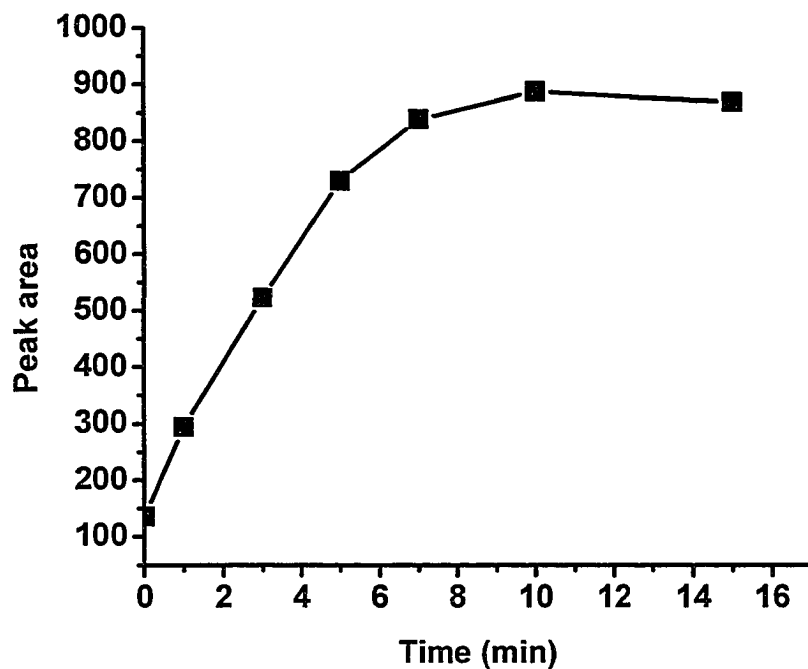


Figure 3.4 Effect of NDA derivatization reaction time at 60°C on glyphosate peak area.

Experimental conditions: 500 μl of 10 μM glyphosate in 10 mM HCl, 60 μl of 200 mM sodium borate buffer (pH10.4), 40 μl of 1 mM $\text{Ca}(\text{ClO})_2$, 60°C water bath. MEKC separation conditions as in Section 3.2.2.3. Each data point is the average of duplicate reaction. The size of the data points approximately reflects the reproducibility of within 10%.

Second, at this $\text{Ca}(\text{ClO})_2$ concentration, the effect of oxidative reaction time was examined by mixing 500 μl of 10 μM glyphosate, 60 μl of 200 mM sodium borate buffer (pH10.4) and 40 μl of 1 mM $\text{Ca}(\text{ClO})_2$. After reaction at 60°C and subsequent fluorescence labeling, the glyphosate peak area increased at longer reaction time. A plateau at 7 ~ 15 min was observed as longer reaction times did not increase peak area any more (Figure 3.4). A reaction time of 5 min was used throughout this study as a compromise of reaction time and yield.

By comparing the glyphosate results with those obtained by directly labeling glycine, it was determined that 51% of glyphosate was converted to glycine and labeled by NDA at the above optimized conditions while only 9% and 16% of glyphosate were converted at room temperature and 45°C, respectively. So 60°C was chosen as the oxidative reaction temperature instead of 36°C⁴⁴, 43°C⁴⁵ or 48°C⁴⁸ used in previous papers. Higher temperatures were not tested.

Optimization of the NaCN and NDA concentrations were more difficult. Side-product formation was observed in NDA labeling reaction and caused interference with detection of glyphosate. Figure 3.7B shows the electropherogram of a blank experiment in which 20 μl of 40 mM NaCN and 20 μl of 10 mM NDA were mixed with 20 mM pH 9.5 sodium borate buffer. Typically 5 ~ 7 side product peaks were observed. One of the side-products (at ~ 4 min) co-migrated with the glycine labeling product, no matter how the separation conditions were adjusted. Its peak height roughly corresponded to 50 nM glycine, but its peak height and area were highly irreproducible.

These side-reactions were not due to impurities in the NDA, NaCN or any other reagents as their peak area did not increase proportionally with the concentration of these reagents. For example, even a 100-fold increase in NDA or NaCN concentrations compared to those used in Section 3.2.2 resulted in only about a 1~2-fold increase in the side-product peak area. Impurities that may be present in the solvent or glassware were also not responsible for these interfering peaks. Injection of NDA itself or any other reagent did not cause any interference. These side-product peaks only appeared in the presence of both NDA and NaCN and posed severe problems in the detection of nanomolar levels of glyphosate. The side-reaction mechanism is unclear. No similar reports of this problem were found in literature with the exception of a PhD thesis by Kwakman in 1991⁵⁰. However no mechanistic studies were reported. Rather he just presumed that in principle the formation of benzoin condensation side-products induced by cyanide was possible⁵¹. These side-product had highly reproducible migration times, but relatively poor peak area reproducibility (peak area RSD > 50%). This made it very difficult to quantitatively study the factors causing the side-products. Also, due to the high salt concentration in the reaction mixture, identification of these side-products was not possible using mass spectrometry. Thus no further efforts were directed towards identifying these side products or their formation mechanism.

However a number of observations about the side product formation can be made on the basis of my work. The side-product formation can be minimized by using very low NDA and NaCN concentrations (*e.g.*, 2.5 mM and 10 mM, respectively). This may be

because the side-reactions have higher orders of reaction kinetics and thus reach completion more slowly than the labeling reaction of glycine. However, the use of lower reagent concentrations necessitates a large increase in the reaction time. To find a compromise between reaction rate and minimization of side-product peaks, the effect of NDA concentration was examined using 20 μ l of 0.625 ~ 10 mM (concentration before mixing). Figure 3.5 shows that the glyphosate peak area increased up to 2.5 mM NDA, above which no further increase was observed. Similarly, the glyphosate peak area increased from 20 μ l of 5 ~ 10 mM NaCN (concentration before mixing) but showed no significant change above 10 mM (Figure 3.6). Note that the NDA and NaCN concentrations were always in great excess in this work, so the effect of reagent concentration on glycine labelling is due to reaction kinetics rather than stoichiometry. 20 μ l of 2.5 mM NDA and 20 μ l of 10 mM NaCN were selected as the optimal reaction conditions because under these conditions the labeling reaction rate was not greatly affected but the side-products were almost negligible. In Figure 3.7 one can see that almost no side-reaction was observed when 2.5 mM NDA and 10 mM NaCN were used (Blank B) but the side-product peaks appeared when reagent concentrations were increased to 10 mM NDA and 40 mM NaCN (Blank A, the recommended reagent concentrations in most papers ⁴⁷).

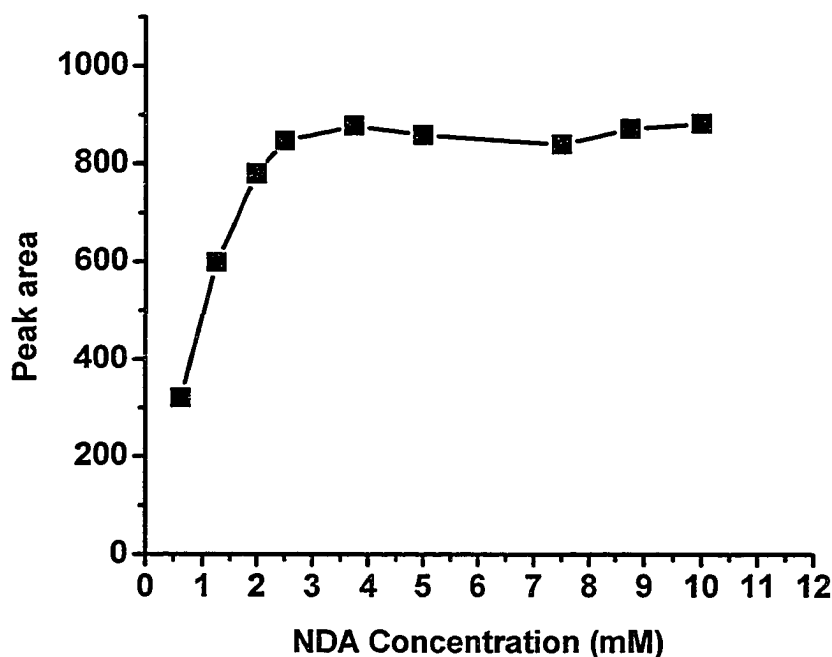


Figure 3.5 Effect of NDA concentration on glycine labeling. First glyphosate was oxidized by mixing 500 μ l of 10 μ M glyphosate in 10 mM HCl, 60 μ l of 200 mM sodium borate buffer (pH10.4) and 40 μ l of 1 mM $\text{Ca}(\text{ClO})_2$ and reacting in 60°C water bath for 5 min. To 600 μ l of glyphosate conversion reaction mixture, add 20 μ l of 10 mM NaCN and 20 μ l NDA. Reaction at room temperature for 3 min. Other reaction conditions are as described in Section 3.2.2.2. Each data point is the average of duplicate reactions. The size of the data points approximately reflects the reproducibility of within 10%.

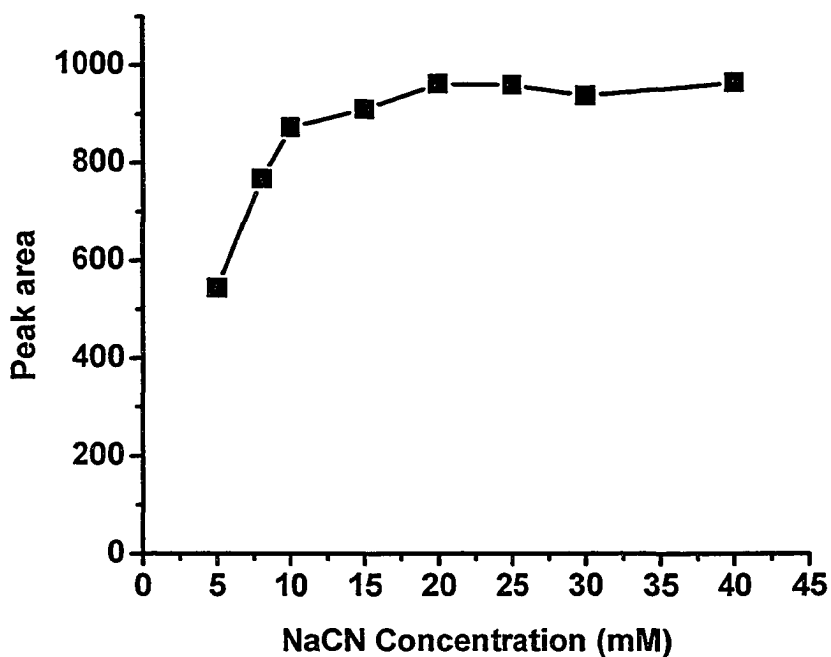


Figure 3.6 Effect of NaCN concentration on glycine labeling. First, glyphosate was oxidized by mixing 500 μ l of 10 μ M glyphosate in 10 mM HCl, 60 μ l of 200 mM sodium borate buffer (pH10.4) and 40 μ l of 1 mM $\text{Ca}(\text{ClO})_2$ and reacting in 60°C water bath for 5 min. To 600 μ l of glyphosate conversion reaction mixture, add 20 μ l of 2.5 mM NDA and 20 μ l NaCN. Reaction at room temperature for 3 min. Other reaction conditions are as described in Section 3.2.2.2. Each data point is the average of duplicate reactions. The size of the data points approximately reflects the reproducibility of within 10%.

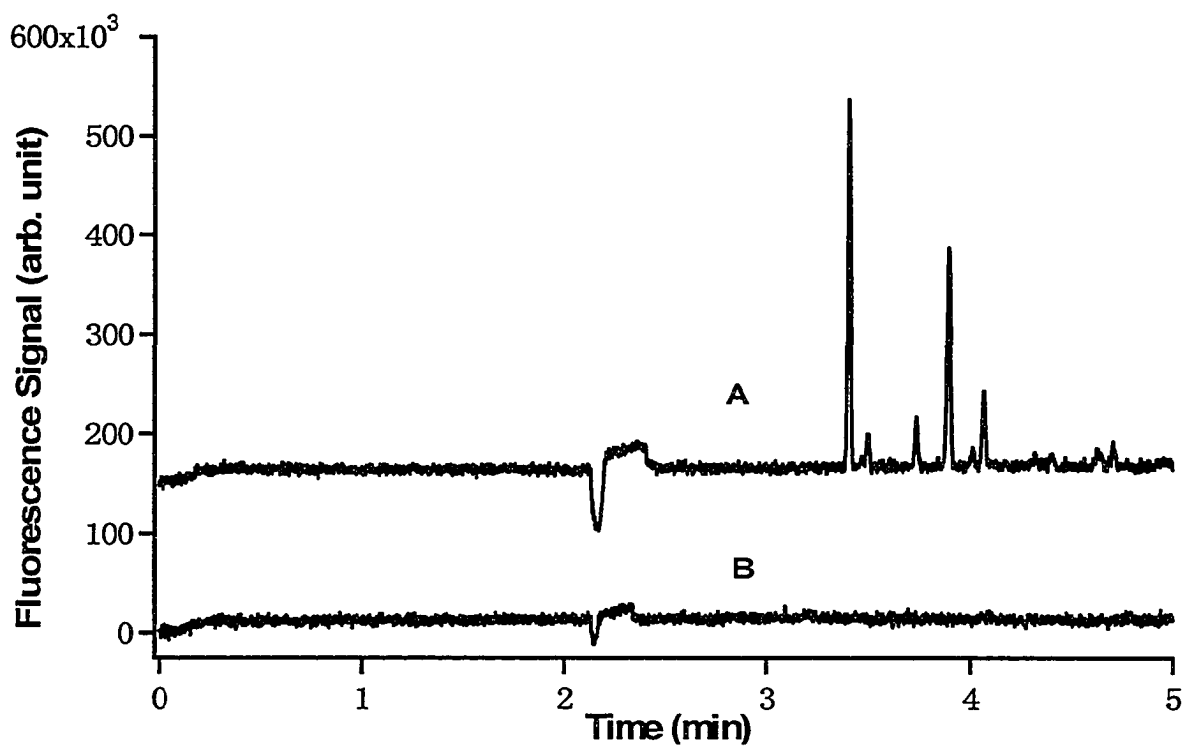


Figure 3.7 Typical electropherogram of side-reaction products in blank reaction. 600 μl of 20 mM pH 9.5 sodium borate was mixed with (A) 20 μl of 40 mM NaCN and 20 μl of 10 mM NDA; (B) 20 μl of 10 mM NaCN and 20 μl of 2.5 mM NDA. Reaction at room temperature for 3 min. Other reaction conditions are as described in Section 3.2.2.2.

3.3.2 Preconcentration on AG1-X8 resin tip

Fifty milliliters of 50 nM glyphosate was pumped through AG1-X8 resin tip at 1, 3, 5 and 8 ml/min, respectively. The glyphosate was then eluted at 0.1 ml/min 10 mM HCl, derivatized as described in Section 3.2.2.2 and separated as in Section 3.2.2.3. No significant change (<3.6%) in peak area was observed. Thus the preconcentration was not affected by the flow rate used for sample loading. Five ml/min was used for all subsequent experiments. On the other hand, elution flow rate did strongly affect glyphosate recovery from the anion exchange preconcentration column. Table 3.1 shows that the recovery percentage decreased at increasing flow rate of 10 mM HCl. At 0.1 ml/min, the first 500 μ l effluent had 88% recovery, however at 0.8 ml/min, the recovery of the first 500 μ l was decreased to 62%. Also, the total recovery of first and second 500 μ l fractions went down from 103% at 0.1 ml/min to 86% at 0.8 ml/min. The strong elution rate dependence indicates that it would take more time for the 10 mM HCl to diffuse into the mesopores of resin beads to elute as much glyphosate as possible from the resin preconcentration tip. In all further experiments, a slow elution rate of 0.1 ml/min was used.

The HCl concentration for elution of glyphosate from the anion exchange preconcentration column was fixed at 10 mM. It was not studied in this work because lower HCl concentration would necessitate larger elution volumes and thus low concentration ratio, while higher HCl concentrations would make it difficult to adjust the pH after elution.

Table 3.1 Effect of elution flow rate on the recovery of glyphosate standard ^a

Elution flow rate (ml/min)	Recovery of 1 st 500 µl effluent (%)	Recovery of 2 nd 500 µl effluent (%)	Recovery sum of 1 st and 2 nd fractions (%)
0.1	88 ± 1	15 ± 3	103 ± 1
0.2	72 ± 1	22 ± 3	94 ± 2
0.5	67 ± 2	24 ± 3	91 ± 1
0.8	62 ± 2	24 ± 2	86 ± 0

- a. Experimental conditions: 50 ml of 100 nM glyphosate was pumped through the AG1-X8 resin tip at 5 ml/min and then eluted with 10 mM HCl at different flow rates. Recovery data were calculated based on comparison with direct labelling 500 µl of 10 µM glyphosate as described in Section 3.2.2.2. Other conditions are as in Section 3.2. Average recovery of duplicate SPE runs.

3.3.3 Quantitative analysis of standard glyphosate solutions

Under optimized conditions above, 50 ml of 1 ~ 100 nM glyphosate was concentrated on the AG1-X8 resin tip. Figure 3.8 shows the electropherogram for 50 ml of a 1 nM glyphosate standard, processed as in Section 3.2.2. The corresponding peak area showed a linear relationship in this concentration range with $R^2=0.999$ and zero intercept with the 95% confidence level (Figure 3.9). The concentration limit of detection (LOD) based on a S/N ratio of 3 was 0.2 nM, and reproducibility of peak area

measured at 20 nM (RSD) was 4.9% (n=9).

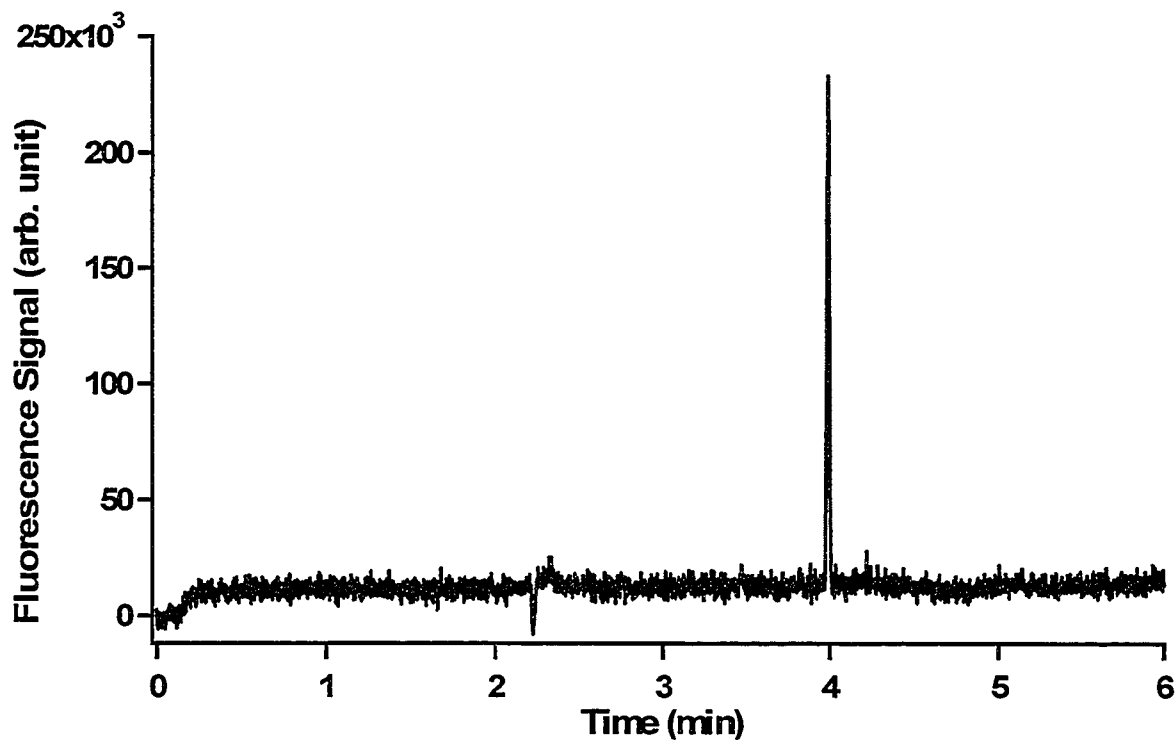


Figure 3.8 Electropherogram of 50 ml of 1 nM glyphosate standard, processed as in Section 3.2.2.

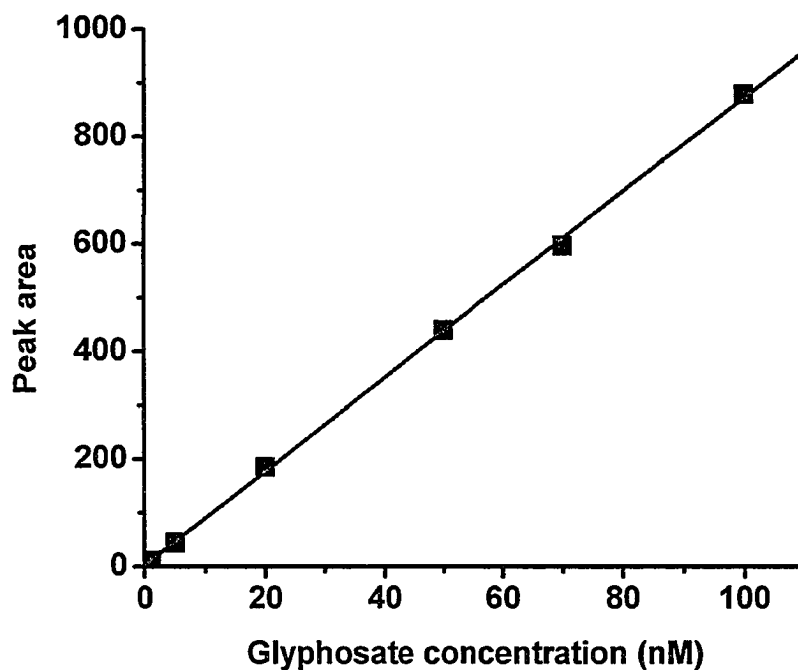
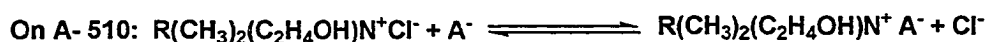
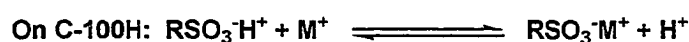


Figure 3.9 Calibration curve of glyphosate standards. Experimental conditions as described in Section 3.2.2. Each data point is the average of duplicate reactions. The size of the data points approximately reflects the reproducibility of within 8%.

3.3.4 Clean-up of real samples

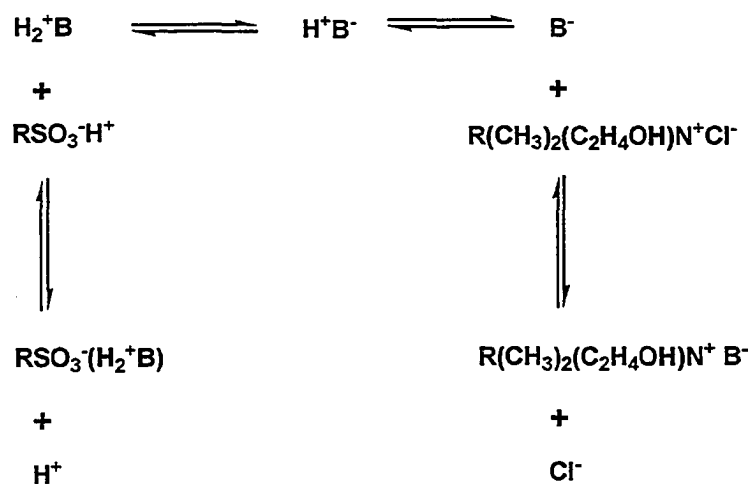
When 50 ml of river water sample spiked at the level of 50 nM glyphosate was pumped directly through the AG1-X8 resin tip, only 7% of the glyphosate was recovered. This low recovery percentage was attributed to the large amount of inorganic ions (and organic compounds as well) present in the sample that can compete with glyphosate and interfere with the ion exchange retention mechanism⁴⁵. Similar to Patsias's work⁴⁴, a clean-up cartridge filled with 300 mg of mixture of Purolite A-510 macroporous type II strong base anion exchange resin(chloride form) and Purolite C-100H strong acid cation exchange resin (hydrogen form) at a mass ratio of 60:40 was coupled on-line before the AG1-X8 resin tip (Figure 3.2b). This mixing ratio is selected because both resins have roughly the same exchange capacity. When the spiked river water sample passes through the clean-up cartridge, interfering inorganic ions (and some organic compounds as well) are retained on the cartridge, as shown below:



Scheme 3.1 the behavior of interfering ionic species on the mixed-bed ion exchange resin

However, glyphosate is an amphoteric compound with pKa₁ 0.8 (1st phosphonic), pKa₂ 2.3 (carboxylic), pKa₃ 6.0 (2nd phosphonic), and pKa₄ 11.0 (amine)² and can be written

simply as HB. When it flows through the mixed resin,



Scheme 3.2 the behavior of glyphosate on the mixed-bed ion exchange resin

The ion exchange reactions on both types of resins would pull the equilibrium $\text{H}_2^+\text{B} \rightleftharpoons \text{H}^+\text{B}^- \rightleftharpoons \text{B}^-$ in the opposite directions. As a result, glyphosate is not retained in the mixed resin column and thus has low loss on cleanup cartridge. To examine how much glyphosate was retained on the mixed bed clean-up cartridge and thus lost, 50 ml of 100 nM glyphosate standard solution was pumped through clean-up cartridge and then the anion exchange preconcentration tip at 5 ml/min. The glyphosate peak area after derivatization was compared with the result for same sample solution passed directly through the preconcentration tip only. 55% of the incoming glyphosate can pass through the cleanup cartridge. Given that 88% of glyphosate can be recovered using AG1-X8 resin tip (Table 3.1), an overall recovery of 48% was obtained.

Prior to analysis it was necessary to check if the sample matrix will overwhelm the capacity of the cleanup cartridge. First, 50 ml of river water spiked at 100 nM

glyphosate was processed but it was found that only 10%, 3% and 2% of glyphosate was recovered for the three consecutive runs using the same clean-up cartridge. This result indicated that the river water contains too many interfering species. Thus 5 ml of the spiked water samples was 10-fold diluted and the resultant 50 ml of diluted sample solution was processed as in Section 3.2.2. Only two runs were performed on each new cleanup cartridge. Good linearity was observed from 40 ~2000 nM with $R^2=0.999$ and zero intercept with the 95% confidence level (spiked concentrations before 10-fold dilution, Figure 3.10). The concentration limit of detection was 5.8 nM. Reproducibility of peak area at 500 nM was $RSD = 6.3\%$ ($n=9$). Consecutively using the same clean-up cartridge showed that for the first 7 runs the observed peak areas remained essentially constant (<3% change in peak area) and then started decreasing gradually (Figure 3.11).

3.4 Conclusion

In this chapter, an off-line preconcentration technique based on ion-exchanger, was used to extract glyphosate from river water sample, followed by conversion, fluorescence labeling and CZE-LIF analysis. Detection limits of 0.2 nM were obtained for glyphosate standard solutions. This is comparable to the lowest LOD reported⁴⁴. For spiked river water sample, a clean-up procedure is required to eliminate other ionic compounds present in river water but nearly half of the glyphosate was lost. Future work is needed to minimize the loss of glyphosate on clean-up cartridge and improve the

recovery.

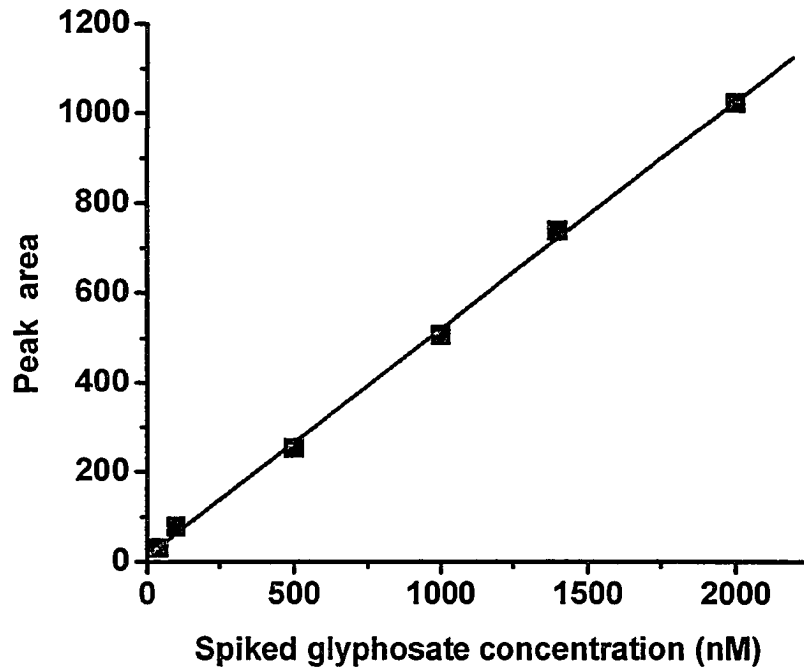


Figure 3.10 Calibration curve of spiked river water sample. 5 ml of river water was spiked by glyphosate, diluted to 50 ml and then processed as in Section 2.2.2. Each data point is average of duplicate measurement. The size of the data points approximately reflects the reproducibility of within 8%.

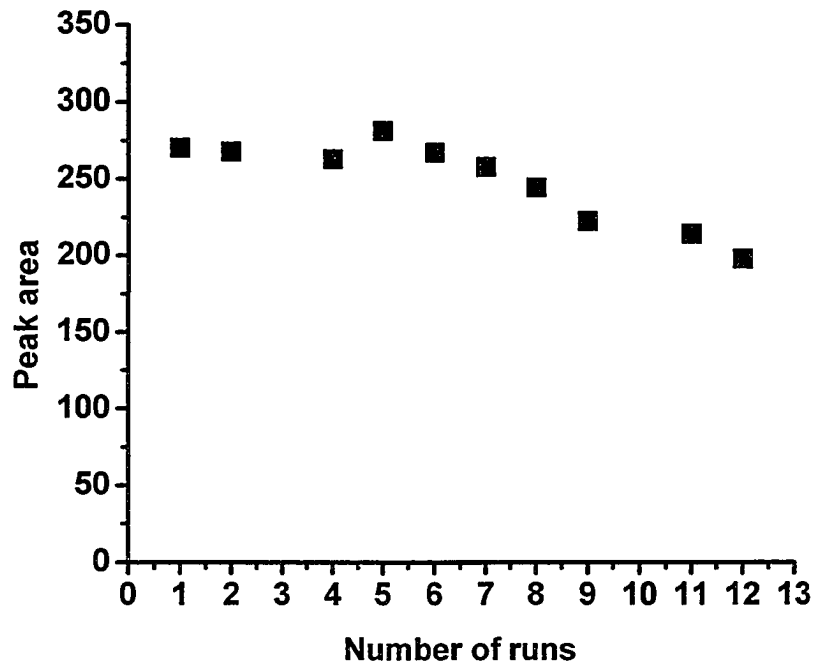


Figure 3.11 Lifetime of a Purolite mixed resin clean-up cartridge. Each data point is average of duplicate measurement at two clean-up cartridges. The size of the data points approximately reflects the reproducibility of within 8%.

3.5 References

- (1) Takacs, P.; Martin, P. A.; Struger, J. *Pesticides in Ontario, a critical assessment of potential toxicity of agricultural products to wildlife, with consideration for endocrine disruption. Volume 2, Triazine herbicides, Glyphosate, and Metolachlor*, 2002.
- (2) Glyphosate Factsheet (a) <http://www.cetos.org/criticalhabitat/glyphosate.pdf>; (b) <http://www.safe2use.com/poisons-pesticides/pesticides/organo/glyphosate.htm>; (c) <http://infoventures.com/e-hlth/pesticide/glyphos.html>; (d) http://www.soils.wisc.edu/virtual_museum/glyphosate/glyphosate_tx.html.
- (3) Alferness, P. L.; Iwata, Y. *Journal of Agricultural and Food Chemistry* **1994**, *42*, 2751-2759.
- (4) Hernandez, F.; Serrano, R.; Miralles, M. C.; Font, N. *Chromatographia* **1996**, *42*, 151-158.
- (5) Kataoka, H.; Ryu, S.; Sakiyama, N.; Makita, M. *Journal of Chromatography A* **1996**, *726*, 253-258.
- (6) Mogadati, P. S.; Louis, J. B.; Rosen, J. D. *Journal of Aoac International* **1996**, *79*, 157-162.
- (7) Sakiyama, N.; Kataoka, H.; Makita, M. *Journal of Chromatography A* **1996**, *724*, 279-284.
- (8) Royer, A.; Beguin, S.; Tabet, J. C.; Hulot, S.; Reding, M. A.; Communal, P. Y. *Analytical Chemistry* **2000**, *72*, 3826-3832.

- (9) Stalikas, C. D.; Pilidis, G. A. *Journal of Chromatography A* **2000**, *872*, 215-225.
- (10) Stalikas, C. D.; Pilidis, G. A.; Karayannis, M. I. *Chromatographia* **2000**, *51*, 741-746.
- (11) Alferness, P. L.; Wiebe, L. A. *Journal of AOAC International* **2001**, *84*, 823-846.
- (12) Hori, Y.; Fujisawa, M.; Shimada, K.; Hirose, Y. *Journal of Analytical Toxicology* **2003**, *27*, 162-166.
- (13) Tseng, S. H.; Lo, Y. W.; Chang, P. C.; Chou, S. S.; Chang, H. M. *Journal of Agricultural and Food Chemistry* **2004**, *52*, 4057-4063.
- (14) Sen, N. P.; Baddoo, P. A. *International Journal of Environmental Analytical Chemistry* **1996**, *63*, 107-117.
- (15) Ridlen, J. S.; Klopff, G. J.; Nieman, T. A. *Analytica Chimica Acta* **1997**, *341*, 195-204.
- (16) Mori, H.; Sato, T.; Nagase, H.; Takada, K.; Nagasaka, M.; Yamazaki, F. *Japanese Journal of Toxicology and Environmental Health* **1998**, *44*, 245-255.
- (17) Vreeken, R. J.; Speksnijder, P.; Bobeldijk-Pastorova, I.; Noij, T. H. M. *Journal of Chromatography A* **1998**, *794*, 187-199.
- (18) Ohno, C.; Otaki, M.; Mori, Y.; Hisamatsu, Y.; Nakazawa, H. *Journal of the Food Hygienic Society of Japan* **1999**, *40*, 75-79.
- (19) Le Fur, E.; Colin, R.; Charreteur, C.; Dufau, C.; Peron, J. J. *Analisis* **2000**, *28*, 813-818.
- (20) Takano, I.; Nagayama, T.; Kobayashi, M.; Ito, M.; Tamura, Y.; Takada, C.;

- Kimura, N.; Kitayama, K.; Yasuda, K. *Journal of the Food Hygienic Society of Japan* **2000**, *41*, 242-245.
- (21) Takahashi, K.; Horie, M.; Aoba, N. *Journal of the Food Hygienic Society of Japan* **2001**, *42*, 304-308.
- (22) Veiga, F.; Zapata, J. M.; Marcos, M. L. F.; Alvarez, E. *Science of the Total Environment* **2001**, *271*, 135-144.
- (23) Le Bot, B.; Colliaux, K.; Pelle, D.; Briens, C.; Seux, R.; Clement, M. *Chromatographia* **2002**, *56*, 161-164.
- (24) Lee, E. A.; Zimmerman, L. R.; Bhullar, S. S.; Thurman, E. M. *Analytical Chemistry* **2002**, *74*, 4937-4943.
- (25) Rubio, F.; Veldhuis, L. J.; Clegg, B. S.; Fleeker, J. R.; Hall, J. C. *Journal of Agricultural and Food Chemistry* **2003**, *51*, 691-696.
- (26) Nedelkoska, T. V.; Low, G. K. C. *Analytica Chimica Acta* **2004**, *511*, 145-153.
- (27) Cikalo, M. G.; Goodall, D. M.; Matthews, W. *Journal of Chromatography A* **1996**, *745*, 189-200.
- (28) You, J.; Kaljurand, M.; Koropchak, J. A. *International Journal of Environmental Analytical Chemistry* **2003**, *83*, 797-806.
- (29) Goodwin, L.; Startin, J. R.; Keely, B. J.; Goodall, D. M. *Journal of Chromatography A* **2003**, *1004*, 107-119.
- (30) Safarpour, D.; Katz, S. *Abstracts of Papers of the American Chemical Society* **2002**, *223*, U57-U57.

- (31) Molina, M.; Silva, M. *Electrophoresis* **2002**, *23*, 1096-1103.
- (32) Khrolenko, M.; Dzygiel, P.; Wieczorek, P. *Journal of Chromatography A* **2002**, *975*, 219-227.
- (33) Goodwin, L.; Hanna, M.; Startin, J. R.; Keely, B. J.; Goodall, D. M. *Analyst* **2002**, *127*, 204-206.
- (34) Chang, S. Y.; Liao, C. H. *Journal of Chromatography A* **2002**, *959*, 309-315.
- (35) Molina, M.; Silva, M. *Electrophoresis* **2001**, *22*, 1175-1181.
- (36) Hooijschuur, E. W. J.; Kientz, C. E.; Dijksman, J.; Brinkman, U. A. T. *Chromatographia* **2001**, *54*, 295-301.
- (37) Safarpour, H.; Asiaie, R. *Electrophoresis* **2005**, *26*, 1562-1566.
- (38) Ishiwata, T. *Bunseki Kagaku* **2004**, *53*, 863-864.
- (39) Clegg, B. S.; Stephenson, G. R.; Hall, J. C. *Journal of Agricultural and Food Chemistry* **1999**, *47*, 5031-5037.
- (40) Stalikas, C. D.; Konidari, C. N. *Journal of Chromatography A* **2001**, *907*, 1-19.
- (41) Grey, L.; Nguyen, B.; Yang, P. *Journal of Aoac International* **2001**, *84*, 1770-1780.
- (42) Watanabe, S. *Journal of the Food Hygienic Society of Japan* **2004**, *45*, 38-43.
- (43) Hidalgo, C.; Rios, C.; Hidalgo, M.; Salvado, V.; Sancho, J. V.; Hernandez, M. *Journal of Chromatography A* **2004**, *1035*, 153-157.
- (44) Patsias, J.; Papadopoulou, A.; Papadopoulou-Mourkidou, E. *Journal of Chromatography A* **2001**, *932*, 83-90.

- (45) Mallat, E.; Barcelo, D. *Journal of Chromatography A* **1998**, *823*, 129-136.
- (46) Sancho, J. V.; Hernandez, F.; Lopez, F. J.; Hogendoorn, E. A.; Dijkman, E.; vanZoonen, P. *Journal of Chromatography A* **1996**, *737*, 75-83.
- (47) Demontigny, P.; Stobaugh, J. F.; Givens, R. S.; Carlson, R. G.; Srinivasachar, K.; Sternson, L. A.; Higuchi, T. *Analytical Chemistry* **1987**, *59*, 1096-1101.
- (48) Abdullah, M. P.; Daud, J.; Hong, K. S.; Yew, C. H. *Journal of Chromatography A* **1995**, *697*, 363-369.
- (49) Sundaram, K. M. S.; Curry, J. *Journal of Liquid Chromatography & Related Technologies* **1997**, *20*, 511-524.
- (50) Kwakman, P. J. M. Ph.D Thesis, Vrije University, Netherlands, **1991**.
- (51) Ternay, A. T. *Comtemporary Organic Chemistry*, 2nd ed.; W. B. Saunders: Philadelphia, **1979**.

Chapter 4. A Capillary-Tip Chromatographic Beads-Packed Monolithic Preconcentrator – Fabrication, Characterization and Application in Determination of Herbicides Using Capillary Electrophoresis – Laser Induced Fluorescence Detection

4.1 Introduction

Capillary electrophoresis (CE) has become one of the major separation techniques¹, despite complaints about its poor detection sensitivity almost since its invention. This is especially true when ultraviolet detection is used. For decades analytical chemists have worked to solve this problem in different ways. More sensitive detection schemes have been coupled to capillary, including sheath-flow laser-induced fluorescence detection (LIF), electrochemical detection and mass spectrometry². Another way is to use a conventional detector and enrich the analytes from diluted sample solutions in either an off-line or on-line manner. On-line enrichment methods are usually preferred because they have a lower sample usage and less time-consuming steps³.

As described in Chapter 1, on-line pre-concentration techniques may be classified into two groups: (a) electrophoresis-based stacking or sweeping; and (b) solid phase extraction (SPE)-based pre-concentration. In stacking or sweeping, a discontinuous buffer system within the capillary causes the acceleration/deceleration of the analyte migration upon crossing the interface of discontinuous buffer zones⁴⁻¹⁰. The high salt stacking in Chapter 2 is an example of this approach. An advantage of stacking and sweeping pre-concentration is that no modifications need be done inside the capillary or

on capillary inner wall. However stacking and sweeping pre-concentration factors are very sensitive to the sample matrix. In SPE-based pre-concentration methods, a SPE material is immobilized inside the capillary to selectively capture analytes when the sample solution passes through ^{7, 11}. In-capillary frits are usually required to retain the SPE material within the capillary. These frits can cause serious problems such as bubble formation and mismatched EOF ¹². Harrison's group reported the use of weirs to retain octadecylsilane (ODS) packing in a 330 pl chamber on a microfluidic device for up to 500-fold on-chip preconcentration of BODIPY ^{13, 14}.

Alternatively, SPE materials can be held in place by monolith techniques ^{15, 16}, as described in Section 1.3.2. For example, Baryla and co-worker ¹⁶ reported a monolithic methacrylate polymer fabricated at the inlet end of a capillary by photo-initiated polymerization to pre-concentrate S-propranolol in the low nanomolar range. Sol-gel monolith chemistry has been widely used in separation sciences ¹⁷. The fabrication, characterization and applications of sol-gel monoliths have been extensively reviewed ^{17, 18}. Many papers have explored chromatographic beads entrapped in a silica sol-gel monolith for capillary electrochromatography (CEC) or capillary liquid chromatography ¹⁸⁻²³. However, the separation performance of such columns is usually modest ²⁰ due to difficulties in fabricating homogeneous monolith columns. This indicates that a sol-gel monolith may not be suitable for high-performance separations. However they still show promise for preconcentration purposes.

The objective of the research in this chapter is the development of a capillary-tip on-line pre-concentrator for charged analytes after fluorescence derivatization. The selected test analytes are ampropylfos (AMPR) and glufosinate (GLUF), as shown in

Figure 4.1. They are widely employed as non-selective, post-emergence contact herbicides. As discussed in Chapter 3, it is important to detect herbicide residues in natural environment and foods as these residues can cause problems to human health. Polymeric chromatographic beads PRP-1 were entrapped into an alkoxide sol-gel monolith to pre-concentrate the analytes at the capillary tip. The retained analytes were then eluted as a highly-concentrated short sample plug and separated by capillary electrophoresis and detected by LIF. The proposed method may be applied to detect residues of these herbicides in soil, water, foods, vegetables and fruits.

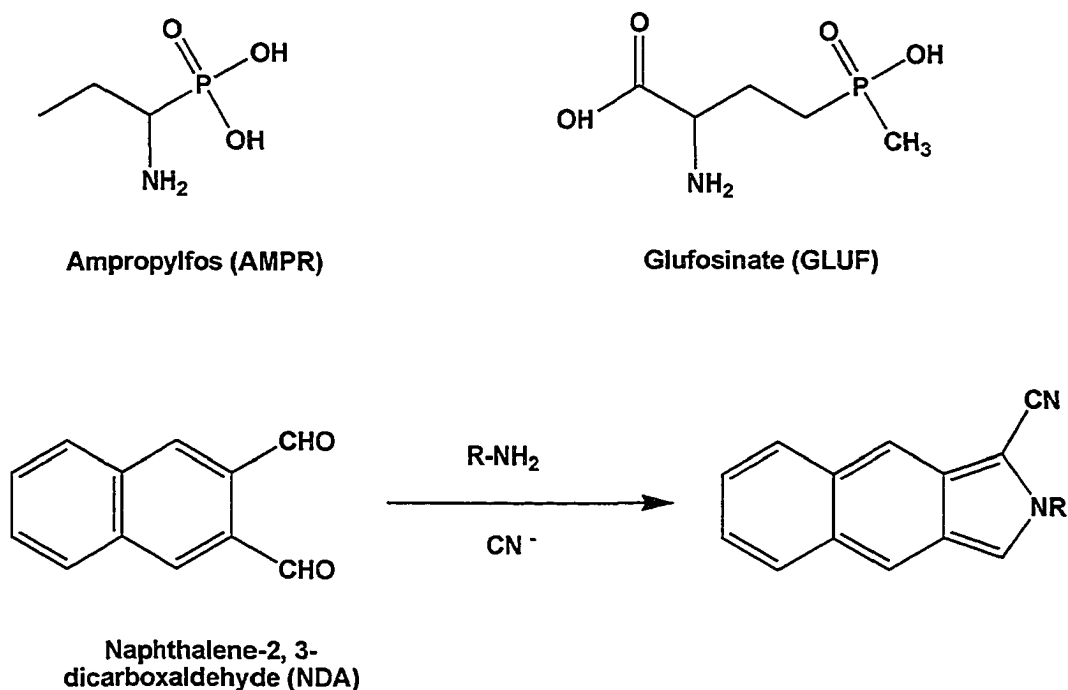


Figure 4.1 Molecular structures of test analytes and derivatization products. R stands for non-amino group moieties in AMPR/GLUF.

4.2 Experimental

4.2.1 Reagents and Materials

Poly (ethylene glycol) (PEG, typical Mn 10,000), sodium hydroxide (min. 98%), tetramethyl orthosilicate (TMOS, 98%), ampropylfos (3-aminopropylphosphonic acid, AMPR, 99%), sodium cyanide (99.98%), and naphthalene-2, 3-dicarboxaldehyde (NDA, 98%) were purchased from Aldrich (Milwaukee, WI, USA). Glufosinate ammonium (GLUF, 97.5%) was from Riedel-de Haën Laborchemikalien GmbH & Co.KG (Seelze, Germany). The structures of the test analytes AMPR, GLUF, and their NDA-derivatives are shown in Figure 4.1. Sodium tetraborate was from BDH (Poole, England). Acetonitrile (HPLC grade) was from Fisher (Fair Lawn, NJ, USA). Acetic acid was from Anachemia (Rouses, NY, USA). Sodium chloride was from EMD Chemicals (Gibbstown, NJ, USA). All solutions were prepared with Nanopure 18 M Ω water (Barnstead, Chicago, IL, USA) except NDA which was in acetonitrile. All CE running buffers and eluents were filtered with 0.45 μ m MILLEX[®]-HA mixed cellulose esters filter units (Millipore, Molsheim, France) before use.

PRP-1 bulk packing 3 μ m (lot No: 600F) was purchased from Hamilton (Reno, Nevada, USA). This is a polystyrene divinylbenzene HPLC packing possessing 100 Å mesopores. B-D 1-ml syringe and 26G1/2 sterile needles were from Beckton, Dickinson and Company (Franklin Lakes, NJ, USA).

4.2.2 Fabrication of PRP-1 packed monolith

A 120 cm-long 75 μ m-i.d 360 μ m-o.d fused-silica capillary (Polymicro, Phoenix, AZ) was conditioned by rinsing at 20 psi with 1 M NaOH for 60 min, 0.1 M NaOH for 30 min and finally water for 60 min. After conditioning, the long capillary was cut into

about 15 cm-long segments and placed in a 120°C drying oven for 2 hours.

The alkoxide-based sol-gel solution was prepared by adding 2.5 ml of 10 mM acetic acid to 220 mg PEG in a 5 ml beaker. The solution was stirred gently to dissolve the PEG, then the beaker was semi-buried into an ice bath and 1 ml of TMOS was added. The solution was allowed to react with stirring for 45 min. The interface between the two layers disappeared after about 30 min and finally a homogeneous sol-gel solution was obtained.

The PRP-1 beads were entrapped in the silica sol-gel monolithic segments as follows. First weigh 75 mg of PRP-1 beads into a 1.5 ml micro-centrifuge tube. Next, 500 µl of the freshly prepared sol-gel solution was added. The suspension was immediately vortexed vigorously for 3 min on a MV1 mini vortexer (VWR International, West Chester, PA, USA) to ensure thorough mixing, and then sonicated on a 75HT sonicator (VWR) for 1 min to degas. The PRP-1 sol-gel suspension solution was charged into 15 cm-long capillary segments using a 1-ml syringe connected to the capillary through a 26G1/2 sterile needle and a 5 mm x 0.015" i.d. PE-20 polyethylene tubing (Clay Adams, Parsippany, NJ, USA). The packed capillary segments were checked carefully for uniform filling and distribution using a 200X optical microscope (BH-2, Olympus, Lake Success, NY, USA). If the capillary was uniformly filled, both ends of the capillary were sealed by connecting to a 5 mm x 0.015" i.d. polyethylene tubing and immersed into a 40°C water bath for incubation overnight (about 18 h). After incubation, the packed monolith was flushed briefly with water and acetonitrile, and then checked again using the 200X optical microscope for monolith structure uniformity. These packed capillary segments were filled with acetonitrile and both ends were sealed with

polyethylene tubing for storage. No degradation was observed for storage times up to four weeks.

Immediately before use, a pre-conditioning procedure was required. From the PRP-1 packed monolith segment, a ~1-mm segment was cut using a capillary cutting stone (Beckman). This short monolith segment was attached to the inlet tip of a bare capillary using a short polyethylene tubing as shown in Figure 4.2. The pre-conditioning procedure was carried out by rinsing with 25 mM sodium borate buffer at 20 psi for 60 min, followed by running buffer for 5 min.

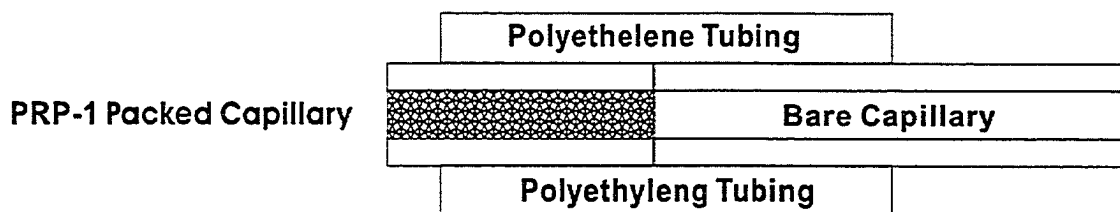


Figure 4.2 PRP-1 packed monolith tip attached to the inlet of bare capillary. Not drawn to scale.

4.2.3 SEM imaging

All SEM experiments were performed on a JSM6301 FVX scanning electron microscope (Japan Electron Optics Ltd.) located in the Department of Earth and Atmospheric Sciences, University of Alberta. As described in Section 4.2.2, the 1-mm PRP-1 packed monolith segment was attached to the inlet end of a capillary cartridge, pre-conditioned, rinsed briefly with water and air-dried. Then the preconditioned PRP-1

tip was fixed vertically to the SEM sample holder using epoxy resin. Silver paint was applied to the base of the capillary tubes to provide a line of conductivity to the stub. 200Å of gold was sputtered onto the segment (2 min sputtering time). SEM images were taken at an acceleration voltage of 1 kV and a working distance of 8 ~ 19 mm.

4.2.4 Fluorescence derivatization

Diluted mixed analyte solutions were prepared from 1 mM stock solutions of AMPR and GLUF. To a 4 ml glass vial were added 200 µl of diluted analyte solution, 200 µl of 20 mM NaCN and 80 µl of 5 mM NDA, and then diluted by 25 mM pH 9.4 sodium borate buffer to a total volume of 4 ml. The reaction mixture was vortexed briefly and allowed to react at room temperature in the dark for 30 min. This reaction solution was diluted 100-fold in 15 mM pH 4.8 sodium acetate buffer containing 100 mM NaCl before sample injection.

4.2.5 CE separation

All CE experiments were performed on a P/ACE 2100 capillary electrophoresis system (Beckman Instruments, Fullerton, CA, USA) equipped with a laser-induced fluorescence detector and *P/ACE Station* software (version 1.2, Beckman) for instrument control and data acquisition. The P/ACE 2100 instrument had been upgraded to include many features of a P/ACE 5000 series instrument, including the ability to simultaneously apply both voltage and pressure. A 415 nm violet diode laser (model LDCU 12/4673, Power Technology Inc., Little Rock, AR, USA) was used as the excitation source. The laser was coupled to the LIF detector through an SMA fiber optic receptacle, a 1-m

multimode fiber optic patchcord with a 100/140- μm (core/cladding) diameter and SMA 906 connectors (Polymicro Technologies, Phoenix, AZ, USA). An XB84-500DF25 band pass filter (Omega Optical, Brattleboro, VT, USA) was used to collect the fluorescence signal at 500 ± 12.5 nm. The laser output power was 0.2 mW as measured at the outlet of optic fibre. Data were collected at 10 Hz with a detector response time of 0.1 s. The capillary was always thermostated at 25°C.

CE separations were performed at 20 kV (normal polarity) across a 37 cm-long (30 cm to the detection window), 50 μm -i.d fused-silica capillary. The CE running buffer was 15 mM pH 4.8 sodium acetate buffer unless stated otherwise. Before use each new bare capillary was conditioned by flushing at 20 psi with 1 M NaOH for 10 min, distilled water for 10 min, 0.1 M NaOH for 5 min and distilled water for 10min.

For CE experiments without the PRP-1 tip, injections were 3 s hydrodynamic at 0.5 psi. Between runs the capillary was washed at 20 psi with 0.1 M NaOH for 2 min, distilled water for 2 min and running buffer for 5 min.

For CE experiments with the PRP tip, a 1-mm PRP-1-packed monolith segment was cut and attached to the inlet tip of the 37 cm bare capillary using a short polyethylene tubing, as shown in Figure 4.2. The complete running procedure was as follows: The sample was injected at 20 psi for 5 min, followed by a 0.3 min rinse at 20 psi with running buffer. After injection of eluent containing 15 mM pH 4.8 sodium acetate buffer and acetonitrile (40:60) at 0.5 psi for 5 s, the 5 min electropherogram was initiated upon application of 20 kV voltage plus 0.5 psi forward pressure. Between runs, the PRP-1 tip and capillary were washed at 20 psi with eluent for 0.5 min and then 15 mM pH 4.8 acetate buffer for 1 min. At the end of day, the PRP-1 tip was discarded and the bare

capillary was cleaned by rinsing at 20 psi with 0.1 M NaOH for 15 min and distilled water for 15 min.

4.3 Results and Discussion

4.3.1 Fabrication and pre-conditioning of the PRP-1 monolith tips

The monolith fabrication procedure was adapted from the method of Tanaka and coworkers²⁴. However, our monolith is employed solely as an inert support for the HPLC packing beads. Thus no mesopores are needed. In our recipe no urea was used nor was the monolith heated above 100°C. The lack of mesopores allowed simplification of Tanaka's procedure and may bring us some extra advantages if biological recognizing elements are used to selectively extract analytes from sample solutions in future work.

Figure 4.3 shows scanning electron micrograms (SEM) of the polystyrene divinylbenzene PRP-1 chromatographic beads. The PRP-1 beads are nominally 3 μm in diameter. Most beads agree well to this nominal size. However, there is significant dispersivity evident in Figure 4.3a, where beads range in diameter from 1.5 to 4.7 μm . Figure 4.3b is a close-up image of a single PRP-1 bead. In particular, one can note the roughened surface of the bead. This textured surface will be used later to identify the beads *versus* the sol-gel skeleton.

Figure 4.4 shows the alkoxide monolith without entrapped beads after incubation at 40°C overnight. One can see that after incubation the alkoxide silica sol-gel has become a porous network structure attached firmly to the surface of capillary. The sol gel skeleton is about 1 μm in diameter and contains throughpores of approximately 2~10 μm in diameter. These values are smaller than Tanaka's monolith (2 and 8 μm , respectively,

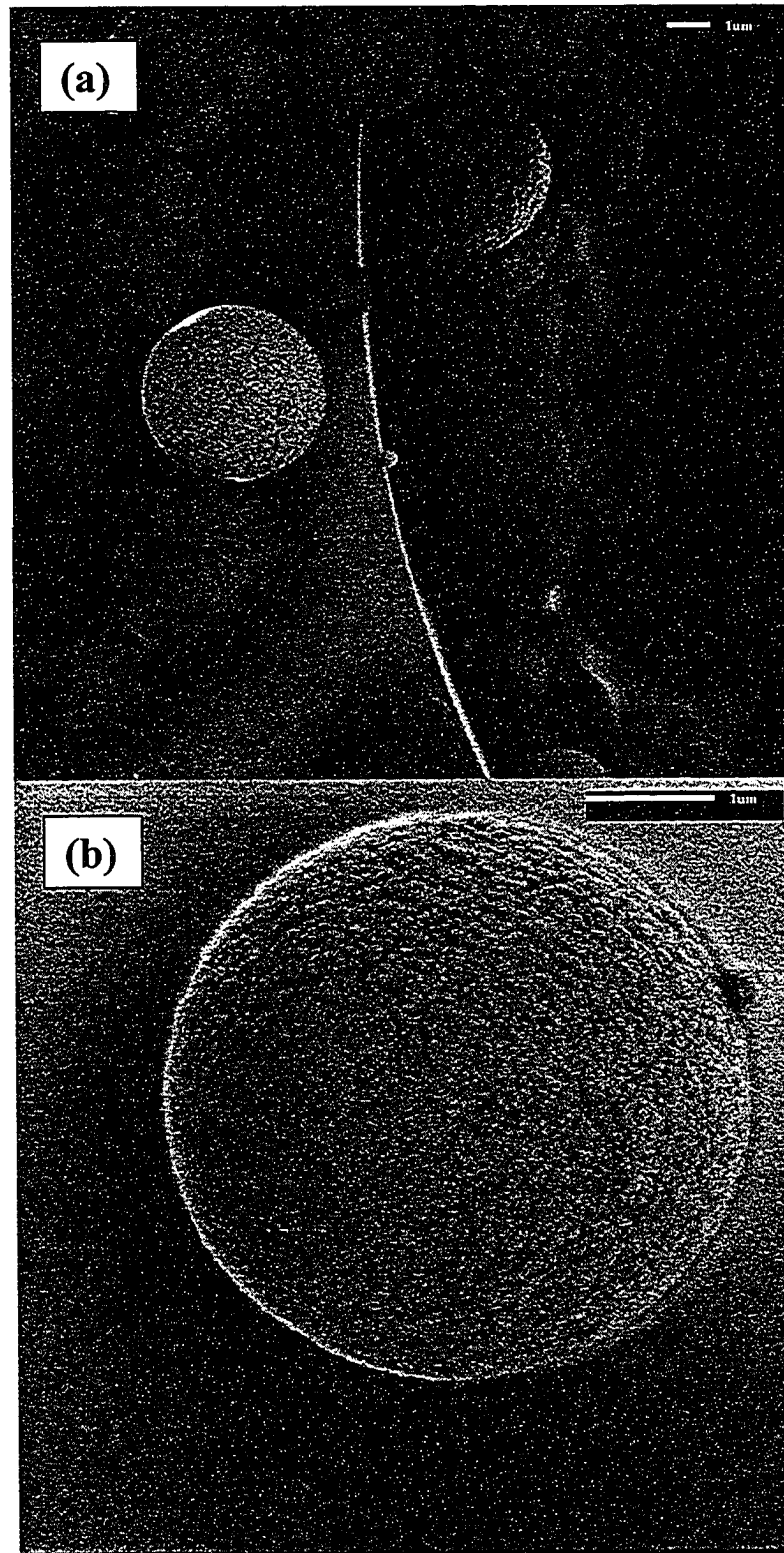


Figure 4.3 PRP-1 beads, Magnification: (a) 5000X; (b) 15,000X.

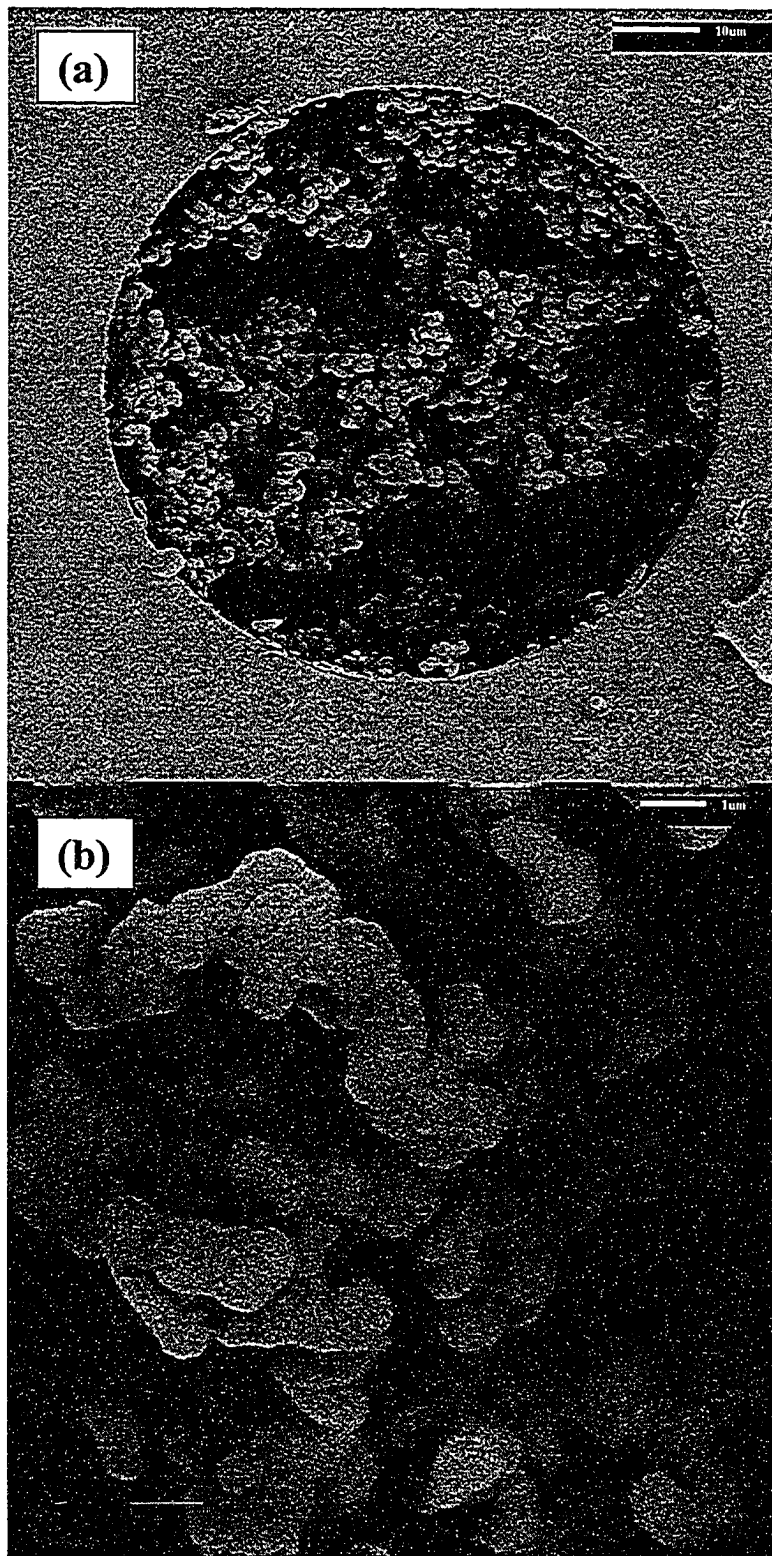


Figure 4.4 Sol-gel monolithic structure (without packed PRP-1 beads). Magnification: (a) 1000X; (b) 7500X

Reference ²⁴, Table 2), although the cross-section images looks very similar to Tanaka's monolith (Ref ²⁴, Figure 1a). CE experiments were performed as described in Section 4.2.5 but 1 mm sol-gel monolith tip without packed PRP-1 beads was used. No detectable peaks were observed and thus it was confirmed that no analytes used in this work were retained on capillary wall or silica monolith without embedded PRP-1 beads.

The porous structure of the monolith can provide an inert support to immobilize HPLC beads ²¹⁻²³. The particle entrapment eliminates the need to fabricate frits to retain the chromatographic beads. In this work the PRP-1 beads were added to the sol-gel solution and charged into the capillary. The capillary was then incubated overnight at 40°C. Figure 4.5 shows the SEM images of PRP-1 beads entrapped in our sol-gel monolith. It is evident in Figure 4.5b that almost all PRP-1 beads are completely encapsulated by a thin sol-gel silica coating "shell". The presence of the "shell" is also indicated by the fusion of particles due to the formation of a sol-gel silica "bridge" between the individual particles. It is believed that these bridges provide the chromatographic bed with its structural integrity. Similar bridges are evident in Dulay and co-workers' studies ²³, but are not evident in Chirica and Remcho's work ^{21,22}. Chirica and Remcho attributed immobilization of their Nucleosil C18 HPLC particles to a small amount of irregularly shaped silica fragments located between the particles in their SEM images (reference ²¹, Figure 2). In contrast, Dulay and co-workers showed SEM images of their monolith in which the HPLC particles appear imbedded within the bulk sol-gel silica (reference ²³, Figure 1b). The entire interstitial space between the HPLC particles is filled with a featureless sol-gel silica, i.e., no skeletal silica structure is evident ²³. This implies that the presence of this interstitial silica shell depends more on the

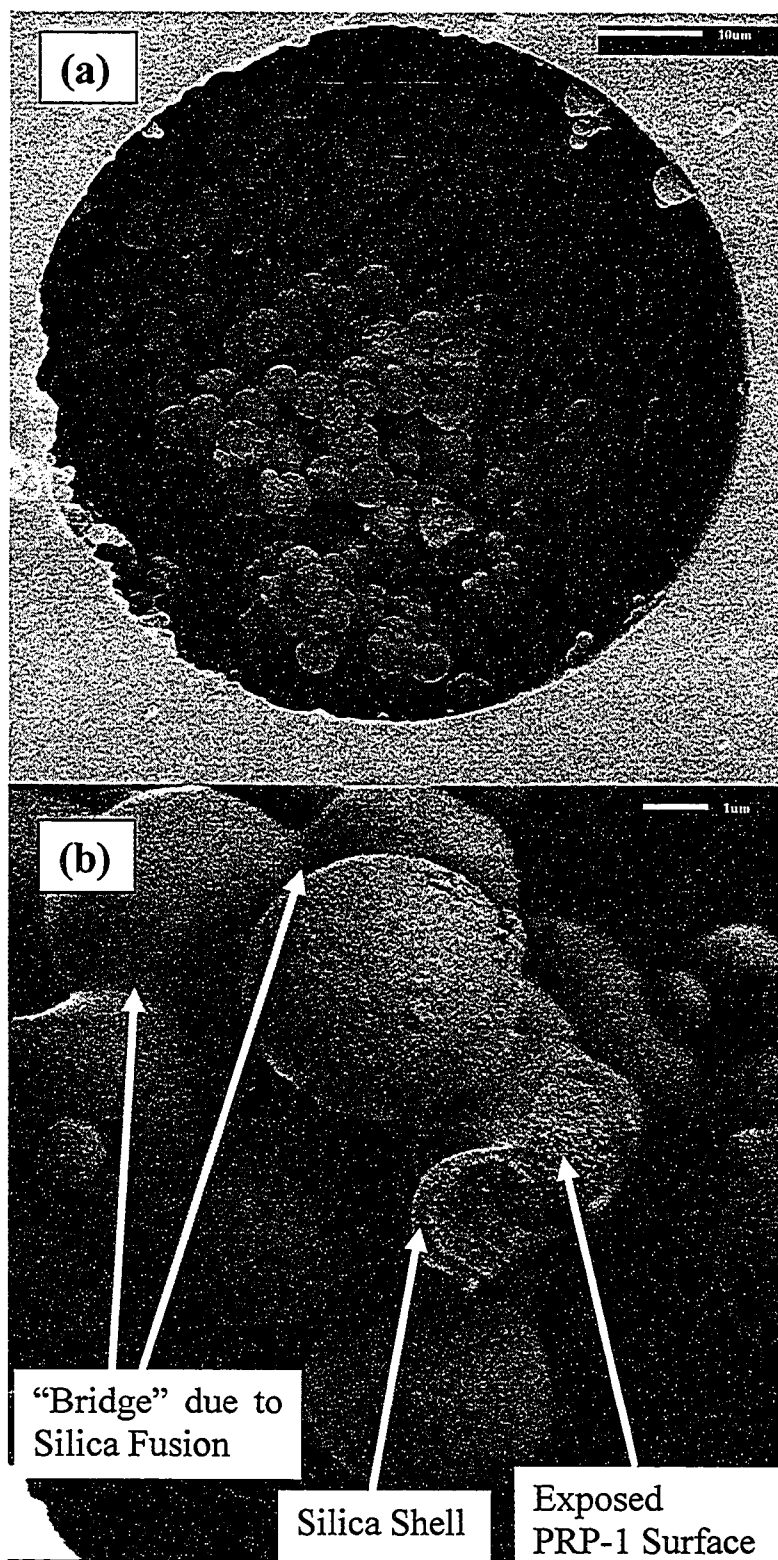


Figure 4.5 PRP-1-packed monolith, before pre-conditioning. Magnification: (a) 1200X; (b) 7500X.

fabrication protocols of the sol-gel monoliths, not on the material properties of the entrapped HPLC beads because both groups used the same type of chromatographic particles.

In Figure 4.3b it was shown that the PRP-1 beads display a textured or roughened surface. Thus the presence or absence of this texturing feature allows an assessment of whether the surface of the beads are exposed or covered by the sol-gel. Figure 4.5b shows that only a very small fraction of the beads have surface that is exposed to the solution. The presence of the sol-gel shell surrounding the PRP-1 beads strongly affects its chromatographic retention. For instance, CE experiments with packed monoliths such as shown in Figure 4.5 displayed a poor pre-concentration performance for derivatized AMPR and GLUF. In Figure 4.7A, only a small AMPR peak was observed, and GLUF, although with three times concentration injected as AMPR, was barely detectable. Thus, while the sol-gel provides structural integrity to the PRP-1 bed, the formation of a shell around each particle interferes with analyte access to the stationary phase.

A simple solution to this problem is what we called the *pre-conditioning* procedure. That is, rinsing the PRP-1 beads packed monolith with 25 mM pH 9.4 sodium borate buffer at 20 psi for 60 min. The SEM images in Figure 4.6 show that after 60 min pre-conditioning the shell encapsulating PRP-1 beads has been partially dissolved and peeled off. As a result, much more of the surface of the PRP-1 beads is exposed to the sample solution. The increased exposure of the PRP-1 surface results in greater retention of the analytes. Figure 4.7 illustrates the effect of increasing the time during which the PRP-1 monolith is pre-conditioned with 25 mM sodium borate (pH 9.4). Each monolith was mounted onto the inlet of the separation capillary, and then a mixture of 5 nM AMPR

and 15 nM GLUF was loaded onto the capillary for 5 min at 20 psi. The analytes were then eluted and separated as detailed in Section 4.2.5. Under these conditions, the electropherograms (Figure 4.7B ~ G) contain a negative dip caused by the acetonitrile and indicating the combined EOF and pressure flow, and then peaks for AMPR and finally GLUF. As the pre-conditioning time is increased (from Figure 4.7A to 4.7G), the peak heights for both AMPR and GLUF increase dramatically. This indicates that monoliths that have been pre-conditioned for longer periods of time can pre-concentrate AMPR and GLUF more effectively. However, the peaks for the two analytes do not increase in same proportion. Prior to pre-conditioning only AMPR peak is detected (Figure 4.7A). As the pre-conditioning is performed, the GLUF peak appears (10 min pre-conditioning, Figure 4.7B), and increases in size quickly (Figures 4.7C-4.7G) but remains smaller than the AMPR peak despite GLUF being three times more concentrated.

The two key observations from Figure 4.7 are that the pre-conditioning improves analyte preconcentration by the PRP-1 tips and that there is some sample discrimination in this preconcentration. The mechanism hidden behind these behaviors may be as follows. Before pre-conditioning, the PRP-1 beads are almost completely coated by the silica shell, as shown in Figure 4.5. Silica has an isoelectric point of around 2.5²⁵. Thus, the silica shell is negatively charged in the pH 4.8 buffers used in this work. The negatively charged shell surface would strongly repel the negatively charged analytes, *i.e.*, the analytes would experience Donnan exclusion²⁶ and most of the analytes will be lost. At pH 4.8 the derivatization product of GLUF would be more negatively charged than AMPR (discussed in Section 4.3.2.1). As a consequence, the GLUF would experience greater Donnan exclusion upon approaching the totally entrapped PRP-1 beads. Thus

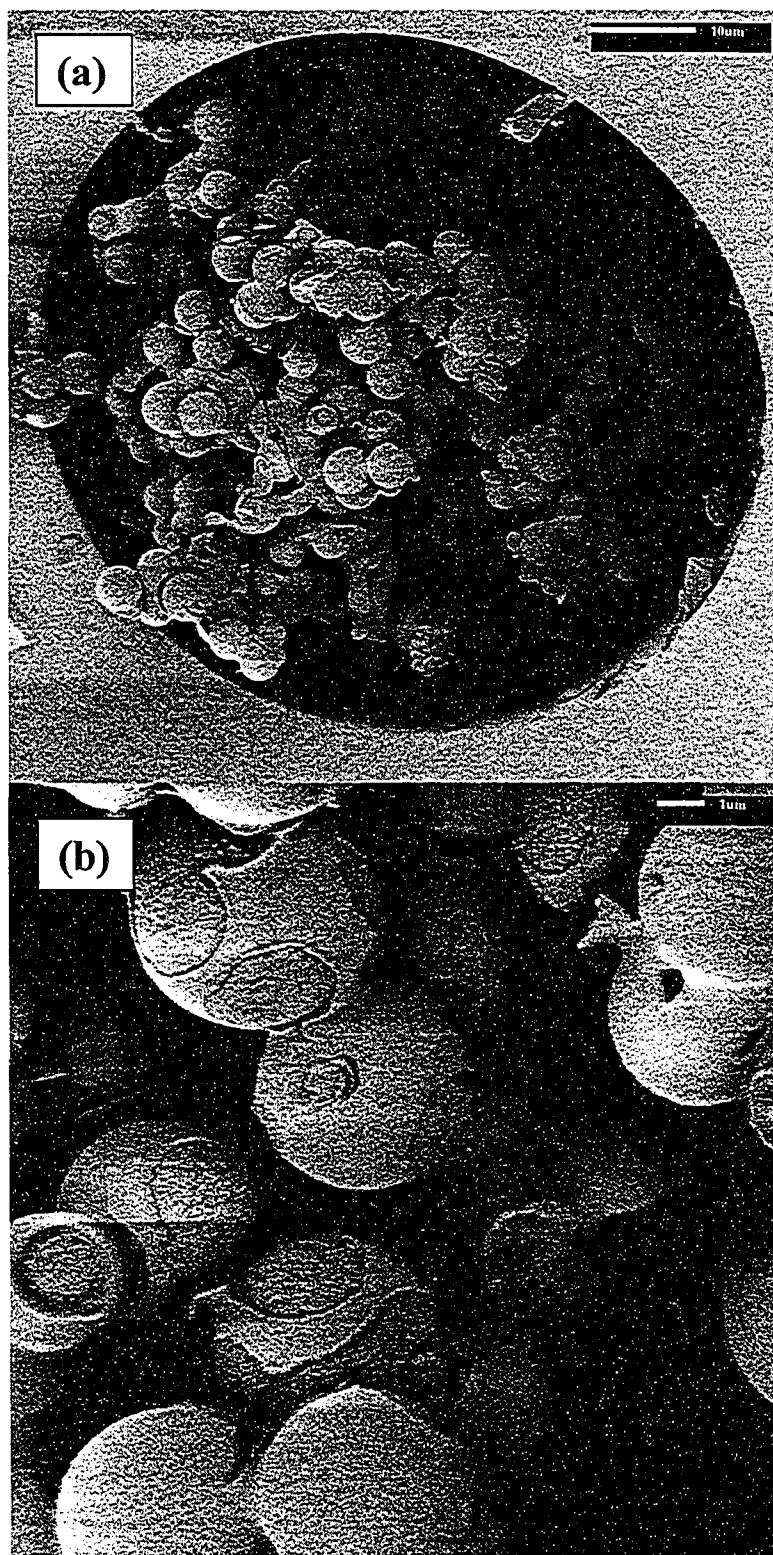


Figure 4.6 PRP-1-packed monolith, after pre-conditioning with 25 mM borate solution at 20 psi for 60 min. Magnification: (a) 1200X; (b) 5500X

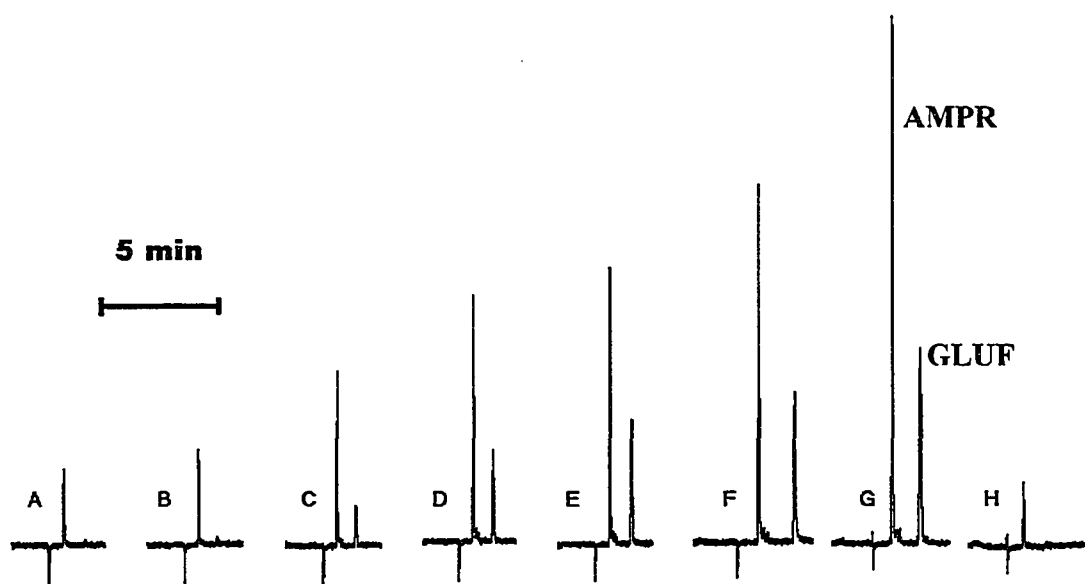


Figure 4.7 Effect of pre-conditioning time. A) Before pre-conditioning, B) ~ G) after pre-conditioning with 25 mM pH 9.4 sodium borate buffer at 20 psi for each period of 10 min, H) after pre-conditioning with 15 mM pH 4.8 sodium acetate buffer at 20 psi for 60 min.

this Donnan exclusion resulted in low pre-concentration of AMPR and no detectable GLUF in Figure 4.7A. As pre-conditioning proceeds, the silica shell dissolves partially, resulting in exposure of more and more of the PRP-1 bead surface to the sample solution, as shown in Figure 4.6. This reduced the Donnan exclusion caused by the silica shell, allowing greater and greater pre-concentration of the analytes. Also, as GLUF initially experiences greater Donnan exclusion, its peak heights increase more dramatically than AMPR.

As a control study of the pre-conditioning procedure, a PRP-1 monolith tip was pre-conditioned with 15 mM pH 4.8 sodium acetate buffer at 20 psi for 60 min. No

dissolution of the sol-gel would be expected at this pH. The resultant electropherogram (Figure 4.7H) is identical to that in Figure 4.7A (no pre-conditioning), showing only a low AMPR peak and no GLUF. The SEM image in Figure 4.8 also confirms that the coating shell remains almost intact. This indicates that the pre-conditioning procedure is not simply a physical phenomenon due to erosion by the hydrodynamic flow. Rather chemical dissolution is important. Using the pH 9.4 sodium borate buffer a 60 min conditioning time seems optimal for this project. High pre-concentration levels were obtained without undermining the monolithic structure. If the pre-conditioning time was longer than 90 min or the pH of the pre-conditioning buffer was higher than 9.4, the monolith was totally dissolved. All further experiments were performed on PRP-1 monolith segments that were pre-conditioned for 60 min with 25 mM pH 9.4 sodium borate buffer.

4.3.2 Operation of the Pre-concentration Tip

Typically in CZE the EOF arising from the negative charge of the bare capillary inner wall is responsible for the bulk solution flow. In our work, the low pH (4.8) of the running buffer results in a slow EOF (about $1.2 \times 10^{-4} \text{ cm}^2/\text{Vs}$) in the absence of any pre-concentrator. When the short monolith tip (~1 mm) was attached to the inlet of a normal bare CZE capillary, as shown in Figure 4.2, it induced a resistance to flow. Fortunately, the PRP-1 tip has good permeability and the use of a short monolith segment caused only very low flow resistance. Thus, application of a low forward pressure (0.5 psi), in addition to the 20 kV running voltage, allowed separations to be performed in only 5 min. The simultaneous application of pressure and voltage is known as pressure-assisted

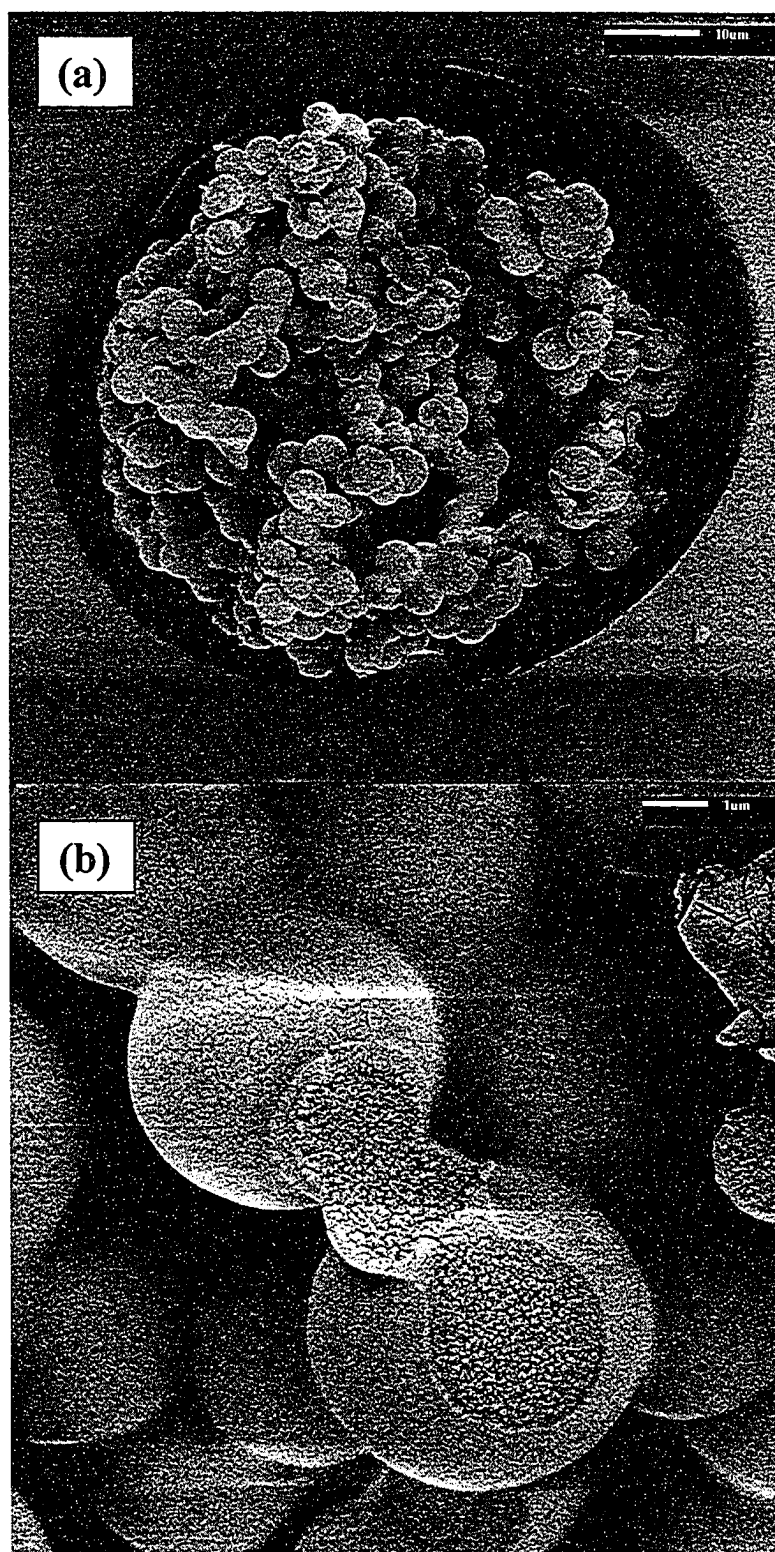


Figure 4.8 PRP-1-packed monolith, after pre-conditioning with 15 mM pH 4.8 acetate buffer at 20 psi for 60 min. Magnification: (a) 1100X; (b) 7500X.

capillary electrophoresis or capillary electrokinetic chromatography^{1,27}.

Between runs the PRP-1 tip was rinsed at 20 psi with eluent (15 mM pH 4.8 sodium acetate buffer and acetonitrile (40:60)) for 0.5 min to remove any strongly retained compounds that may be present in real samples. A subsequent 1 min rinse at 20 psi with running buffer (15 mM pH 4.8 sodium acetate) washes out the organic solvent, and thus prepares the PRP-1 tip for the pre-concentration step. Sample solution was injected at 20 psi for 5 min. The PRP-1 tip was then washed with running buffer to remove interstitial sample solution in the PRP-1 tip and bare capillary. The retained analytes were then eluted using a 5 s injection of eluent at 0.5 psi. In this work the eluting strength was not studied as the current organic solvent ratio is strong enough to elute all extracted analytes on the PRP-1 beads.

4.3.2.1 Charge state of analytes

Both AMPR and GLUF contain primary amino groups. These amine functionalities are derivatized with the fluorogenic dye NDA so that the products can be detected using fluorescence. The structures of the analytes and their NDA-derivatives are shown in Figure 4.1. In addition, the derivatization adds a large hydrophobic group to AMPR and GLUF. This enables retention of the derivatization products on the hydrophobic PRP-1 beads, the HPLC packing beads entrapped in monolith. However, derivatives of AMPR and GLUF are negatively charged at the pH used for pre-concentration (pH 4.8) in this work. This negative charge enables their separation by CZE after elution from the PRP-1 tip.

In the CZE running buffer, the charge state of the derivatization products affects

both their separation and preconcentration performance. No literature pKa data are available for the derivatization products. Nonetheless, we can estimate their pKa. Underivatized AMPR has $pK_{a1} = 0.62$ and $pK_{a2} = 5.53$ for the phosphonic acid and $pK_{a3} = 10.46$ for the protonated ammonium ion²⁸. Similarly, propyl phosphonic acid (*i.e.*, AMPR without the amino group) has $pK_{a1} = 2.49$ and $pK_{a2} = 8.18$ ²⁹. In comparing these two compounds one finds that the AMPR pK_a values decrease by ~ 2 units because the protonated ammonium ion, as a strong electron-withdrawing substituent, causes an acid-strengthening effect³⁰. The protonated ammonium ion also strongly repels approaching hydronium and thus makes the phosphonic acid group easier to release hydronium. After derivatization, delocalization of the lone electron pair on the nitrogen atom into the aromatic benz[f]isoindole ring makes it harder to protonate the nitrogen and the acid-strengthening effect is greatly reduced. As a result, it would be expected that the pK_a values of the phosphonic acid group would increase by 1-2 units.

GLUF has a $pK_{a1} = 1.17$ for carboxylic acid, $pK_{a2} = 2.69$ for the phosphonic acid and $pK_{a3} = 9.42$ for the protonated ammonium ion³¹. The pK_{a1} of the carboxylic acid in GLUF is much lower than normal carboxylic acids for the same reason as with AMPR. However, the protonated ammonium ion in GLUF does not have a significant effect on the phosphonic acid (pK_{a2}), as the ammonium is far from the phosphonic acid group. After derivatization, we expect GLUF's pK_{a1} to increase by 1-2 units, but pK_{a2} to remain essentially unchanged.

In this work, buffers ranging from pH 8.5 to 4.8 were used. Thus, based on the above discussion, a number of predictions about the charge state of the derivatization products can be made. First, the GLUF derivatization product will have a greater

negative charge than the AMPR derivatization product. Second, the negative charge of both derivatization products will decrease with pH. Third, from pH 8.5 to 4.8, the negative charge of the GLUF derivatization product will decrease more slowly than that of the AMPR derivatization product.

4.3.2.2 Effect of sample solution pH

During initial experiments, we tried using 25 mM pH 8.5 sodium borate buffer to dilute the sample and as the CZE running buffer for the pre-concentration and separation, respectively. Figure 4.9A shows that the AMPR and GLUF derivatization products are baseline resolved ($R_s = 1.7$). However both analytes are not equally preconcentrated. Although the GLUF concentration was three times of AMPR, the GLUF peak area was only 65% of the AMPR peak. This indicates that the AMPR derivatization product has a stronger affinity for the PRP-1 beads than GLUF. Both the AMPR and GLUF derivatization products have similar aromatic benz[f]isoindole rings that would dominate their hydrophobicity. Thus the difference in pre-concentration is consistent with the GLUF derivatization product being more negatively charged and less retained, as discussed above.

To achieve better resolution, 15 mM pH 4.8 sodium acetate buffer was used as the CZE running buffer. The mixed reaction solution was diluted with 15 mM pH 4.8 sodium acetate buffer or 25 mM pH 8.5 borate buffer to final concentrations of 5 nM AMPR and 15 nM GLUF. CZE separations were performed in 15 mM pH 4.8 sodium acetate buffer in both cases (Figures 4.9B and 4.9C, respectively). The analytes were well separated, presumably because there is a more significant difference in the charge of

the analytes at pH 4.8 than pH 8.5 (in accordance with the predictions in Section 4.3.2.1). More interesting is that, compared with Figure 4.9A, the AMPR peak area increased by 136% when the sample was prepared in 15 mM pH 4.8 sodium acetate buffer. Similarly the GLUF peak area also increased by 85%. However, when the sample was in 25 mM pH 8.5 borate buffer (as in Figure 4.9A), there was < 10% change in peak area for either analyte. Since 60:40 acetonitrile/water is strong enough to elute all extracted analytes on PRP-1 beads and no residual analytes can be detected, the different response must be attributed to different affinity and preconcentration efficiency on the PRP-1 beads. From the predictions in Section 4.3.2.1, both analytes would have a lower negative charge at pH 4.8 than pH 8.5, and thus would absorb with higher efficiency at the lower pH. The increase in pre-concentration efficiency was more evident for AMPR because the GLUF derivatization product has a larger negative charge than the AMPR derivatization product. In both Figures 4.9A and 4.9C, where the sample solution was in 25 mM pH 8.5 sodium borate, there was no change in affinity. Thus, preconcentration of the analytes is a strong function of the sample pH.

Figure 4.10 shows the effect of the sample injection time on the observed peak area. The AMPR peak area increased almost linearly with injection time up to 8 min. The peak area then leveled-off, and thereafter slowly decreased with longer injections. GLUF showed a similar behavior by gradually increasing with injection time up to ~5 min and thereafter decreasing slowly, however GLUF peak area was much lower than AMPR even at 3-fold concentration as AMPR.

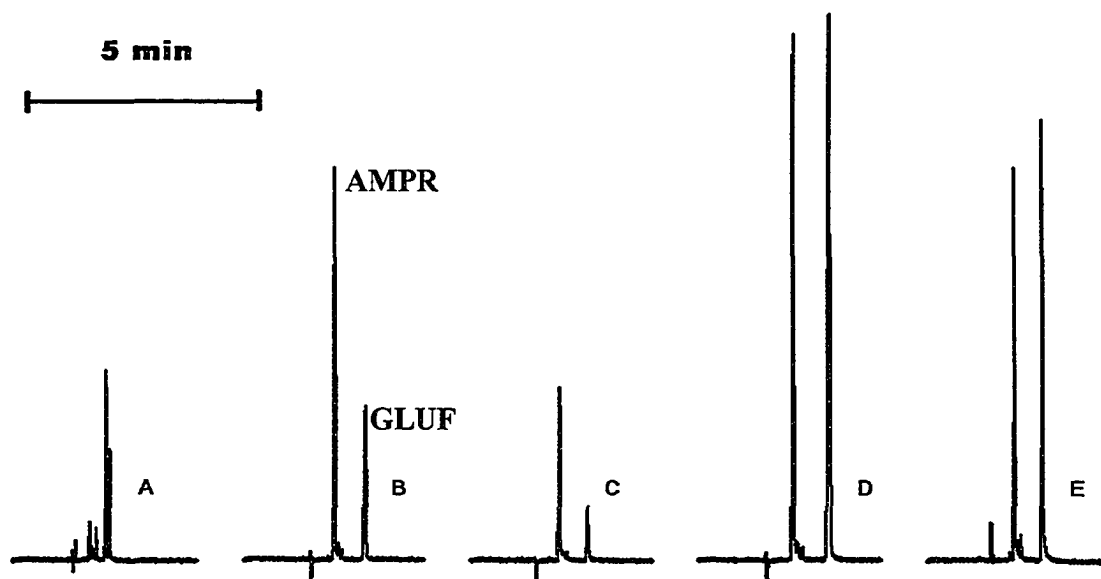


Figure 4.9 Pre-concentration effect by changing pH and salt concentration. 5nM AMPR and 15 nM GLUF, A) Dissolved in 25 mM pH 8.5 sodium borate buffer, CE running buffer: 25 mM pH 8.5 sodium borate. B) Dissolved in 15 mM pH 4.8 sodium acetate buffer, CE running buffer: 15 mM pH 4.8 sodium acetate. C) Dissolved in 25 mM pH 8.5 sodium borate buffer, CE running buffer: 15 mM pH 4.8 sodium acetate. D) Dissolved in 15 mM pH 4.8 sodium acetate buffer containing 100 mM NaCl, CE running buffer: 15 mM pH 4.8 sodium acetate. E) Dissolved in 25 mM pH 8.5 sodium borate buffer containing 100 mM NaCl, CE running buffer: 15 mM pH 4.8 sodium acetate.

These observations are in good agreement with the pK_a predictions in Section 4.3.2.1. That is, in the pH 4.8 buffer, the GLUF derivatization product is more negative than AMPR and thus was less hydrophobic and more weakly retained on the PRP-1 beads. The linear portion of the AMPR curve in Figure 4.10 indicates that AMPR has a

relatively strong affinity for PRP-1 beads. It is not surprising to see that GLUF derivatization product, more negatively charged and thus less hydrophobic, equilibrates with the column earlier. Longer injection of sample solution caused lowering of the peak area for both analytes and the mechanism is still unclear.

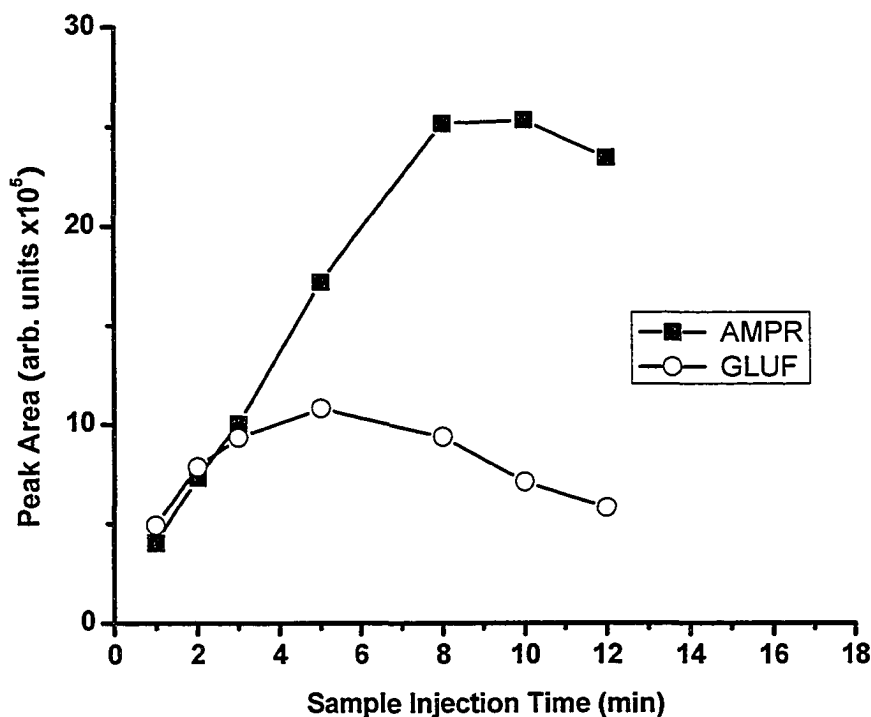


Figure 4.10 Effect of sample injection time at 20 psi in the absence of 100 mM NaCl. 5 nM AMPR and 15 nM GLUF. Each data point is the average of duplicate injections. The size of the data points approximately reflects the reproducibility of within 5%.

4.3.2.3 Effect of salt in sample solutions

Addition of 100 mM NaCl to the sample solutions caused an enhancement in the preconcentration of both analytes. Figure 4.9D shows that the peak areas of AMPR and

GLUF increased by 48% and 316%, respectively, compared with Figure 4.9B. Similar increases were also observed if the sample solutions were dissolved in 25 mM pH 8.5 sodium borate buffer (Figure 4.9E vs. 4.9C). When the added NaCl concentration was increased from zero to 150 mM, the GLUF peak area showed a 5.3-fold increase but AMPR increased only 0.8 fold. GLUF showed greater enhancement since it was more negatively charged as discussed below. However, if the NaCl concentration is too high (> 100 mM) it is difficult to completely rinse out the remaining NaCl with the CE running buffer. If some of the concentrated NaCl is present in the capillary upon application of the voltage it distorts the capillary current and deteriorates the separation. 100 mM NaCl was added in all other experiments.

The effect of sample injection time for samples containing 100 mM NaCl is shown in Figure 4.11. As the injection time was increased from 1 min to 15 min, the AMPR peak area increased roughly linearly up to 15 min and then showed a negative deviation from linearity for longer injections. Compared with Figure 4.10, AMPR had linear relationship with injection time over a much wider range of injection time (15 min vs. 8 min) and leveled-off started at much higher sample volumes and more slowly. On the other hand, GLUF had a much greater peak area than in Figure 4.10. The leveling-off of signal was still observed for GLUF, but the decay in the GLUF peak area appeared more slowly than in Figure 4.10 where the sample did not contain salt.

Addition of NaCl generated a region called the ionic atmosphere around the charged analytes and near the charged silica sol gel. As a result, the electrostatic interactions between them were greatly attenuated, due to: (1) The Donnan exclusion of the analytes was reduced since the ionic atmosphere decreased the repulsion between the

negatively charged analytes and the silica surface. This would allow analytes to reach the PRP-1 bead surface more easily. (2) The effective charge of the analytes appeared to be decreased and they acted more hydrophobic. Attenuation of the repulsion between the negatively charged analytes adsorbed on the surface of the PRP-1 bead can increase the maximum absorption capacity of the beads. As a result, more analytes can be adsorbed onto PRP-1 bead based on the “salting out” mechanism³². No studies were performed in this work to explain which effect was dominant, or whether other types or valences of salts would cause a different effect.

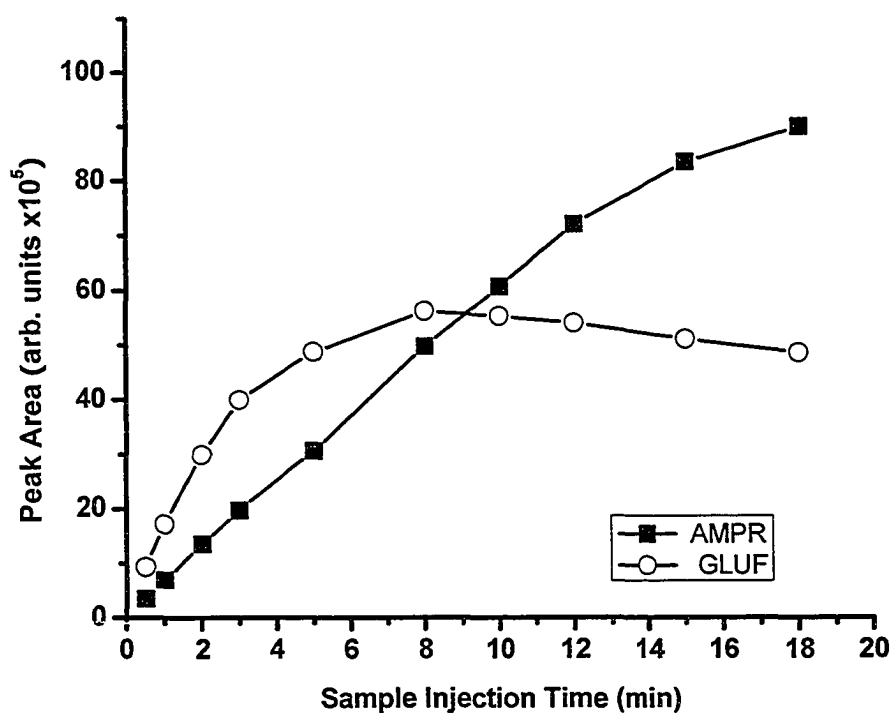


Figure 4.11 Effect of sample injection time at 20 psi in the presence of 100 mM NaCl. 5 nM AMPR and 15 nM GLUF. Each data point is the average of duplicate injections. The size of the data points approximately reflects the reproducibility of within 5%.

4.4 Quantitative studies

Quantitative studies were performed using AMPR/GLUF standard solutions and the optimized conditions described in Section 4.2. The PRP-1 tip yielded excellent pre-concentration performance. Figure 4.12 shows that using a 1 mm long PRP-1 entrapped monolith tip the peak area for AMPR and GLUF were enhanced by 790 and 130-fold, respectively in the absence of 100 mM NaCl in the sample. Addition of 100 mM NaCl to sample solutions increased the enrichment ratios to 1260 and 580, respectively. Figure 4.13 and 4.14 show that linear response was observed for 0.125 nM -12.5 nM AMPA and 0.375 nM - 37.5 nM GLUF. The correlation coefficients (R^2) were greater than 0.998 and the intercepts were equal to zero within the 95% confidence interval. The detection limits for AMPR and GLUF based on an S/N ratio of 3 were 20 pM and 65 pM, respectively. Repetitive determinations (n=10) were performed using a 5 nM AMPR / 15 nM GLUF standard. Relative standard deviations (RSD) for peak area measured using 0.125 nM AMPR/0.375 nM GLUF on the same monolith tip were 3.7% and 3.9% (n=6), respectively. Tip to tip reproducibility was 6.2% (n=5) for monolith tips cut from the same 15 cm-long monolith capillary segment. The reproducibility was typically 6 ~ 10% (n=5) for monolith tips cut from different 15 cm-long monolith capillary segments, depending on the monolith fabrication/packing homogeneity.

Although not evident in Figure 4.13, addition of a PRP-1 monolith tip caused broadening of the peaks relative to normal CZE. The theoretical plates were 77000 and 28100 for AMPR and GLUF respectively in normal CZE (Figure 4.12A). With the PRP-1 tip (Figure 12C) the efficiencies were reduced to 26900 and 15000 respectively. This may be mostly attributed to the parabolic flow profile in the pressure-driven system^{1,27}.

After preconditioning with 25 mM sodium borate buffer as described in Section 4.2.2, a PRP-1 tip yields good reproducibility (RSD<6%) for 20 ~ 35 runs. The failure time of such a PRP-1 packed monolith tip is indicated by sudden increases in migration times or decreases in peak area. At this point, a new monolith tip should be installed.

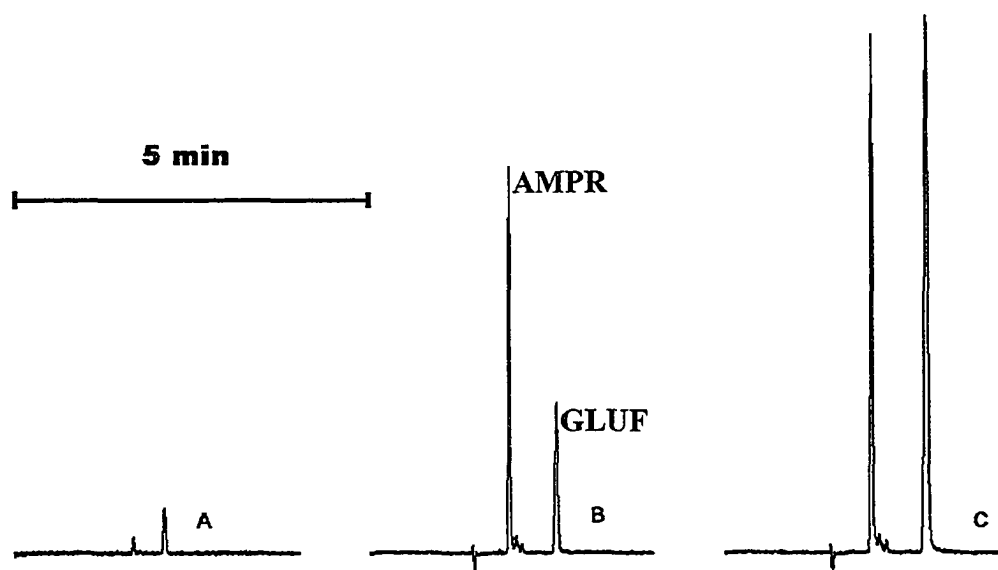


Figure 4.12 Performance comparisons. A) 0.5 μ M AMPR-1.5 μ M GLUF in CZE without PRP-1 tip, B) 5 nM AMPR-15 nM GLUF without added NaCl, in CZE with PRP-1 tip, C) 5 nM AMPR-15 nM GLUF with 100 mM NaCl, in CZE with PRP-1 tip.

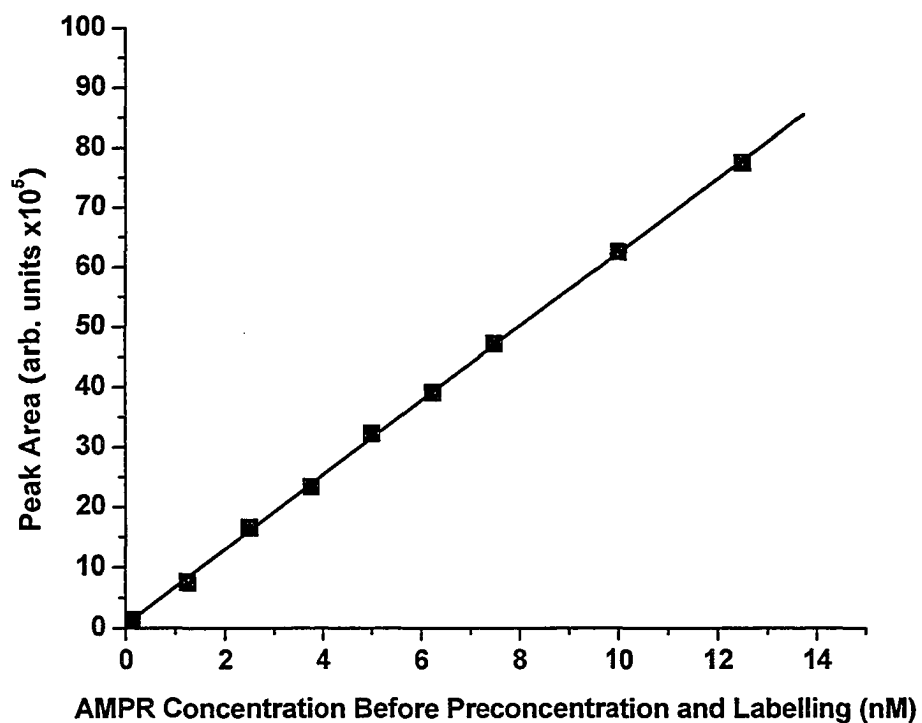


Figure 4.13 AMPR calibration curve. The experimental conditions are as in Section 4.2. Each data point is the average of duplicate reactions. The size of the data points approximately reflects the reproducibility of within 5%.

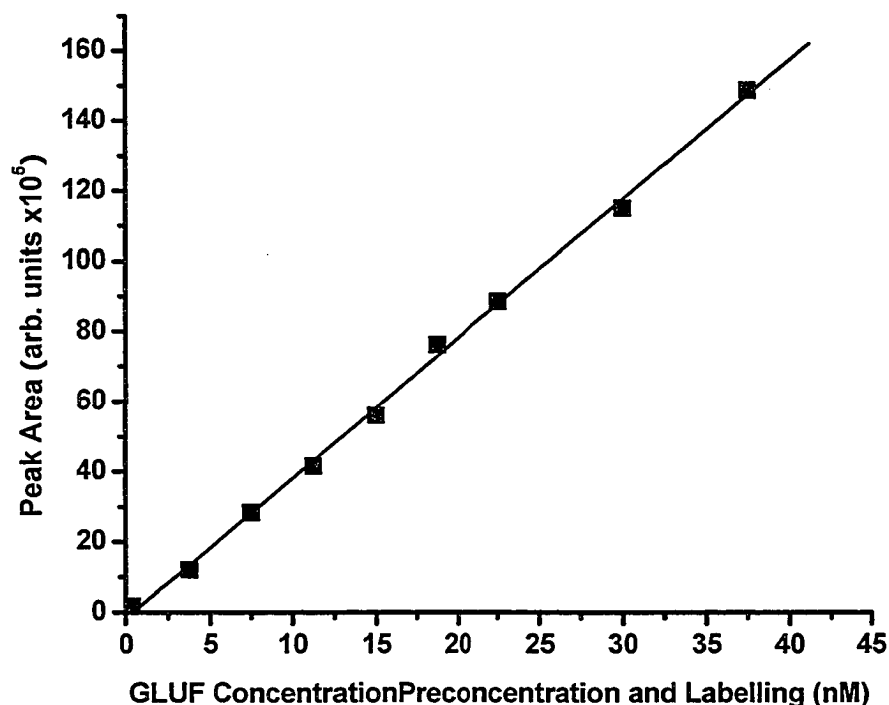


Figure 4.13 GLUF calibration curve. The experimental conditions are as in Section 4.2. Each data point is the average of duplicate reactions. The size of the data points approximately reflects the reproducibility of within 5%.

4.5 Conclusions and future work

In this Chapter, I have presented a successful demonstration of capillary-tip on-line pre-concentration. After fluorescence derivatization, two herbicides were pre-concentrated onto PRP-1 beads entrapped in a sol-gel monolith tip and then eluted for subsequent CZE separation and LIF detection. Pre-concentration efficiency can be greatly enhanced by: (1) adjusting the buffer pH to change charge status of analytes; (2) adding salt to increase affinity of charged analytes on hydrophobic phase; (3) using more

hydrophobic derivatization reagent, but this option was not studied in this work.

Although the mechanism of enrichment in this work was based on the hydrophobic nature of the analytes, other mechanisms, such as ion-exchange, affinity interactions may also be employed in future works to develop more sensitive and selective capillary-tip pre-concentrator. To achieve this goal, however, some problems remain to be resolved: (1) in this research, the higher pH limit for silica monolith is only ~ 8.5. Other monolith materials such as polymeric monolith are needed to be able to work at higher pH and for longer lifetime ¹⁷. (2) For the separation of natural analytes after extraction/elution from pre-concentration tip, a MEKC method must be designed compatible for the previous online extraction/elution procedures. (3) The online SPE preconcentration based on hydrophobic interactions has low selectivity. Other retention mechanisms using immunoaffinity antibodies or molecularly-imprinted polymer (MIP) are promising for highly selective recognition ⁷. (4) The application of low pressure is required to facilitate CE separation in this research. This leads to a parabolic flow profile and lower separation efficiency. The extraction/elution and CE separation processes may be allowed in different channels in an on-chip SPE preconcentration – CE system. Thus the resistance from monolith tip can be eliminated and forward pressure is no longer needed.

4.6 References

- (1) Li, S. F. C. *Capillary Electrophoresis: Principles, Practice and Applications*; Elsevier: Amsterdam, **1992**.
- (2) Swinney, K.; Bornhop, D. J. *Electrophoresis* **2000**, *21*, 1239-1250.
- (3) Majors, R. E. *LC-GC North America* **2001**, *19*, 14-22.
- (4) Lin, C. H.; Kaneta, T. *Electrophoresis* **2004**, *25*, 4058-4073.
- (5) Urbanek, M.; Krivankova, L.; Bocek, P. *Electrophoresis* **2003**, *24*, 466-485.
- (6) Kim, J. B.; Terabe, S. *Journal of Pharmaceutical and Biomedical Analysis* **2003**, *30*, 1625-1643.
- (7) Sentellas, S.; Puignou, L.; Galceran, M. T. *Journal of Separation Science* **2002**, *25*, 975-987.
- (8) Quirino, J. P.; Kim, J. B.; Terabe, S. *Journal of Chromatography A* **2002**, *965*, 357-373.
- (9) Molina, M.; Silva, M. *Electrophoresis* **2002**, *23*, 3907-3921.
- (10) Stroink, T.; Paarlberg, E.; Waterval, J. C. M.; Bult, A.; Underberg, W. J. M. *Electrophoresis* **2001**, *22*, 2375-2383.
- (11) Guzman, N. A.; Majors, R. E. *LC-GC Europe* **2001**, June, 1-9.
- (12) Robson, M. M.; Cikaló, M. G.; Myers, P.; Euerby, M. R.; Bartle, K. D. *Journal of Microcolumn Separations* **1997**, *9*, 357-372.
- (13) Oleschuk, R. D.; Shultz-Lockyear, L. L.; Ning, Y. B.; Harrison, D. J. *Analytical Chemistry* **2000**, *72*, 585-590.
- (14) Jemere, A. B.; Oleschuk, R. D.; Ouchen, F.; Fajuyigbe, F.; Harrison, D. J. *Electrophoresis* **2002**, *23*, 3537-3544.

- (15) Yu, C.; Davey, M. H.; Svec, F.; Frechet, J. M. J. *Analytical Chemistry* **2001**, *73*, 5088-5096.
- (16) Baryla, N. E.; Toltl, N. P. *Analyst* **2003**, *128*, 1009-1012.
- (17) Tanaka, N.; Kobayashi, H.; Nakanishi, K.; Minakuchi, H.; Ishizuka, N. *Analytical Chemistry* **2001**, *73*, 420a-429a.
- (18) Allen, D.; El Rassi, Z. *Electrophoresis* **2003**, *24*, 3962-3976.
- (19) Ratnayake, C. K.; Oh, C. S.; Henry, M. P. *HRC-Journal of High Resolution Chromatography* **2000**, *23*, 81-88.
- (20) Ratnayake, C. K.; Oh, C. S.; Henry, M. P. *Journal of Chromatography A* **2000**, *887*, 277-285.
- (21) Chirica, G. S.; Remcho, V. T. *Electrophoresis* **2000**, *21*, 3093-3101.
- (22) Chirica, G.; Remcho, V. T. *Electrophoresis* **1999**, *20*, 50-56.
- (23) Dulay, M. T.; Kulkarni, R. P.; Zare, R. N. *Analytical Chemistry* **1998**, *70*, 5103-5107.
- (24) Motokawa, M.; Kobayashi, H.; Ishizuka, N.; Minakuchi, H.; Nakanishi, K.; Jinnai, H.; Hosoya, K.; Ikegami, T.; Tanaka, N. *Journal of Chromatography A* **2002**, *961*, 53-63.
- (25) Tohver, V.; Smay, J. E.; Braem, A.; Braun, P. V.; Lewis, J. A. *Proceedings of the National Academy of Sciences of the United States of America* **2001**, *98*, 8950-8954.
- (26) Tarter, J. G. *Ion Chromatography*; Marcel Dekker Inc.: New York, **1987**.
- (27) Soga, T.; Ueno, Y.; Naraoka, H.; Matsuda, K.; Tomita, M.; Nishioka, T. *Analytical Chemistry* **2002**, *74*, 6224-6229.

- (28) Troev, K.; Hagele, G.; Kreidler, K.; Olschner, R.; Verwey, C.; Roundhill, D. M. *Phosphorus Sulfur and Silicon and the Related Elements* **1999**, *148*, 161-176.
- (29) Crofts, P. C.; Kosolapoff, G. M. *Journal of the American Chemical Society* **1953**, *75*, 3379-3383.
- (30) Perrin, D. D.; Dempsey, B.; Serjeant, E. P. *pKa Prediction for Organic Acids and Bases*; Chapman and Hall Ltd: London, **1981**.
- (31) Hagele, G.; Szakacs, Z.; Ollig, J.; Hermens, S.; Pfaff, C. *Heteroatom Chemistry* **2000**, *11*, 562-582.
- (32) Neue, U. D. *HPLC Columns: theory, technology, and practice*; Wiley-VCH, Inc: New York, **1997**.

Chapter 5. Capillary Gel Electrophoresis with Laser Induced Fluorescence and Detergent Differential Fractionation for Characterization of Cancer Cell Proteins *

5.1. Introduction

As a powerful separation technique, capillary electrophoresis (CE) has gained great success in DNA sequencing ¹. Due to the acceleration in DNA analysis made possible by capillary array systems based on CE, the Human Genome project was finished ahead of schedule ^{2,3}. In the meantime, CE has also been explored for protein mapping ⁴. For example, high-efficiency CZE methods have been developed for mapping of the proteins within a single-cell ⁵. Although this is very challenging, it is still worthwhile since CE method is easily automated and provides much higher speed than the classic SDS-polyacrylamide gel electrophoresis (SDS-PAGE) method.

Commonly used CE methods for proteins include capillary zone electrophoresis (CZE), capillary isoelectric focusing (CIEF) and capillary gel electrophoresis (CGE) ⁴. CGE for protein analysis has the advantage of providing molecular weight information for proteins and can be regarded as the capillary format of the widely used SDS-PAGE. UV is

* This chapter describes preliminary doctoral studies performed in the laboratory of Dr. Norman Dovichi. A version of this chapter has been published as S. Hu, J. Jiang, L.M. Cook, D.P. Richards, L. Horlick, B. Wong and N.J. Dovichi. "Capillary sodium dodecyl sulfate-DALT electrophoresis with laser-induced fluorescence detection for size-based analysis of proteins in human colon cancer cells", *Electrophoresis* 23 (2002) 3136-3142.

the popular detection mode for SDS-CGE, but it lacks detection sensitivity and it also requires the use of a UV-transparent sieving polymer. Compared with UV detection, laser-induced fluorescence (LIF) provides much higher detection sensitivity and has no special requirements for the sieving polymer.

In CGE, replaceable polymer matrices are often employed instead of cross-linked polyacrylamide. These replaceable polymers include linear polyacrylamide (LPA)^{6, 7}, polyethylene oxide (PEO)^{8, 9}, dextran⁹⁻¹¹, pullulan^{12, 13} and hydroxypropyl cellulose¹⁴. As discussed in Chapter 1.1.5.3, such linear polymers can form an entangled network with dynamic mesh sizes for size-based sieving of macromolecules. Guttman¹⁵⁻¹⁷ and Cottet¹⁸ *et al.* studied the separation mechanism of PEO polymer solution and the effect of operational variables on its resolution capability. Their research work indicated that PEO could be a good sieving polymer matrix for proteins.

Detergent differential fractionation (DDF)¹⁹⁻²¹ is a cell fractionation method that involves sequential extraction of cells or tissues with a series of detergent-containing buffers. Ramsby and co-workers partitioned eukaryotic cells into: (1) cytosolic and proteins and soluble cytoskeletal elements, (2) membrane and organellar proteins, (3) nuclear membrane and soluble nuclear proteins, (4) detergent-resistant cytoskeletal filaments with nuclear matrix proteins by using digitonin/EDTA, Triton-100/EDTA, Tween-40/deoxycholate extraction buffers and cytoskeletal solubilization buffer, respectively²⁰. These subcellular fractions can be subject to further analysis, most often by SDS-PAGE or two-dimensional (2-D) gel electrophoresis, to obtain biochemical and

immunochemical information. DDF is simple, reproducible and ultracentrifuge-independent. Furthermore, it does not cause damage to the structures and functions of the subcellular compartments and can enrich low-abundance species. Thus DDF has numerous potential applications^{19,22}.

In this study, a CGE-LIF method was developed for protein separation by using PEO (MW=100,000) as the sieving polymer. We also combined this method with DDF to characterize the protein profiles from HT29 human colon adenocarcinoma cells. Four different profiles show different information regarding the protein composition in the four sequential fractions.

5.2. Experimental

5.2.1 Apparatus

The CE-LIF system with a sheath-flow cuvette was a home-built system²³. A 0~30 kV high voltage was provided by a DC power supply (CZE1000, Spellman, Plainview, NY, USA). Separation was performed in a 40 cm-long, 51 μm -i.d, 140 μm -o.d, fused-silica capillary (Polymicro Technologies, Phoenix, AZ, USA) which had been coated with linear polyacrylamide to eliminate electroosmotic flow (EOF) as described by Hjerten²⁴. The 488nm laser beam from an argon ion laser (Model 2211-15SL, Uniphase, San Jose, CA, USA) operated at 12 mW was focused at $\sim 30 \mu\text{m}$ from the smoothly-cut tip of the capillary by a 6.3 \times objective (Melles Griot, Nepean, ON, Canada). The resultant fluorescence was filtered with a 630DF30 bandpass filter (Omega Optical, Brattleboro, VT, USA), collected

with a 60×, 0.7NA microscope objective (MO0060LWD, Universe Kokagu, Oyster Bay, NY, USA) and then detected with a photomultiplier tube (R1477, Hamamatsu, Middlesex, NJ, USA) operated at 900V. Data sampling was accomplished with a 16-bit data acquisition board (NB-MIO16XH-18, National Instruments, Austin, TX, USA) connected to a Macintosh computer. All data were analyzed by Igor Pro software (Version 3.14, Wavemetrics, Lake Oswego, OR, USA).

5.2.2 Reagents

Acrylamide was obtained from Life Technologies (Burlington, ON, Canada). Tris (hydroxymethyl) aminomethane (Tris), 2-(cyclohexylamino)-ethanesulphonic acid (CHES), γ -methacryloxypropyltrimethoxysilane (MAPS), phenylmethylsulfonyl fluoride (PMSF), piperazine-N,N'-bis (2-ethanesulfonic acid) (PIPES), Triton-100, Tween-40, sodium deoxycholate (DOC) and model proteins including β -lactoglobulin (MW=18,400), carbonic anhydrase (MW=29,000), ovalbumin (MW=45,000), BSA (MW=66,000) and conalbumin (MW=78,000) were purchased from Sigma (St. Louis, MO, USA). Ammonium persulfate (APS) was from Boehringer Mannheim Biochemical (Indianapolis, IN, USA). N, N, N', N'- tetramethylethylenediamine (TEMED) was from Bio-Rad (Richmond, CA, USA). 3-(2-furoyl) quinoline-2- carboxaldehyde (FQ, Figure 5.1) and KCN were obtained from Molecular Probes (Eugene, OR, USA). Digitonin and PEO (MW=100,000) were from Aldrich (Milwaukee, WI, USA).

5.2.3 Separation of model proteins

The protein mixture solution was prepared from 10 μM stock solutions of each model protein: β -lactoglobulin, carbonic anhydrase, ovalbumin, BSA and conalbumin. 5 μl of the mixture solution was mixed with 5 μl 5 % SDS solution and then heated at 90 $^{\circ}\text{C}$ for 10 min to denature the proteins. After cooling in ice for a while, 5 μl of the denatured protein solution and 5 μl of 2 mM KCN solution were added sequentially into a 500- μl microcentrifuge tube containing 100 nmol previously dried FQ²³. After vortexing for a while, the mixture was incubated at 65 $^{\circ}\text{C}$ for 5 min and then diluted with 40 μl of running buffer. The running buffer contained 100 mM Tris, 100mM CHES and 0.1 % (w/v) SDS (pH 8.6). The final concentration of each protein was 100 nM.

The sample was electrokinetically injected at -100 V/cm for 5 s and then separated at -300 V/cm. Unless stated otherwise, PEO sieving buffer was prepared by dissolving an appropriated amount of PEO at 2.5% (W/V) concentration in the running buffer. Before use, the sieving buffer was degassed for 30 min by ultrasonication.

5.2.4 Differential detergent fractionation of HT29 cancer cells

HT29 cells, cultured as reported in previous work⁵, were washed with phosphate -borate saline buffer (PBS) five times before use. The digitonin/EDTA, Triton-100/EDTA, Tween-40/DOC and detergent-resistant residue extraction buffers were prepared according to Ramsby's protocol²⁰, however a modified fractionation procedure was employed in this work. The cell suspension containing around 10^6 cells were added into a T25 flask and

evenly dispersed over only one surface so that the cells were adsorbed onto its inner wall of only one side. The excess PBS was then sucked out of the flask, and 1 ml of digitonin/EDTA extraction buffer was added. The flask was placed on fresh ice and rocked for 15 min. The extraction solution was transferred into a test tube, aliquoted and stored at -80 °C. To rinse the cells, 2 ml of ice-cold PBS was added into the T25 flask, rocked for 1 min and then aspirated. As done above, 1ml of Triton-100/EDTA extraction buffer, 500 µl of Tween/DOC extraction buffer and 300 µl of detergent-resistant residue extraction buffer were added into the flask and rocked for 30 min, 20 min and 20 min, respectively, and then the resultant extraction solutions were collected, aliquoted and stored at -80 °C. Between these sequential fractionation steps, 2 ml of ice-cold PBS was used to wash out the residual solution from the previous fractionation step. For the detergent-resistant residue extraction, no ice was used because 5 % SDS solution will curdle and cannot rinse the stickled cells continuously.

An aliquot of each of the four DDF cell fractionations was thawed and vortexed. Then 5 µl of the sample solution was mixed with 5 µl of 5% SDS and heated at 95 °C for 10 min. After denaturization, the cell fraction was labeled with FQ as described in Section 5.2.3 and subjected to CGE analysis as done for model proteins.

5.3 Results and discussion

In this work FQ is used to label proteins^{5, 23, 25}, as described in Section 5.2.3 (Figure 5.1). This reagent is a fluorogenic dye working well with 488 nm Argon-ion laser. No

background fluorescence results from unreacted dyes until it reacts with proteins.

Detection limits as low as picomolar has been reported for proteins²³.

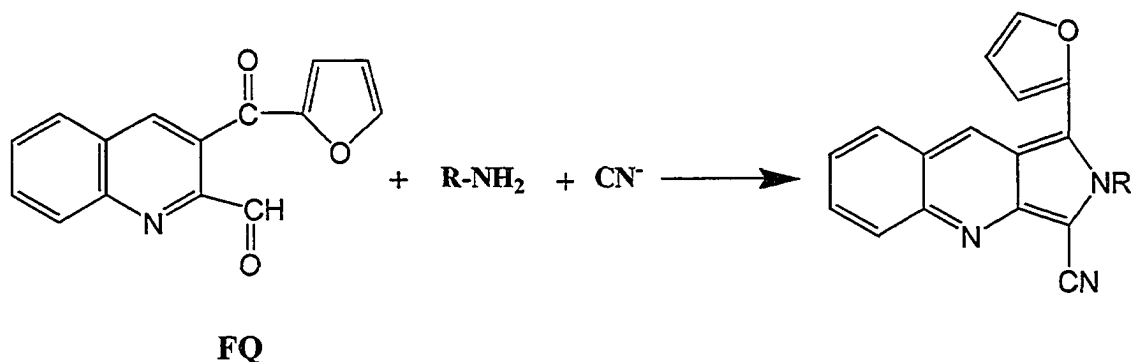


Figure 5.1 Molecular structure of FQ and its fluorescence labeling reaction.

5.3.1 Separation of standard proteins

Five standard proteins, which have molecular weights ranging from 18,400 to 78,000, were used to demonstrate the CGE-LIF separation of proteins based on their molecular weights. Previous studies¹⁵⁻¹⁸ have shown that the sieving capability of PEO increases as PEO chain length (and thus MW) or PEO concentration increases. 1 ~ 4 % PEO (MW=100,000) have been reported for separation of proteins, but we found it was difficult to prepare PEO sieving matrix using concentrations higher than 2.5 %. More than 2.5 % PEO could not dissolve completely even if it was sonicated for a few hours. So the sieving capability of 1.5 - 2.5 % PEO was examined in this work. As shown in Figure 5.2, five model proteins elute in the order of their molecular weights. The small peak before peak 1

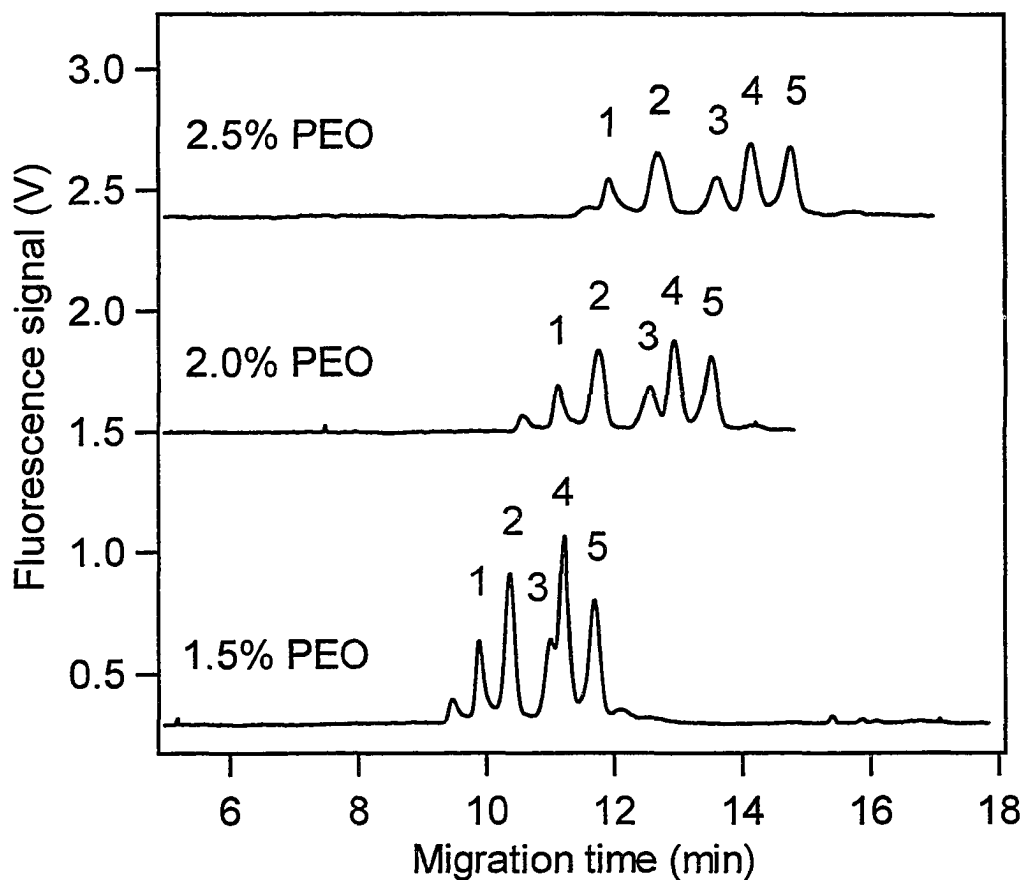


Figure 5.2 Effect of PEO concentration on the separation of five model proteins

Peak identification: (1) β -lactoglobulin; (2) carbonic anhydrase; (3) ovalbumin; (4) BSA; (5) conalbumin. Fluorescence derivatization conditions as in Section 5.2.3. Protein concentration: 100 nM each; Injection: 100 V/cm for 5 s; Separation: 300 V/cm; Sieving matrix: 100 mM Tris-100 mM CHES-0.1% SDS-PEO, pH 8.6.

is an impurity from carbonic anhydrase. Obviously, PEO concentration has a significant effect on the separation of model proteins, especially for ovalbumin and BSA. If 1.5% PEO was used, ovalbumin almost co-eluted with BSA. However, the resolution of ovalbumin and BSA increases as the PEO concentration increases. When 2.5% PEO was used, all standard proteins were separated with baseline resolution.

The effect of electric field strength on the separation of the five model proteins was also studied (shown in Figure 5.3). As expected, no significant improvement was observed using different electric field strength. 300 V/cm was used for all further experiments. Buffers other than Tris within the sieving matrix were also tested (i.e., other biological buffers such as 4-(2-hydroxyethyl)-1-piperazineethanesulfonic acid (HEPES), Tricine or {(2-hydroxymethyl) ethyl}-amino}-l-propanesulphonic acid (TAPS)). However, Tris provides the best resolution for these standard proteins.

The migration time, limits of detection (LOD), and reproducibility of the migration times of these proteins are presented in Table 5.1. These statistical data were obtained with 2.5% PEO sieving matrix under the separation voltage of 300 V/cm. It can be seen that model proteins with higher MW yield lower LOD. This is due to FQ reacting with the ϵ -amine of lysine of these proteins. A higher MW protein will possess more lysine residues and thus more FQ molecules label these proteins, so higher detection sensitivity was observed. It was also found the migration times of the model proteins have a linear relationship with the logarithm of the molecular weights of these standard proteins (shown in Figure 5.4). Regression analysis yielded the linear expression:

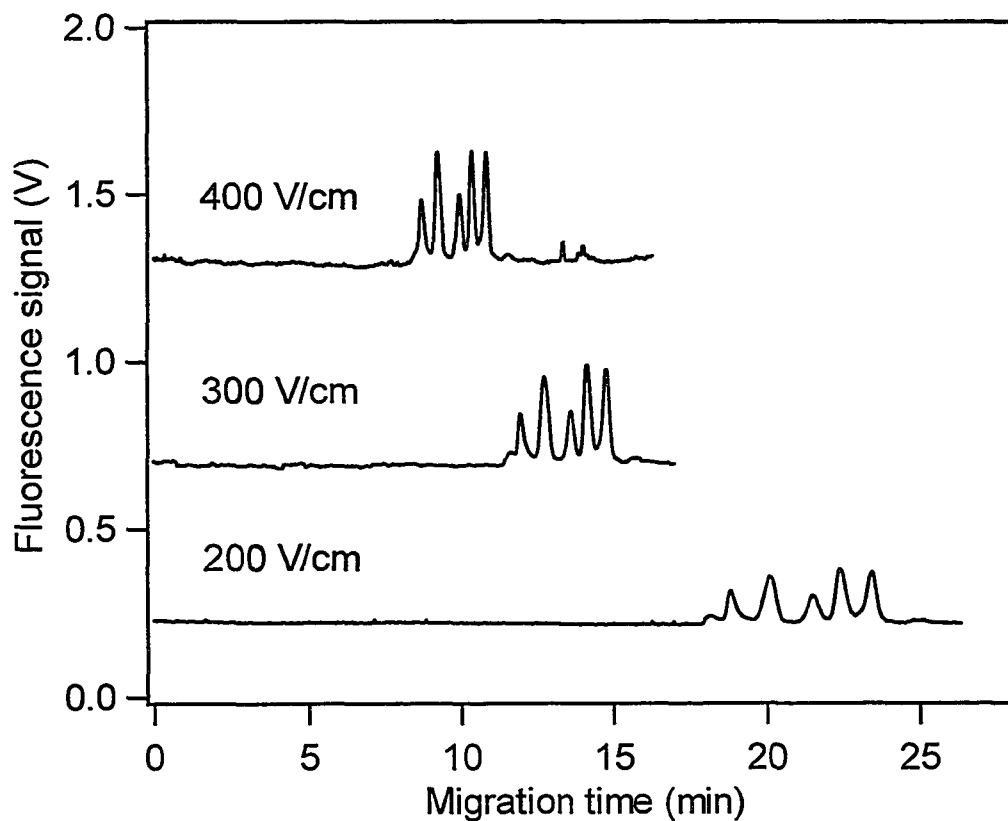


Figure 5.3 Effect of electric field on the separation of standard proteins. Fluorescence derivatization conditions as in Section 5.2.3. Protein concentration: 100 nM each; Injection: 100 V/cm for 5 s; Sieving matrix: 100 mM Tris-100mM CHES-0.1% SDS-2.5 % PEO, pH 8.6.

Table 5.1 CGE-LIF for separation of five standard proteins

Protein	Migration time (min)*	Concentration LOD (nM) †	Mass LOD (amol) †
β -lactoglobulin (MW=18,4000)	12.124 \pm 0.16 (1.3%)	6.56	37.5
Carbonic anhydrase (MW=29,000)	12.952 \pm 0.18 (1.4%)	5.62	30.2
Ovalbumin (MW=45,000)	13.924 \pm 0.21 (1.5%)	2.71	13.9
BSA (MW=66,000)	14.467 \pm 0.24 (1.6%)	2.17	10.5
Conalbumin (MW=78,000)	15.137 \pm 0.26 (1.7%)	1.92	8.9

Experimental conditions: Fluorescence derivatization conditions as in Section 5.2.3.

Injection: 100 V/cm for 5 s; Separation: 300 V/cm; Sieving matrix: 100 mM Tris- 100mM CHES-0.1% SDS-2.5% PEO, pH 8.6.

* mean \pm standard deviation (RSD) (n=16)

† S/N=3

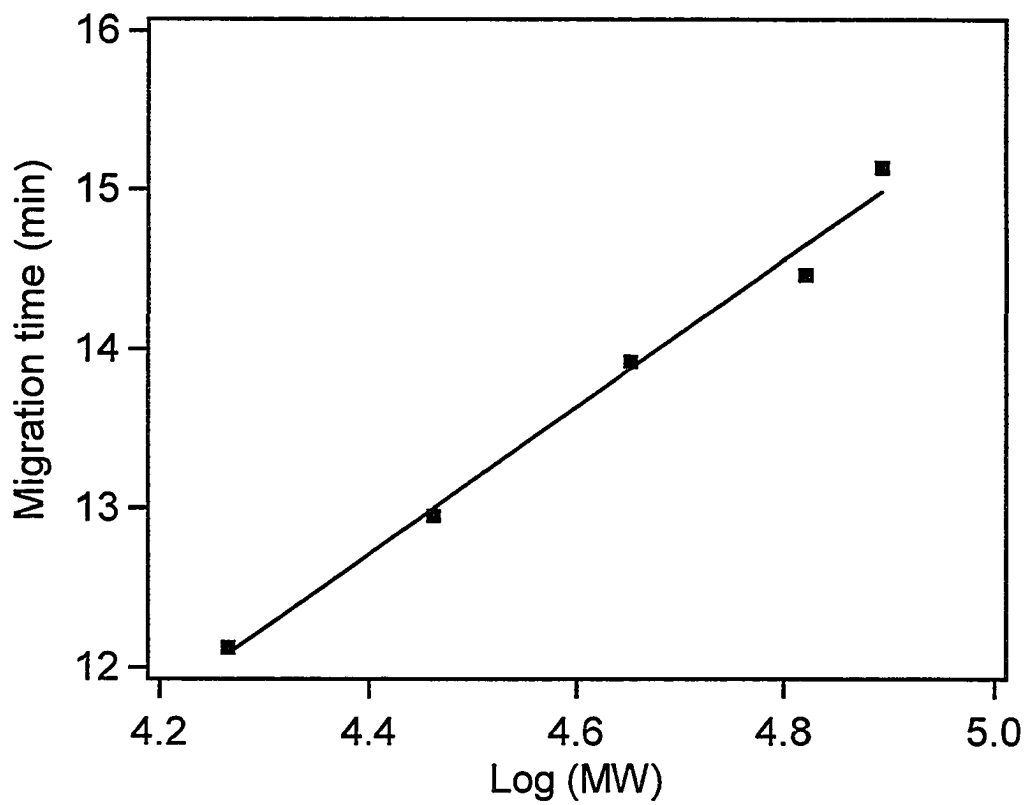


Figure 5.4 Plot of migration time of standard protein vs. log (MW). Experimental conditions as in Table 5.1

$$t = 4.62 \times \log MW - 7.62 \quad (R=0.9945) \quad (\text{Eqn 5.1})$$

where t is migration time (min), MW is molecular weight (Dalton), and R is the correlation coefficient. This demonstrates that these proteins were separated based on their size.

Blank experiments were performed by using the same procedure as for standard proteins. No peak was observed, demonstrating that the sieving matrix does not interfere with the labeling experiment and separation. In addition, note that we used linear polyacrylamide to coat the capillary to eliminate the EOF²⁴. This coating should not be used for $pH > 9$. Our coated capillary can be used with $pH 8.6$ running buffer for ~ 10 days.

5.3.2 Characterization of HT29 cell proteins by CGE-LIF with DDF

Similar to model proteins, DDF fractions of HT29 cancer cells were denatured by SDS, labeled with FQ and then analyzed by CGE-LIF using 2.5% PEO as the sieving buffer.

Figure 5.5 shows the electropherogram of cytosolic fraction obtained by CGE-LIF.

Baseline resolution was not achieved due to the complexity of the cell protein composition.

Most proteins fall into the molecular weight range of 13,700 \sim 155,000. Between 18 to 23

min, however, a couple of sharp peaks migrate after the largest of our molecular weight

standards. These peaks might result from some proteins with molecular weights over

400,000. However, a reducing agent was not used in these experiments to disrupt disulfide

bonds. Thus, some of the late-migrating peaks may be due to protein conjugates.

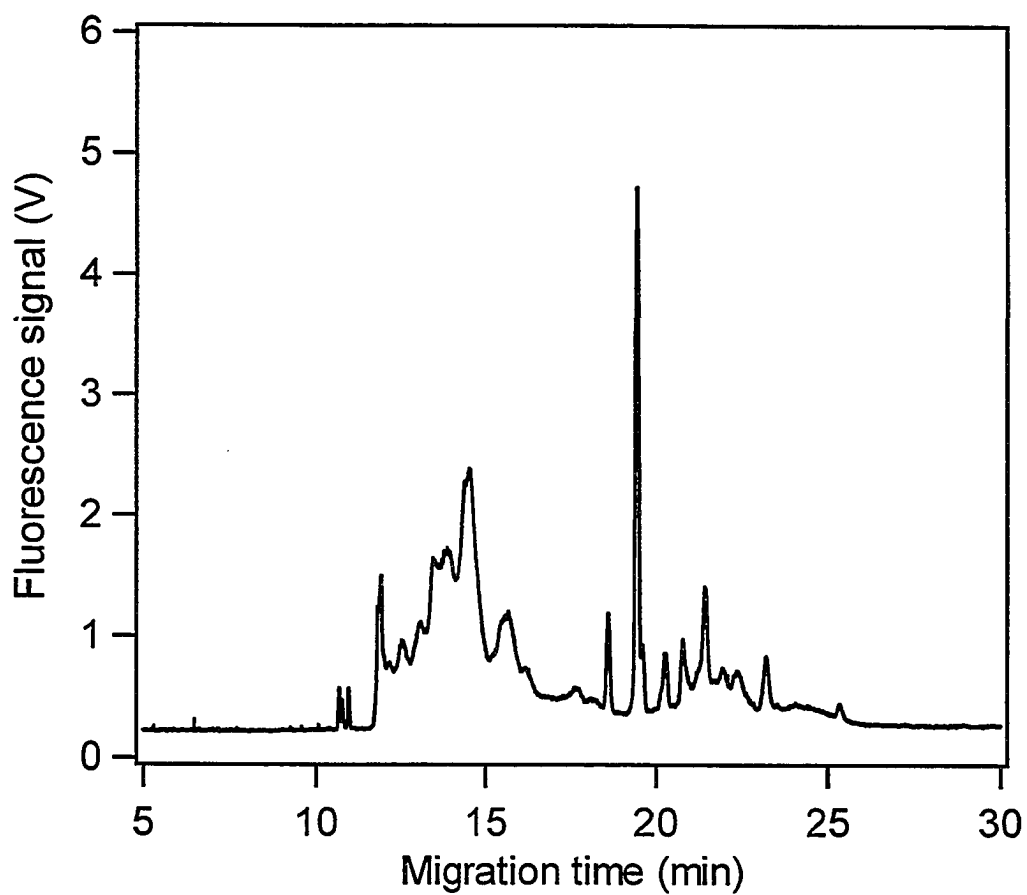


Figure 5.5 CGE-LIF electropherogram of the cytosolic fraction of HT29 cell extract.

Experimental conditions: DDF processing and fluorescence derivatization conditions as in Section 5.2.4. Injection: 100 V/cm for 5 s; Separation: 300 V/cm; Sieving matrix: 100 mM Tris-100 mM CHES-0.1% SDS-2.5 % PEO, pH8.6.

Figure 5.6 shows the CGE-LIF electropherogram of the membrane/organelle fraction, which presents the profile with the poorest resolution in the four fractions. This result is not surprising because the membrane of cells and cell organelles consist of many kinds of highly viscous membrane proteins and lipoproteins, which are notoriously difficult to separate and analyze by SDS-PAGE^{26,27}. However, Figure 5.6 indicates that proteins within the membrane/organelle fraction can be roughly divided into two groups, 11-16 min and 18-20 min, based on their molecular weights.

Figures 5.7 and 5.8 show, respectively, the CGE electropherograms of the nuclear fraction and the detergent-resistant cytoskeletal fraction. Similar to the cytosolic fraction proteins, the nuclear fraction proteins (Figure 5.7) are distributed almost over the whole molecular weight range. Comparatively speaking, the detergent-resistant cytoskeletal fraction (Figure 5.8) has the simplest protein profile in the four cell fractions. Two pairs of peaks were present in low molecular weight range (19.5/23.8 kDa and 55.4/64.4 kDa) and one broad peak present in higher MW range.

The protein profiles obtained for the four sequential protein fractions of HT29 cells are quite different, either in the expressed amount or in the molecular weight distribution. Taking into account the difference of the final extraction volumes in the four fractionation steps, as pointed out by Ramsby *et al*²⁰, the cytosolic and membrane/organelle proteins obviously make up most of the proteins expressed in the HT29 cells.

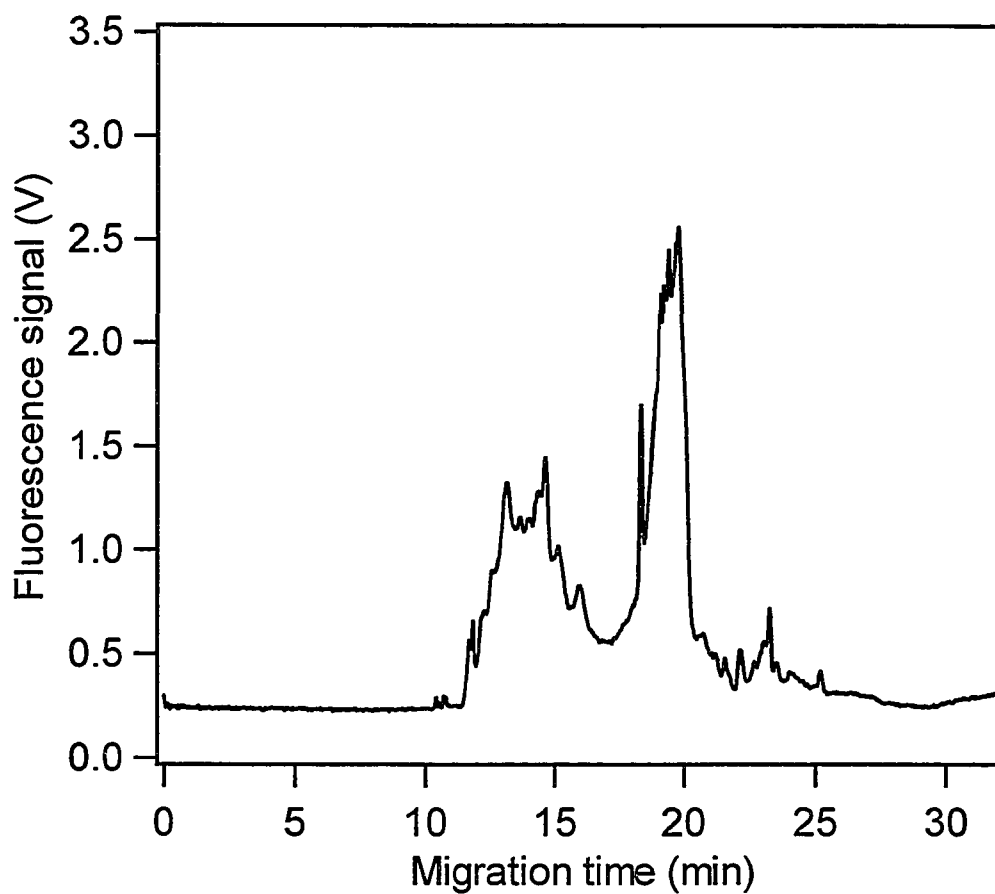


Figure 5.6: CGE-LIF electropherogram of the membrane/organelle fraction of HT29 cell extract. All conditions as in Figure 5.5.

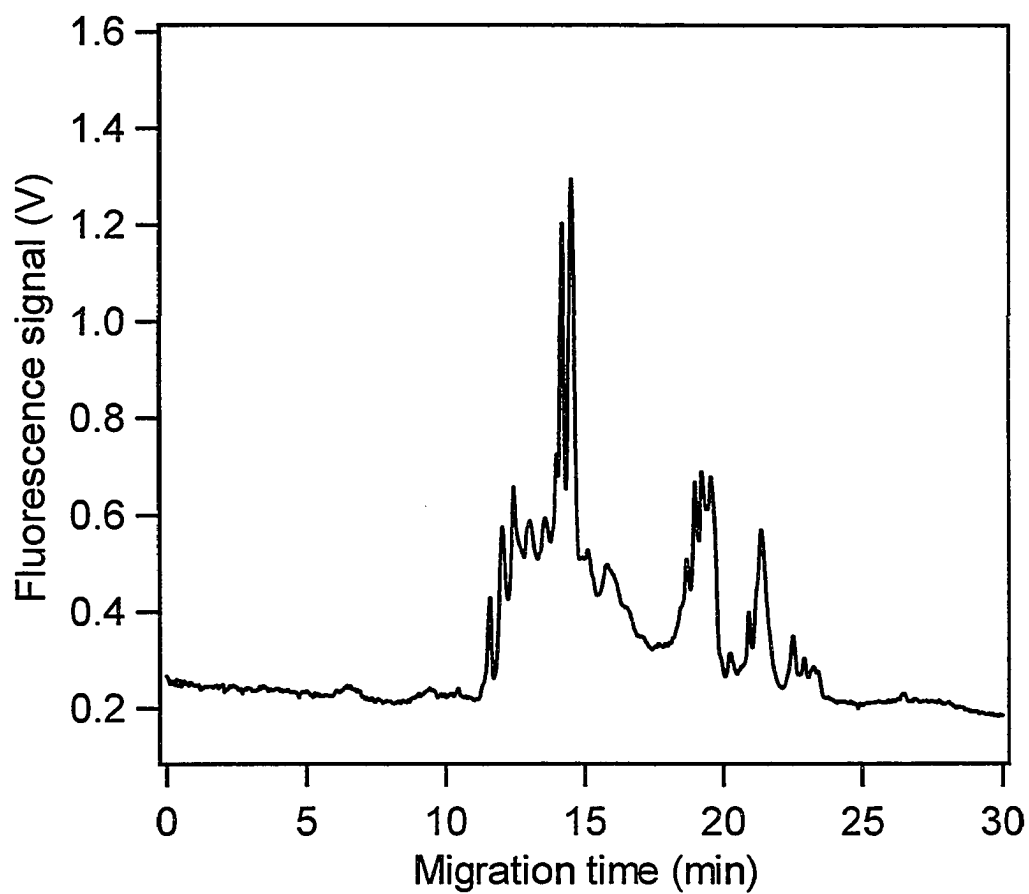


Figure 5.7 CGE-LIF electropherogram of the nuclear fraction of HT29 cell extract. All conditions as in Figure 5.5.

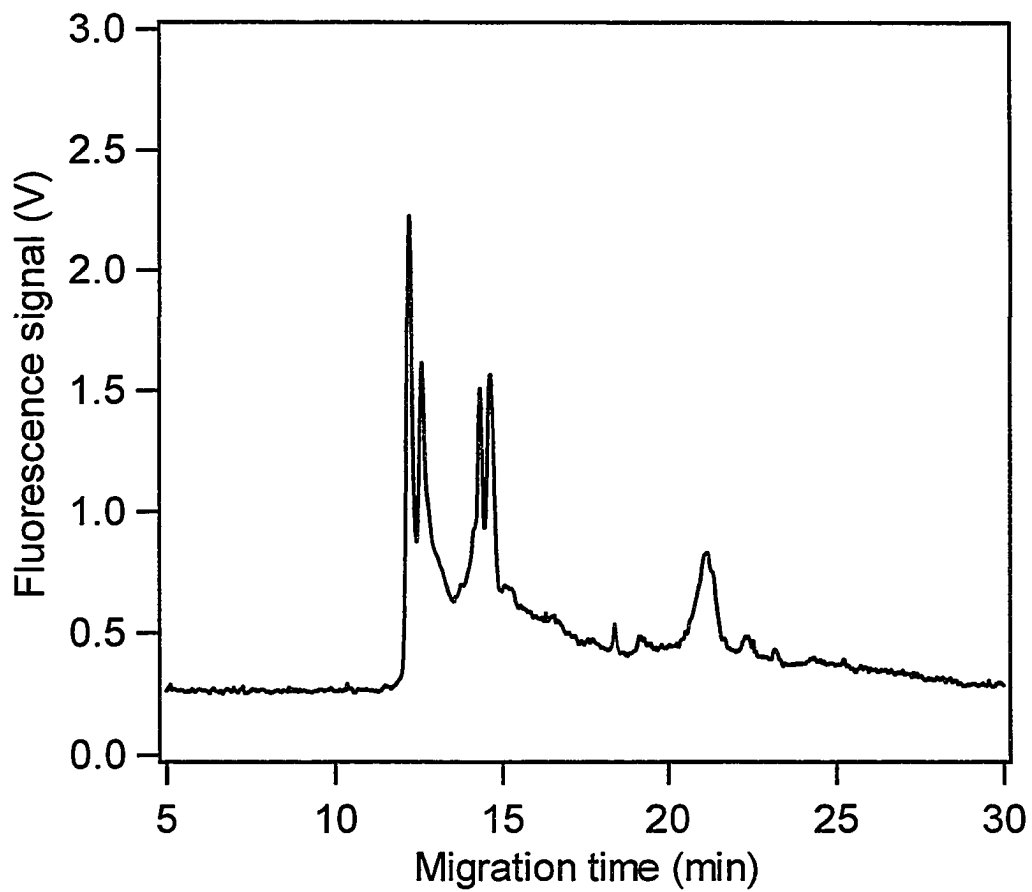


Figure 5.8 CGE-LIF electropherogram of the cytoskeletal fraction of HT29 cell extract
. All conditions as in Figure 5.5.

As expected, it is almost impossible to separate the over-thousands of proteins in a complicated cell such as HT29 by normal one-dimensional CE. However, the DDF technique gives us an approach to extract sequentially different groups of components from cell extract and probably link the obtained CE results to the protein profiles and biological properties of each group of proteins. Two-Dimensional CE with LIF detection has been developed in Dovichi's group to provide higher resolution and fingerprint identification of cell proteins²⁸.

5.4 Conclusions

In this chapter, a CGE-LIF method using PEO sieving matrix was developed for the size-based separation of five model proteins, and then applied to the analysis of HT29 cell protein fractions obtained by detergent differential fractionation (DDF). This method is highly sensitive and provides much higher speed than classical SDS-PAGE. Although different protein profiles have been demonstrated for the four sequential fractions from HT29 cancer cells, further work is still needed to enhance the resolution and get more of the information offered by DDF. Similar to 2-D gel electrophoresis, if this CGE method were combined with another CE mode to perform a 2-D CE, much more detailed information would be gained. Such a 2D-CE methodology would be a novel and powerful tool in proteomics studies.

5.5 References

- (1) Dovichi, N. J. *Electrophoresis* **1997**, *18*, 2393-2399.
- (2) Roberts, L.; Davenport, R. J.; Pennisi, E.; Marshall, E. *Science* **2001**, *291*, 1195.
- (3) Dovichi, N. J.; Zhang, J. Z. *Angewandte Chemie-International Edition* **2000**, *39*, 4463-4468.
- (4) Krylov, S. N.; Dovichi, N. J. *Analytical Chemistry* **2000**, *72*, 111r-128r.
- (5) Zhang, Z. R.; Krylov, S.; Arriaga, E. A.; Polakowski, R.; Dovichi, N. J. *Analytical Chemistry* **2000**, *72*, 318-322.
- (6) Widhalm, A.; Schwer, C.; Blaas, D.; Kenndler, E. *Journal of Chromatography* **1991**, *549*, 446-451.
- (7) Manabe, T.; Oota, H.; Mukai, J. *Electrophoresis* **1998**, *19*, 2308-2316.
- (8) Benedek, K.; Guttman, A. *Journal of Chromatography A* **1994**, *680*, 375-381.
- (9) Guttman, A.; Horvath, J.; Cooke, N. *Analytical Chemistry* **1993**, *65*, 199-203.
- (10) Ganzler, K.; Greve, K. S.; Cohen, A. S.; Karger, B. L.; Guttman, A.; Cooke, N. C. *Analytical Chemistry* **1992**, *64*, 2665-2671.
- (11) Karim, M. R.; Janson, J. C.; Takagi, T. *Electrophoresis* **1994**, *15*, 1531-1534.
- (12) Nakatani, M.; Shibukawa, A.; Nakagawa, T. *Journal of Chromatography A* **1994**, *672*, 213-218.
- (13) Nakatani, M.; Shibukawa, A.; Nakagawa, T. *Electrophoresis* **1996**, *17*, 1210-1213.
- (14) Hu, S.; Zhang, Z. R.; Cook, L. M.; Carpenter, E. J.; Dovichi, N. J. *Journal of Chromatography A* **2000**, *894*, 291-296.

- (15) Guttman, A.; Shieh, P.; Hoang, D.; Horvath, J.; Cooke, N. *Electrophoresis* **1994**, *15*, 221-224.
- (16) Guttman, A. *Electrophoresis* **1995**, *16*, 611-616.
- (17) Guttman, A. *Electrophoresis* **1996**, *17*, 1333-1341.
- (18) Cottet, H.; Gareil, P.; Viovy, J. L. *Electrophoresis* **1998**, *19*, 2151-2162.
- (19) Ramsby, M. L.; Makowski, G. S.; Khairallah, E. A. *Electrophoresis* **1994**, *15*, 265-277.
- (20) Ramsby, M. L.; Makowski, G. S. *2-D Proteome Analysis Protocols*; Humana Press Inc., 1999.
- (21) Patton, W. F. *Journal of Chromatography B-Analytical Technologies in the Biomedical and Life Sciences* **1999**, *722*, 203-223.
- (22) Ramsby, M. L.; Kreutzer, D. L. *Investigative Ophthalmology & Visual Science* **1993**, *34*, 3207-3219.
- (23) Pinto, D. M.; Arriaga, E. A.; Craig, D.; Angelova, J.; Sharma, N.; Ahmadzadeh, H.; Dovichi, N. J.; Boulet, C. A. *Analytical Chemistry* **1997**, *69*, 3015-3021.
- (24) Hjerten, S. *Journal of Chromatography* **1985**, *347*, 191-198.
- (25) Craig, D. B.; Polakowski, P. M.; Arriaga, E.; Wong, J. C. Y.; Ahmadzadeh, H.; Stathakis, C.; Dovichi, N. J. *Electrophoresis* **1998**, *19*, 2175-2178.
- (26) Santoni, V.; Molloy, M.; Rabilloud, T. *Electrophoresis* **2000**, *21*, 1054-1070.
- (27) Gu, S.; Chen, J.; Dobos, K. M.; Bradbury, E. M.; Belisle, J. T.; Chen, X. *Molecular & Cellular Proteomics* **2003**, *2*, 1284-1296.

- (28) Michels, D. A.; Hu, S.; Dambrowitz, K. A.; Eggertson, M. J.; Lauterbach, K.;
Dovich, N. J. *Electrophoresis* **2004**, *25*, 3098-3105.

Chapter 6. Summary and Future Work

6.1 Summary

In this thesis, several on-capillary preconcentration techniques were utilized for enhancing detection sensitivity of capillary electrophoresis with LIF detection. Chapter 2 gives an example of high-salt stacking used for preconcentration of neutral analytes in MEKC. The concentration ratio is determined by the affinity of the analytes for micelles. To achieve baseline resolution of the three very hydrophobic fluorescence derivatization products of alkylphosphonic acids, 40% acetonitrile was added to the MEKC buffer. This decreases the affinity of analytes for the cholate micelles. However, ~ 10 fold preconcentration ratio was still achieved. Also the addition of 400 mM NaCl to the dilution buffer enabled high salt stacking while still maintaining baseline resolution. Limits of detection for methyl, ethyl and propylphosphonic acids were 0.13 μM , 0.13 μM and 0.14 μM injected, respectively, which were better than most prior methods.

Chapter 3 discussed offline preconcentration of glyphosate using ionic exchange resin packed in a pipette tip, followed by fluorescence labeling and CE-LIF analysis. The unexpected interference in NDA labeling reaction was studied and minimized through the use of lower reactant concentrations than had been recommended by the literature. Using my optimized reaction conditions and the off-line resin packed pipette tip, about 88 fold preconcentration was observed. Detection limits of 0.2 nM were achieved for glyphosate standards, which was comparable to the lowest LOD reported. With river water, the matrix necessitated an additional clean-up step which degraded the LOD to 6 nM.

A more desirable approach is online preconcentration as reported in Chapter 4. SPE-based on-capillary preconcentration was developed successfully. PRP-1 HPLC

beads were entrapped in a silica sol-gel monolith in short segment of capillary. This SPE capillary was attached to the separation capillary and used to extract hydrophobic analytes from dilute sample solutions. Since the analytes must be charged even after fluorescence derivatization to be separated by CZE mode, the charge states of analytes were found to affect the extraction ratio. For highly charged analytes, low extraction ratio was observed. The extraction ratios were improved significantly by reducing the electrostatic repelling either by reducing the pH or by adding salt to the sample solution. Examination of the silica sol-gel monolith by SEM found that a silica shell encapsulated almost all of the PRP-1 beads. This sol gel shell was negatively charged, and so was responsible for repulsion of the anionic analytes. This problem was solved by partial digestion of the monolith using pH 9.4 borate buffer. Under optimized conditions, 1260 and 580 folds enhancement of detection sensitivity were achieved for AMPR and GLUF, respectively. The detection limits for AMPR and GLUF were 20 pM and 65 pM, respectively. However, a further study on the formation of the shell is necessary, which will be discussed in Section 6.2.1.

Chapter 5 is a preliminary study on CGE-LIF analysis of proteins using PEO polymer sieving matrix. For the first time, detergent differential fractionation (DDF) technique was combined with CGE for studying the protein profiles of the different fractions of a cancer cell extract. This work was an important first step towards 2-D CGE which should provide the higher resolution needed for extracting full information about the complex cell components.

In summary, online preconcentration performance in CE strongly depends on the analyte properties and the concentration mechanism. SPE-based online preconcentration

is preferred as both the concentration ratio and selectivity may be improved significantly by using suitable extraction mechanism. The future work outlined below is primarily focused on improving the extraction performance of SPE-based online preconcentration segment coupled to CE or microfluidic separation systems. Improvements focus on the concentration ratio, selectivity and reliability.

6.2 Future work

6.2.1 Studies on the formation of the encapsulating shell

In Chapter 4, PRP-1 beads capable of extracting hydrophobic analytes were retained in a porous silica sol-gel monolith. However, the encapsulation of the HPLC particles by the sol gel silica shell posed a serious problem to the access of analytes to the PRP-1 beads. A preconditioning step using pH 9.4 borate buffer for 60 min was required to partially dissolve the silica shell and expose the PRP-1 beads to the sample solution. This means extra preparation time before a PRP-1 tip is ready for performing analyses. Optimization of the monolith fabrication protocol is needed to prepare HPLC bead packed monoliths with more exposed SPE surface. In this thesis, the silica sol-gel monolith was fabricated following the protocol of Tanaka's group¹ without further studies of the influence of fabrication conditions on the physical characteristics of the silica shell. Although there have been no reports regarding this problem, the comparison of description and SEM images reported by different groups^{2,3} indicates that the appearance of the silica shell is probably related to the fabrication conditions rather than the chemical or material properties of the immobilized beads. For example, in Dulay *et al*'s work², the SEM images show clearly that the interstitial space between the ODS

particles is almost filled with silica. Whereas, Remcho and co-workers reported a similar alkoxide sol-gel fabrication procedure, yet their SEM images show much less inter-bead silica³. The silica sol-gel process has been studied in detail in the literature⁴, including the gelation and aging kinetics. I believe that the appearance and thickening of the encapsulating shell is a time (and other conditions) dependent process. Therefore it should be possible to prepare a bead-packed monolith with exposed bead surface by changing the monolith fabrication conditions such as the gelation and aging time, temperature and pH.

6.2.2 Other recognizing/preconcentration mechanisms

In this thesis, the preconcentration is based on the hydrophobic nature of the analytes. However all hydrophobic solutes would be adsorbed onto the immobilized PRP-1 beads. Thus the selectivity of this preconcentration process is low. To be compatible with complex sample matrices, a high extraction selectivity is essential. As discussed in Section 1.3, immunoaffinity adsorbents and molecularly-imprinted polymers (MIP) have much higher selectivity for a specific analyte or group of analytes. Immunoaffinity recognizing elements such as antibodies can be immobilized on glass beads⁵ and then entrapped into silica sol-gel monolith using similar fabrication protocol to that in Chapter 4, or bonded directly to the monolithic materials. For example, Hage's group recently reported the immobilization of rabbit immunoglobulin G (IgG) and anti-FITC antibodies on a copolymer monolith of glycidyl methacrylate and ethylene dimethacrylate⁶. Although it is not prepared for on-capillary SPE preconcentration, it is attractive for rapid extraction of analytes from complex biological matrix and can be developed into capillary-tip immunochemical preconcentrator.

Similarly, MIP adsorbents can be prepared either as chromatographic particles or monolith segments⁷. MIP particles could be entrapped in the same manner as in Chapter 4. Alternatively, a MIP monolith may be fixed covalently to the methacryloxypropyl-trimethoxysilane derivatized capillary inner surface by *in situ* polymerization^{8,9}. Lai's group recently reported monolithic MIP phase in a pipette tip inserted into sample loading vial of microchip CE system¹⁰. It is expected that such a MIP monolith fabricated in capillary can be used for on-capillary extraction of specific analyte.

6.2.3 Applications in MEKC mode

Neutral analytes have a higher affinity for reversed phase packings than charged solutes. Thus higher concentration ratios can be achieved for neutral solutes. However, organic solvents have to be used to elute the extracted analytes from the SPE segment. This results in a concentrated sample plug containing a high percentage of organic solvent. The high concentration of organic solvent causes two problems. First, the micelles (usually SDS) near the sample plug will dissolve immediately when organic solvent in sample plug dissipates into SDS micelles-containing buffer, making MEKC impossible. Second, the hydrophobic analytes have higher affinity for organic solvent in sample plug than micelle phase in MEKC buffer. Thus the analytes will always stay in the sample plug rather than partition into the micelles, resulting in no separation occurring.

Chapter 2 gives some hints to a solution to these problems. In Chapter 2, the injected sample plug contains 50% DMF and the MEKC buffer has 40% acetonitrile and 40 mM sodium cholate. Unlike SDS, cholate micelles can tolerate up to 50% acetonitrile

¹¹. The addition of acetonitrile to the MEKC buffer decreases the difference in the affinity of analytes for sample plug and MEKC buffer. Thus baseline resolution of three linear alkylphosphonic acids was observed.

A potential solution to the above problems is proposed as follows: the neutral analytes already extracted onto PRP-1 beads could be eluted by a short plug of elution buffer containing 40% acetonitrile. Then most of the analytes are washed out for subsequent MEKC separation in running buffer containing 40% acetonitrile and cholate. The cholate concentration can be varied to adjust the retention factor. A long segment of eluent is required to elute the strongly retained analytes from the PRP-1 beads. High-salt stacking could be used to focus such analytes prior to MEKC separation.

6.2.4 Other monolith materials and CE separation channel layout

One of the drawbacks of the alkoxide sol-gel monolith is that it is not stable at high pH buffer (> pH 9). This limits silica monoliths to low pH applications. Under low pH conditions, the EOF is low and so low-pressure has to be applied to facilitate fast separations, as in Chapter 4. The application of pressure leads to lower separation efficiency due to the generation of a parabolic flow profile. If the SPE preconcentration and subsequent CE separation were performed in different capillaries or channels, it would not be necessary to apply a pressure across both the preconcentration column and the separation channel. A potential multi-channel microfluidic format with LIF detection for preconcentration and separation is shown in Figure 6-1. Sample solution is first introduced into the preconcentration channel from port P1 and the analytes are adsorbed onto the immobilized SPE adsorbents. CE running buffer in port P2 would be used to

wash out excessive sample solution. Then a short plug of eluting buffer is injected hydrodynamically from port P3 to elute the adsorbed analytes. CE running buffer in P2 is pumped into preconcentration channel to bring the concentrated sample plug into separation channel, followed by CE separation and LIF detection.

An alternative solution to the pH limitation of silica monolith would be to use polymeric monoliths¹² which are stable over a wide pH range. At high pH the EOF would be strong enough to pump the flow of buffer solution against the resistance from the SPE segment in the absence of applied pressure. For polymeric monolith, charged functionalities can be introduced to control EOF¹²⁻¹⁵. MIP reorganization sites may be incorporated into the polymeric monolith, as discussed above and in Chapter 1.

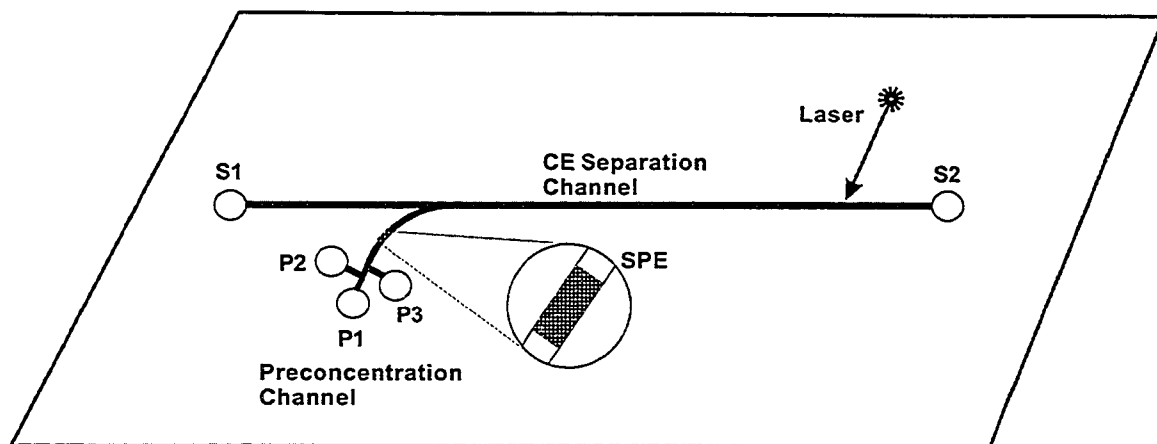


Figure 6.1 A potential microfluidic format with LIF detection for SPE preconcentration and separation performed on different channels. Figure is not drawn to scale. S1 and S2: CE running buffer and electrodes; P1: sample loading; P2: CE running buffer; P3: eluting buffer; SPE: immobilized SPE adsorbent.

6.3 References

- (1) Motokawa, M.; Kobayashi, H.; Ishizuka, N.; Minakuchi, H.; Nakanishi, K.; Jinnai, H.; Hosoya, K.; Ikegami, T.; Tanaka, N. *Journal of Chromatography A* **2002**, *961*, 53-63.
- (2) Dulay, M. T.; Kulkarni, R. P.; Zare, R. N. *Analytical Chemistry* **1998**, *70*, 5103-5107.
- (3) Chirica, G. S.; Remcho, V. T. *Electrophoresis* **2000**, *21*, 3093-3101.
- (4) Hench, L. L.; West, J. K. *Chemical Reviews* **1990**, *90*, 33-72.
- (5) Guzman, N. A. *Journal of Chromatography B-Analytical Technologies in the Biomedical and Life Sciences* **2000**, *749*, 197-213.
- (6) Jiang, T.; Mallik, R.; Hage, D. S. *Analytical Chemistry* **2005**, *77*, 2362-2372.
- (7) Haupt, K. *Analyst* **2001**, *126*, 747-756.
- (8) Spegel, P.; Schweitz, L.; Nilsson, S. *Electrophoresis* **2003**, *24*, 3892-3899.
- (9) Schweitz, L.; Spegel, P.; Nilsson, S. *Electrophoresis* **2001**, *22*, 4053-4063.
- (10) Revesz, E.; Lai, E. P. C., 88th Canadian Chemistry Conference and Exhibition, Saskatoon, Canada, **2005**, 141.
- (11) Landers, J. P. *Handbook of Capillary Electrophoresis*, 3rd ed.; CRC Press, **1996**.
- (12) Tanaka, N.; Kobayashi, H.; Nakanishi, K.; Minakuchi, H.; Ishizuka, N. *Analytical Chemistry* **2001**, *73*, 420a-429a.
- (13) Wu, R. N.; Zou, H. F.; Ye, M. L.; Lei, Z. D.; Ni, J. Y. *Electrophoresis* **2001**, *22*, 544-551.
- (14) Hilder, E. F.; Svec, F.; Frechet, J. M. *Journal of Chromatography A* **2004**, *1044*, 3-22.

(15) Hilder, E. F.; Svec, F.; Frechet, J. M. J. *Electrophoresis* **2002**, *23*, 3934-3953.

Appendix: Curriculum Vitae

Jiang Jiang

Department of Chemistry

University of Alberta, Edmonton, Alberta, Canada, T6G 2G2

Education

- Ph.D., Analytical Chemistry, University of Alberta, Edmonton, Canada 1999-2005
Thesis: Preconcentration Techniques in Capillary Electrophoresis with Laser-Induced Fluorescence Detection
- M.S., Analytical Chemistry, Wuhan University, Wuhan, China 1991-1994
Thesis: Application of Chemometrics and Differential Kinetic Analysis for the Determination of Drugs
- B.S., Chemistry, Wuhan University, Wuhan, China 1987-1991

Research Experience

- PhD graduate research 2000-2005
Supervisor: Dr. Charles Lucy. University of Alberta, Edmonton, Canada
- Capillary electrophoresis – laser-induced fluorescence detection.
 - Sample stacking and solid-phase extraction in capillary electrophoresis.
 - Ultra-sensitive detection of herbicides.
- PhD graduate research 1999-2000
Supervisor: Dr. Norm Dovichi. University of Alberta, Edmonton, Canada
- Capillary gel electrophoresis – laser-induced fluorescence detection.
 - Protein profiling of cancer cell extract using detergent differential fractionation.
- Pharmaceutical analysis research 1994-1999
Supervisor: Lijuan Fu. Wuhan Institute for Drug Control, Wuhan, China
- Chemical analysis of antibiotics using HPLC, CE, TLC and UV spectrometry.
- M.S. graduate research 1991-1994
Supervisor: Prof. Ruxiu Cai. Wuhan University, Wuhan, China
- Chemometrics: factor analysis.

- Differential kinetic analysis.
- Drug analysis using UV-vis detection.

Selected Publications

4. Jiang Jiang and Charles A. Lucy, "A Capillary-Tip Chromatographic Beads-Packed Monolithic Preconcentrator – Fabrication, Characterization and Application in Determination of Herbicides Using Capillary Electrophoresis – Laser-Induced Fluorescence Detection", in preparation.
3. Jiang Jiang and Charles A. Lucy, "Determination of Alkylphosphonic Acids Using Micellar Electrokinetic Chromatography with Laser-Induced Fluorescence Detection and High-Salt Stacking", *Journal of Chromatography A*, 966 (2002) 239-244.
2. S. Hu, J. Jiang, L. Cook, D.P. Richards, L. Horlick, B. Wong and N.J. Dovichi, "Capillary SDS-DALT Electrophoresis with Laser-Induced Fluorescence for Size-Based Analysis of Proteins in Human Colon Cancer Cells", *Electrophoresis*, 23(2002) 3136.
1. Li-Juan Fu and J. Jiang, "Determination of Three Components in Cefradine for Injection with Precolumn Derivatization - HPLC", *Chinese Journal of Pharmaceutical Analysis*, 21(2001) 81.

Conference Presentations

3. Jiang Jiang and Charles A. Lucy, "A Capillary-Tip Preconcentrator Based on HPLC Beads Entrapped Sol-Gel Monolith", the 88th Canadian Society for Chemistry Conference (CSC 2005), Saskatoon, Canada, May 28 ~ Jun 1, 2005 (oral).
2. Jiang Jiang and Charles A. Lucy, "Determination of Alkylphosphonic Acids Using Micellar Electrokinetic Chromatography with Laser-Induced Fluorescence Detection and High-Salt Stacking", the 85th Canadian Society for Chemistry Conference (CSC 2002), Vancouver, Canada, July 1-5, 2002 (poster).
1. Jiang Jiang, Shen Hu and Norm J. Dovichi, "Capillary Gel Electrophoresis with Laser-Induced Fluorescence Detection and Detergent Differential Fractionation for Characterization of Cancer Cell Proteins", the 2nd International Conference of the Canadian Proteomics Initiative (CPI 2002), Edmonton, Canada, May 11-14, 2002 (poster, based on work done in Dovichi group).

Internal Report

1. Jeremy E. Melanson, Jiang Jiang, Charles A. Lucy and Camille A. Boulet, "Development of High Sensitivity Capillary Electrophoresis Methods for Degradation Products of Chemical Warfare Agents", Public Works & Government Services (Defense Research Establishment Suffield), 1999 ~ 2002.

Teaching Experience

University of Alberta, Graduate Teaching Assistant for Chem 101/103 Introductory University Chemistry I, II	1999-2001, 2004
Chem 211/213 Quantitative Analysis I, II	2002-2003

Professional Membership

Canadian Society for Chemistry

Honors and Awards

2. Graduate Research Assistant Award (University of Alberta, 2003).
1. Second place poster prize winner at the 2nd International Conference of the Canadian Proteomics Initiative (CPI 2002, Edmonton).